# FAULT DIAGNOSIS OF RAILWAY ASSETS USING ACOUSTIC MONITORING

by

KATSUHITO INOUE

A thesis submitted to
The University of Birmingham
For the degree of
DOCTOR OF PHILOSOPHY

School of Engineering
The University of Birmingham
September 2023

# ABSTRACT

Machines such as point machines and contactors are called Single Throw Mechanical Equipment (STME), and the failure of these machines affects the operation of trains significantly and may cause accidents, resulting in many human casualties and significant economic damage.

Although condition monitoring methods for these machines have been studied, conventional methods using voltage sensors, load sensors, and displacement sensors need to be attached directly to the high-voltage circuit or mechanical portion of the equipment which can be dangerous to attach and maintain, and when a sensor fails, it can adversely affect the functioning of the equipment. In addition, the environment where railway equipment is installed is harsh and there is a high possibility of sensor failure due to exposure to iron powder, dust, oil, and vibration generated from the tracks, wheels, ballast and passing trains. Air-borne acoustic monitoring is attracting attention because these data can be measured in a non-contact way from a certain distance, which means there is less risk of the sensor having a negative impact on the equipment or of the sensor breaking due to vibration or natural environmental factors, reducing the risk of the workers involved in data acquisition and sensor maintenance. Furthermore, it may enable low-cost maintenance by monitoring several pieces of equipment from a single sensor as sound is spread around.

Condition monitoring method using acoustic data has attracted attention and a lot of research has been done but most research targets are rotating machinery such as axles and

bearings. Few studies have applied it to STME, and even in a few cases, it focuses on failures that can be detected by existing fault detection methods.

This thesis proposes a condition monitoring method using acoustic data for STME, and faults to be studied are difficult to detect and diagnose by existing methods. In order to verify the effective diagnostic technique for STME, normal and simulated fault data are acquired from two types of STME, a point machine and a contactor, in this study. A fault diagnosis system is developed using features and classification techniques that are expected to be useful from previous studies. Using the developed method to diagnose the data of each STME, it was found that using the Mel Frequency Cepstral Coefficient (MFCC) as a feature is the most accurate for both STME. As for classifiers, both Support Vector Machine (SVM) and K-Nearest Neighbour (KNN) could diagnose faults with sufficiently high accuracy for both STMEs, but the accuracy using KNN was slightly higher than that using SVM.

The noise tolerance of the proposed method was also evaluated by adding noise artificially. In addition, multiple microphones are used to investigate which location is best for data acquisition. Finally, the transferability of the model, in which the model-trained data from one machine can be used for other machines, is verified using MFCC as a feature. The verification revealed that the combination of MFCC and SVM could improve the transferability performance of the model for several faults.

The verification of this study revealed that fault diagnosis is possible from the acoustic data of the STME by using the proposed method, and since this method is tolerant of noise and its performance of transferability is high, field deployment would be anticipated to be successful.

# ACKNOWLEDGEMENTS

I would like to express my deepest gratitude to my first supervisor, Dr Edward Stewart, for his experienced supervision, dedicated support, and patience throughout my PhD project. His immense knowledge and guidance inspired and helped me in all the time of my research. My PhD would have never been possible without him.

I would like also to thank my second supervisor Dr Mani Entezami, for his advice on data analysis and for giving me the opportunity to measure data in various fields, and Prof Clive Roberts, for his advice and outstanding knowledge, making me broaden my perspective.

I would like to offer my special thanks to Prof Takafumi Koseki, for his advice on proceeding with this research. I would like to show my greatest appreciation to Dr Hiroto Takeuchi, for his experienced guidance and generous support throughout my PhD.

Special thanks to Mr Adnan Zentami and Mr Tanapon Kumpao, for support of data acquisition in Birmingham university, and Mr Koki Yanagawa and staff of Central Japan Railway, for helping data acquisition in Japan. I am also grateful to the Central Japan Railway Company, for giving me the excellent opportunity, all the support during my course. Also, I thank all my friends and colleagues in BCRRE, it was fun and precious spending time with you guys.

Finally, I am deeply grateful to my beloved wife, Seika, for her love, understanding and encouragement. I could not have achieved my PhD without her.

# TABLE OF CONTENTS

***LIST OF FIGURES*** ..... ***I***

***LIST OF TABLES*** ..... ***IV***

***LIST OF ABBREVIATIONS*** ..... ***VI***

***CHAPTER 1 INTRODUCTION*** ..... ***1***

**1.1 Background** ..... **1**

**1.2 Single Throw Mechanical Equipment (STME)** ..... **5**

**1.3 Failures and faults** ..... **6**

**1.4 Hypothesis** ..... **8**

**1.5 Scope of this thesis** ..... **9**

***CHAPTER 2 LITERATURE REVIEW*** ..... ***12***

**2.1 Introduction** ..... **12**

**2.2 Previous research on acoustic monitoring** ..... **12**

2.2.1 Acoustic monitoring methods for rotating machinery ..... 12

2.2.2 Point machines ..... 14

2.2.2.1 Fault modes of point machines ..... 17

2.2.2.2 Acoustic monitoring methods for point machines ..... 21

2.2.3 Contactors ..... 29

2.2.3.1 Fault modes of contactors ..... 30

2.2.3.2 Condition monitoring methods for contactors ..... 31

**2.3 Background noise level** ..... **34**

**2.4 Proposed method ..... 36**

***CHAPTER 3 METHODOLOGY ..... 39***

**3.1 Introduction ..... 39**

**3.2 Features for classification ..... 40**

3.2.1 Mel Frequency Cepstral Coefficient (MFCC) ..... 41

3.2.2 Wavelet Packet Decomposition Energy (WPDE) ..... 43

**3.3 Classification ..... 46**

3.3.1 Support Vector Machine (SVM) ..... 46

3.3.2 K-Nearest Neighbour (KNN) ..... 51

**3.4 Validation ..... 52**

**3.5 Summary ..... 54**

***CHAPTER 4 EXPERIMENT WITH SLOW STME: POINT MACHINE ..... 56***

**4.1 Introduction ..... 56**

**4.2 Experiment using a point machine ..... 57**

**4.3 Classification accuracy ..... 64**

4.3.1 Classification accuracy using MFCC ..... 65

4.3.2 Summary of accuracy using MFCC ..... 72

4.3.3 Classification accuracy using WPDE ..... 72

4.3.4 Summary of accuracy of using WPDE ..... 79

**4.4 The effect of noise ..... 79**

**4.5 Important frequency range of operating sound ..... 81**

**4.6 Summary and findings ..... 83**

*CHAPTER 5 EXPERIMENT WITH FAST STME: CONTACTORS ..... 85*

**5.1 Introduction ..... 85**

**5.2 Experiment using contactors ..... 85**

**5.3 Classification accuracy ..... 98**

**5.4 The effect of noise ..... 105**

**5.5 Summary and findings ..... 115**

*CHAPTER 6 TRANSFERABILITY ..... 117*

**6.1 Introduction ..... 117**

**6.2 Transferability experiment ..... 118**

**6.3 Feature selection ..... 123**

6.3.1 Principal Component Analysis ..... 124

6.3.2 Minimum Redundancy Maximum Relevance ..... 126

**6.4 Feature selection using MRMR ..... 130**

**6.5 Performance variation by fault level ..... 134**

**6.6 The effect of noise ..... 138**

**6.7 Summary and findings in this chapter ..... 141**

*CHAPTER 7 CONCLUSIONS ..... 144*

**7.1 Summary of the findings ..... 144**

**7.2 Recommendation for future works ..... 151**

*LIST OF REFERENCES ..... 154*

# LIST OF FIGURES

Figure 1. Spectrogram of acoustic data of STME ..... 6

Figure 2. P–F curve and definition of fault and failure ..... 8

Figure 3. The structure of an HW point machine ..... 15

Figure 4. The number of point machines used in the UK ..... 16

Figure 5. The parameters of the point machines monitored in previous studies ..... 23

Figure 6. The structure of a contactor ..... 30

Figure 7. Transferability of the model ..... 37

Figure 8. Algorithm for diagnosing STME faults ..... 40

Figure 9. Structure of HW point machine ..... 57

Figure 10. Location of microphones ..... 58

Figure 11. Condition of the slide chair ..... 61

Figure 12. Obstructions between switch rail and stock rail ..... 62

Figure 13. Spectrograms for each condition of signal and power (NR direction) ..... 64

Figure 14. Diagnostic results by MFCC-SVM ..... 67

Figure 15. Diagnostic results by MFCC-KNN ..... 69

Figure 16. Amplitude of operating sound for each direction ..... 69

Figure 17. Sound spectrogram for each microphone ..... 71

Figure 18. Diagnostic results by WPDE-SVM ..... 73

Figure 19. Diagnostic results by WPDE-KNN ..... 74

Figure 20. Structure of the point machine ..... 76

Figure 21. Sound spectrograms for over-tightened and loose nuts (NR direction) ..... 77

Figure 22. Recall of each bandpass filter ..... 82

Figure 23. Structure of the contactor ..... 86

Figure 24. Movement of contactor components through opening and closing ..... 87

Figure 25. Location of measuring equipment and contactors ..... 89

Figure 26. Measuring equipment (inside mic and data recorder) ..... 90

Figure 27. Structure of normal and damaged contactors ..... 91

Figure 28. Simulated fault 1: lack of grease ..... 91

Figure 29. Simulated fault 2: spring weakening ..... 93

Figure 30. Simulated fault 3: obstruction ..... 94

Figure 31. Simulated fault 4: improper pin position ..... 95

Figure 32. Spectrogram for each condition of signal and power ..... 98

Figure 33. Diagnostic results by MFCC-SVM ..... 101

Figure 34. Diagnostic results by MFCC-KNN ..... 102

Figure 35. Diagnostic results by WPDE-SVM ..... 103

Figure 36. Diagnostic results by WPDE-KNN ..... 104

Figure 37. Variation in diagnostic accuracy with noise (up to 80 dB) ..... 110

Figure 38. Spectrogram of the signal with noise (Closed data, 37 dB and 55 dB) ..... 111

Figure 39. Spectrogram of the signal with noise (Closed data, 80 dB and 100 dB) ..... 112

Figure 40. Variation in diagnostic accuracy with noise (up to 100 dB) ..... 113

Figure 41. Transferability of the model in practical development ..... 118

Figure 42. Transferability investigation of this study ..... 118

Figure 43. Location of measuring equipment and contactors ..... 119

Figure 44. Transferability performance (MFCC + SVM) ..... 122

Figure 45. Transferability performance (MFCC + KNN) ..... 123

Figure 46. Distribution of selected features ..... 128

Figure 47. MFCC and sound spectrogram for each condition ..... 129

Figure 48. Sound spectrogram and MFCC for obstruction ..... 129

Figure 49. Distribution of features selected from data C ..... 136

# LIST OF TABLES

Table 1. The number of point machine failures in the UK in 2009 ..... 17

Table 2. Point machine failures from Network Rail's database ..... 18

Table 3. The number of point machine failures in Japan from 1996 to 2005 ..... 19

Table 4. Point machine failures from Network Rail's FMS from 2013 to 2018 ..... 20

Table 5. The parameters of the point machines monitored in previous studies ..... 23

Table 6. Confusion matrix ..... 53

Table 7. Measuring equipment ..... 59

Table 8. Test schedule ..... 60

Table 9. Recall of the fault diagnosis ..... 65

Table 10. Recall of fault diagnosis with 37 dB noise ..... 80

Table 11. Recall of fault diagnosis with 55 dB noise ..... 81

Table 12. Simulated fault modes ..... 88

Table 13. Measuring equipment ..... 89

Table 14. Test schedule ..... 97

Table 15. Recall of the fault diagnosis ..... 99

Table 16. Recall of fault diagnosis with 37 dB noise ..... 106

Table 17. Recall of fault diagnosis with 55 dB noise ..... 107

Table 18. Recall of the fault diagnosis with 80 dB noise ..... 109

Table 19. Test schedule ..... 120

Table 20. Transferability performance for obstruction (MFCC + PCA + SVM) ..... 125

Table 21. Transferability performance for obstruction (MFCC + PCA + KNN) ..... 125

Table 22. Transferability performance for obstruction (MFCC + MRMR + SVM) ..... 126

Table 23. Transferability performance for obstruction (MFCC + MRMR + KNN) ..... 127

Table 24. Transferability performance of closed data (MFCC + MRMR + SVM) ..... 132

Table 25. Transferability performance of open data (MFCC + MRMR + SVM) ..... 133

Table 26. Transferability performance of closed data (MFCC + MRMR + KNN) ..... 133

Table 27. Transferability performance of open data (MFCC + MRMR + KNN) ..... 134

Table 28. Transferability performance for spring weakening for each level ..... 135

Table 29. Effective features for diagnosing each level of spring weakening fault ..... 138

Table 30. Transferability of the fault diagnosis without noise ..... 139

Table 31. Transferability of the fault diagnosis with 55 dB noise ..... 140

# LIST OF ABBREVIATIONS

| | |
|---|---|
| **AE** | Acoustic Emission |
| **ANN** | Artificial Neural Network |
| **BPSO** | Binary Particle Swarm Optimisation |
| **CBM** | Condition-Based Maintenance |
| **CWT** | Continuous Wavelet Transforms |
| **DWT** | Discrete Wavelet Transforms |
| **EMD** | Empirical Mode Decomposition |
| **EEMD-HMSEE** | Ensemble Empirical Mode Decomposition Hilbert Marginal Spectrum Energy Entropy |
| **EVR** | Explained Variance Ratio |
| **FN** | False Negative |
| **FP** | False Positive |
| **FPR** | False Positive Rate |
| **FOAS** | Fibre Optic Acoustic Sensing |
| **IMF** | Intrinsic Mode Function |
| **IEC** | International Electrotechnical Commission |
| **KNN** | K-Nearest Neighbour |
| **LDA** | Linear Discriminant Analysis |
| **MFCC** | Mel Frequency Cepstral Coefficient |
| **MRMR** | Minimum Redundancy Maximum Relevance |
| **MFPE** | Multi-scale Fractional Permutation Entropy |
| **NB** | Naive Bayesian |
| **NR** | Normal to Reverse |
| **PSO-SVM** | Particle Swarm Optimisation Support Vector Machine |

| | |
|---|---|
| **PCA** | Principal Component Analysis |
| **RN** | Reverse to Normal |
| **STFT** | Short Time Fourier Transform |
| **SNR** | Signal-to-Noise Ratio |
| **STME** | Single Throw Mechanical Equipment |
| **SPL** | Sound Pressure Level |
| **SVM** | Support Vector Machine |
| **TBM** | Time-Based Maintenance |
| **TN** | True Negative |
| **TP** | True Positive |
| **TPR** | True Positive Rate |
| **VMD** | Variational Mode Decomposition |
| **WPD** | Wavelet Packet Decomposition |
| **WPDE** | Wavelet Packet Decomposition Energy |
| **WT** | Wavelet Transform |

# CHAPTER 1 INTRODUCTION

## 1.1 Background

When equipment used in railways and substations malfunctions, it causes accidents, resulting in many human casualties and significant economic damage. Therefore, many of the facilities are designed redundantly and carefully maintained to ensure safety. However, despite all the costs and efforts, accidents due to equipment failure do occur. Due to a point machine failure, a derailment happened at Potters Bar and Grayrigg in the UK [1-3]. In 2018, a total of 54 bullet trains were delayed due to the failure of the point machine in Maibara, Japan, affecting about 47,000 people [4]. Also in Japan, in 2021, the moving blade of a contactor in the electrical supply system did not open completely due to age-related deterioration, which caused a power failure for nearly two hours. In addition, at least three other outages have occurred in Japan since 2020 due to malfunctions caused by age-related deterioration of circuit breakers and contactors, resulting in a total outage time of more than four hours [5]. In 2012, a fire broke out in a substation in the USA due to a ground fault caused by degraded contacts in a circuit breaker, resulting in an outage affecting over 5800 customers [6].

A single failure of critical Infrastructure components might have a serious effect, and due to the high impact of accidents, time-based maintenance (TBM), checking all equipment every maintenance cycle, is used for many kinds of them. The cycles are determined by the anticipated time of the worst condition breaking and these cycles are applied to all equipment. Therefore, even though most equipment can be sufficiently maintained with longer cycles, unnecessary and frequent maintenance must be performed on all equipment, which is expensive and time-consuming. In addition, maintenance staff usually collect data from equipment only

during inspections and maintenance, thus they may miss initial faults and the progression of faults as continuous data are not acquired.

To improve this situation, many infrastructure companies are applying condition-based maintenance (CBM) which monitors conditions and performs maintenance only on necessary equipment. In CBM, equipment parameters such as current, vibration, and temperature are monitored by condition monitoring systems. This technology enables the monitoring of the equipment's condition by using sensors, and it allows the maintenance to be performed only on the equipment that needs it. Some systems use a threshold method, which monitors parameters continuously and creates an alarm whenever the monitored parameters exceed a predetermined value. Therefore, it enables the detection of initial faults and the progression of faults in equipment. The use of many condition monitoring technologies has been tried in industry, but some equipment is installed in special conditions and environments, which need to be considered. First, since malfunctions of railway equipment and substation equipment often have a significant impact, sensors should be installed in such a way that they do not affect the functioning of the equipment. Second, sensors need to be protected, as frequent breakdowns of the sensors require time-consuming and expensive maintenance. Third, since some railway equipment is installed inside the tracks, and some use high voltage, maintenance staff, who need to approach these facilities when performing the maintenance, are at a risk of accidents such as collisions with trains and electric shocks. Therefore, a method of collecting data from a certain distance away is desirable.

Voltage sensors, load sensors, displacement sensors, etc., need to be attached directly to the high-voltage circuit or mechanical portion of the equipment, and when a sensor fails, it can adversely affect the functioning of the equipment and cause significant damage. According

to a report by Chubu and Kinki, of the Industrial Safety and Inspection Department of Japan, 69 electrical incidents have occurred due to the failure of measurement sensors in the central region of Japan since 1986 [7]. Since 2020, at least 13 power outages have occurred in Japan due to voltage sensor accidents, with a total of more than 16 hours of outage time. An electric shock also occurred when a worker touched the high-voltage part of a voltage sensor [5].

Acoustic Emission (AE) and vibration sensors are usually attached to target equipment with adhesives, but it is reported that they come off due to vibration and natural environmental factors such as rain and heat [8]. When installed outdoors or near industrial machinery, they are exposed to harsh environments such as ultraviolet rays, rapid temperature changes, rain, and oil. This may cause the sensor to come off or the sensor itself to break down.

Vibration sensors, AE sensors, etc., need to be mounted directly on or very close to the equipment. Current sensors do not need to be installed near the target and are sometimes installed in a control room or a lineside cabinet located a short distance away from the target. However, if the target is installed outdoors, the cables may leak current, and the current used by the target may not be accurately monitored. In addition, if other cables are installed in parallel with the cable between the sensor and the target, electromagnetic noise from the other cables may have an effect, therefore, it is desirable to install the sensors as close to the target as possible to obtain accurate current data. Some railway equipment is installed inside the tracks, and some use high voltage; therefore, installing sensors or acquiring data from equipment can cause collisions with trains or electric shocks. JR East reported that 10 people have been lost in collisions and seven due to electric shocks since 1996 [9, 10].

Air-borne acoustic monitoring is attracting attention because these data can be measured in a non-contact way from a certain distance, which means there is less risk of the

sensor having a negative impact on the equipment or of the sensor breaking due to vibration or natural environmental factors, reducing the risk of the workers involved in data acquisition. Furthermore, it may enable low-cost maintenance by monitoring several pieces of equipment from a single sensor as sound is spread around.

A survey using Scopus shows that the number of papers related to acoustic monitoring in the engineering field started to increase from around 2000. A similar upward trend can be seen in research on condition monitoring using current and vibration, which can be attributed to the fact that signal processing from a large number of sensors, which was difficult in the past, has become possible due to improvements in the performance of computing devices. The number of papers has further increased since the late 2010s. Since then, there has also been increased research on diagnosing diseases by attaching sensors to the human body. This may be due to the development of inexpensive and compact sensors, which has stimulated more research.

Sensor improvement or new technology could make it easier to get acoustic data from equipment. Brambilla *et al.* carried out a project to obtain acoustic data of trains and facilities along a track from existing optical fibres by using Fibre Optic Acoustic Sensing (FOAS) technology [11]. FOAS can be used to monitor acoustic data from optical fibres, around 20,000 km of which already exist running alongside Britain's railways. The implementation of FOAS is expected to provide valuable data to enhance remote condition monitoring of assets, improve train performance, and reduce disruption cost-effectively. Network Rail has announced a contract to develop and trial FOAS [12]. If the data obtained by FOAS are accurate, condition monitoring using acoustic data is expected to become more active.

As described above, condition monitoring using acoustic data has attracted attention and a lot of research has been done but most research targets are rotating machinery such as axles and bearings. Few studies have applied it to Single Throw Mechanical Equipment (STME) such as railway point machines and contactors. This study focuses on the acoustic monitoring of STME, which has not yet been well-studied.

## 1.2 Single Throw Mechanical Equipment (STME)

STME is a type of equipment that switches between two states according to control signals [13]. Point machines, contactors, circuit breakers, and doors are examples of STME. One of the characteristics of STME is that its operation is not periodic like rotating machinery. Due to the different acoustic characteristics, in this study, STME is categorised into two types. One is slow switching speed, such as point machines and doors, and the other is fast switching speed, such as contactors and circuit breakers. The former switches from one state to the other over several seconds by motor, hydraulic, or pneumatic force. The latter uses solenoid coils or spring forces to switch states instantaneously. Spectrograms of the operating sound of a point machine and contactor are shown in Figure 1. The point machine data show the motor running between 0.5 and 3 seconds. Specific frequencies continue for several seconds, and almost no sound above 15 kHz can be identified, and high-power sounds are distributed below 5 kHz. In contrast, the contactor data show the sound of the moving blade accelerated by the solenoid coil impacting the fixed blades between 200 to 300 milliseconds. The sound frequency ranges over a wide range, with some sounds reaching nearly 20 kHz. The high-power sound can also be seen at close to 10 kHz. These data were acquired in an ideal environment such as a laboratory or indoors, but usually, there are noises such as wind and rain or operating sounds of other

machines. Although both types of movement are similar, the characteristics of the operating sound are different because the operating speeds are different.

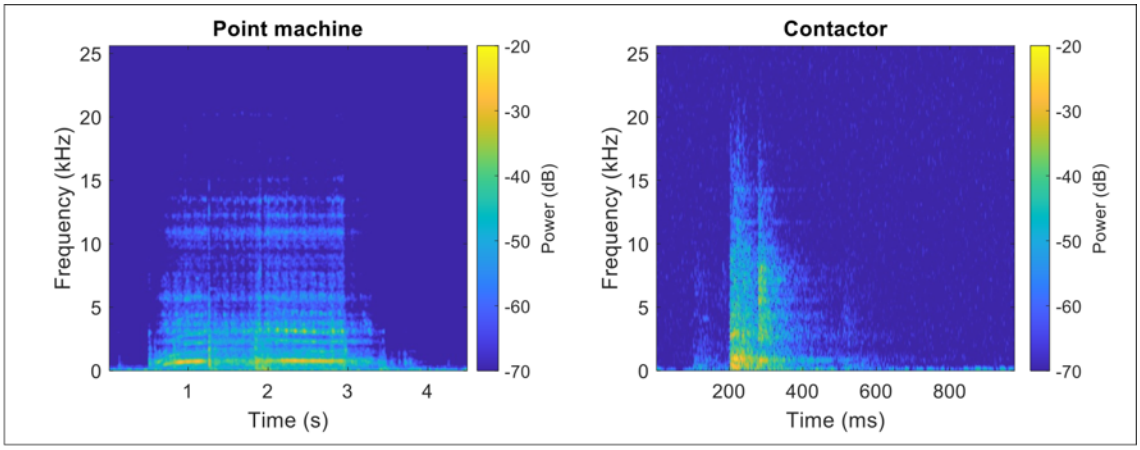


Figure 1. Spectrogram of acoustic data of STME

## 1.3 Failures and faults

This section gives definitions of the terms ‘fault’ and ‘failure’ used in this thesis. According to the International Electrotechnical Commission (IEC) standard, a fault is defined as an ‘abnormal condition that could lead to an error in a system’ and a failure is defined as a ‘loss of ability to perform as required’. An error is defined as the ‘discrepancy between a computed, observed or measured value or condition, and the true, specified or theoretically correct value or condition’ [14-16]. In Moubray’s book, a failure is defined as ‘the inability of any asset to do what its users want it to do’ [17]. He also mentioned ‘potential failure’ and ‘functional failure’. A potential failure is ‘an identifiable condition that indicates that a functional failure is either about to occur or is in the process of occurring’, and a functional failure is ‘the inability of any asset to fulfil a function to a standard of performance which is acceptable to the user’. These two terms are used in the P–F curve, which represents the behaviour of an asset before it fails, as shown in Figure 2. The interval from point P to F is

called the P–F interval, during which appropriate maintenance should be carried out. The definitions of the IEC standard and Moubray's book are also illustrated in Figure 2.

A failure of STME can lead to accidents and major service interruptions, so it is of paramount importance that a failure does not occur. In this study, the terms 'fault' and 'failure' are used as defined by IEC. That is, a fault is a state in which the required operation can be performed even if there is a problem in the machine, and a state in which the required operation cannot be performed is called a failure. The state in which the machine is properly maintained and adjusted is called 'normal'. As described in section 1.1, the CBM system must detect faults before a failure occurs.

Although there are few examples of acoustic monitoring studies for STME, Lee *et al.* and Cao *et al.* have reported fault detection and diagnosis results of a point machine using acoustic data [18, 19]. However, these researchers' experiments do not mention how serious the faults are that can be detected and diagnosed, and those seem to be serious ones or failures. The photographs in Lee *et al.*'s paper show that large blocks of ice and ballast were used in the experiment. Normally, if a gap of more than 3.5 mm is created by an obstruction between the rails of a point machine, the switch rail cannot move to the end, and a detector rod will detect the obstruction and issue an alarm [20]. Cao *et al.* used data on faults that can be detected by detector rods and controller signals, such as no-load, an obstruction so large that the switch rail cannot move completely, and poor contact of the controller contacts. Gear faults were also analysed, but it is unlikely that they will occur in the operating environment, as the gears of a point machine are usually covered. It would be useful if acoustic data could be used to detect and diagnose faults that cannot be detected by conventional detector rods and controller signals.

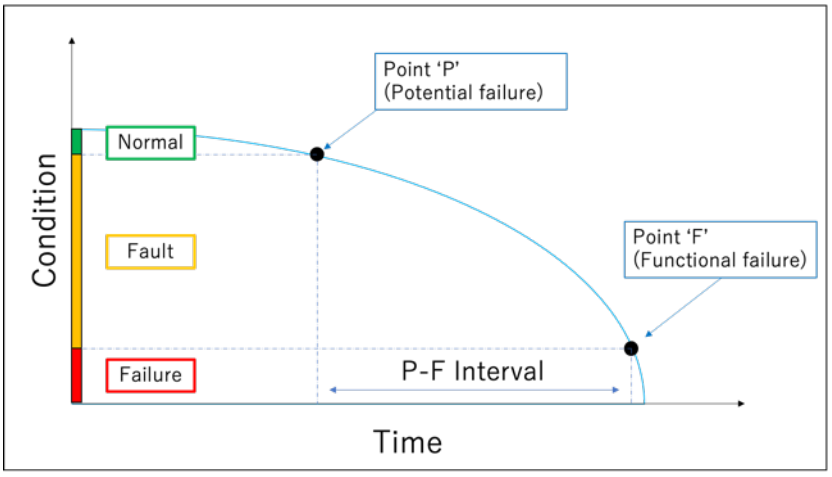


Figure 2. P–F curve and definition of fault and failure

## 1.4 Hypothesis

It is known that rotating machinery faults can cause periodic noise as damaged parts make an abnormal sound every revolution. It is known that each fault of rotating machinery has a basic frequency, and this frequency is usually used to diagnose faults by using frequency analysis and statistical analysis [21, 22]. STME movements, on the other hand, are single-throw, non-linear, and delay may occur in the case of a fault [23, 24]. Therefore, it is difficult to use techniques for rotating machinery for STME.

For this reason, some previous researchers used acoustic recognition techniques to diagnose serious STME faults by capturing differences in time series data. It is expected that in the initial faults of STME that may occur, the components would be damaged or deformed, and the balance of the force on the components transmitted to each component would be disrupted. With this, unusual sounds, and changes in frequency, intensity, and length of the operating sound might happen. Since previous researchers showed that serious faults can be diagnosed using acoustic data, it is possible to diagnose faults, even if they are initial faults, by capturing the occurrence of changes in the operating sound.

This research aims to test the hypothesis that **it is possible to use acoustic methods to detect faults in STME in the early stages of a fault's development**.

To test this hypothesis, normal and simulated fault data using a point machine and contactors are obtained. Fault detection and diagnosis algorithms are developed, and the acquired data are analysed to clarify the following questions.

- Which algorithm is most appropriate? (Discussed in Chapters 4 and 5)
- How accurate is the system and does that vary by fault? (Discussed in Chapters 4 and 5)
- How tolerant is it to noise? (Discussed in Chapters 4 and 5)
- Which place is the most appropriate for the microphone to monitor the target? (Discussed in Chapters 4 and 5)
- Can a fault detection model trained from one machine be transferable to other machines? (Discussed in Chapter 6)

## 1.5 Scope of this thesis

The contents of this thesis are as follows.

Chapter 2: Literature Review

The literature review investigates condition monitoring techniques using acoustic and vibration data of rotating machines and objects that move like STME. Data characteristics, feature extraction methods, and classification methods are summarised. Next, a survey of point machines and contactors is carried out on their structure, operation methods, and faults. Finally, the feature extraction and classification methods for the point machines and contactors are proposed.

Chapter 3: Methodology

First, the algorithm of the proposed method is explained. The theory of the feature and classification methods used is described. In this thesis, Mel-Frequency Cepstrum Coefficients (MFCCs) and Wavelet Packet Decomposition Entropy (WPDE) are used as features and Support Vector Machine (SVM) and k-Nearest Neighbours (KNN) as classification methods.

Chapters 4 and 5: Case studies

Details of the experiments carried out and the analysis results of the data are described in these chapters. Normal and simulated fault data using a point machine and contactors are acquired. First, the optimal feature extraction and classification method for fault diagnosis is investigated by comparing the classification accuracy. Since data are acquired indoors and the effect of background noise is small, white noise is added to the acquired data to simulate an outdoor environment, and the effect on classification accuracy is investigated. Subsequently, to investigate which frequency ranges are important for improving classification accuracy, several bandpass filters are used for data.

Chapter 6: Transferability

Transferability is the ability of a model, trained by data acquired from one machine, to diagnose faults in other machines. Since it is difficult to obtain simulated fault data from all the machines used in the industry, it is necessary to obtain simulated fault data from several machines, train the model with the data, and monitor all the machines with the model. The transferability of the model is essential to realise this. To enhance the transferability performance of the model, a feature selection technique called Minimum Redundancy

Maximum Relevance (MRMR) was used and it was found that the model can have transferability by selecting the features using MRMR.

Chapter 7: Conclusion

This chapter reviews the results of the analysis, summarises the findings of this study in response to the research questions described in the hypothesis section, and draws conclusions. Future works such as problems that may arise in actual use and to be solved also are discussed.

# CHAPTER 2 LITERATURE REVIEW

## 2.1 Introduction

This chapter first describes the background of acoustic monitoring. Many studies have been conducted on rotating equipment, but few have been conducted on machines such as point machines and contactors which have linear actuation. The structure and the investigation results of common failures of point machines and contactors are described. Then, among the condition monitoring research methods for these devices, the ones that can be used for acoustic monitoring are summarised, and the feature extraction and classification methods used in this research are described. Finally, the types and levels of noise that can be added to the acquired data for testing purposes are presented.

## 2.2 Previous research on acoustic monitoring

### 2.2.1 Acoustic monitoring methods for rotating machinery

When there is an abnormality or fault in rotating equipment, an abnormal sound is generated, and the sound is generated at each rotation, thus producing a specific frequency of sound. Acoustic monitoring methods in rotating machinery have been widely researched because of the convenience of acoustic data acquisition and the versatility of frequency analysis.

Heng *et al.* applied a statistical analysis method to sound pressure and vibration signals and found that it is possible to detect the fault of a rolling element bearing by comparing the statistical value [25]. Lu *et al.* used a microphone array to obtain acoustic data of rolling element bearings. They used the basic frequencies associated with different fault locations of bearings, FFT, and near-field acoustic holography techniques to obtain acoustic images in the basic

frequency domain. The features from these images were classified by SVM to diagnose faults with an accuracy of more than 90% [21].

Baydar *et al.* obtained vibration and acoustic signals from a two-stage industrial helical gearbox. They found that the noise content of the acoustic signal changes when the meshing characteristics are disturbed by defects in the teeth. They also calculated the pseudo–Wigner–Ville distribution and found that some faults and their progression could also be detected by monitoring their distribution, the continuity of the meshing frequency, and the frequency activities outside the meshing frequency range [26-29]. They also showed that monitoring by wavelet transform (WT) could also detect faults [27]. WT is one of the methods of time–frequency analysis and uses the wavelet function as the basis function. In this transformation, it is possible to preserve the time-domain information that is lost when determining the frequency response by the Fourier transform.

Liu *et al.* proposed a new rolling bearing fault diagnosis method based on a short-time Fourier transform (STFT) and stacked sparse autoencoders [30]. In this method, a spectrogram was calculated from an acoustic signal, a stacked sparse autoencoder was applied to extract the fault features automatically, and softmax regression was employed to classify the faults. Accuracy was over 97%, and this is better than that of the fault diagnosis method using vibration. However, this method requires high computational resources, which may limit its use in real-time.

Glowacz *et al.* used a technique called the Method of Selection of Amplitudes of Frequency – Multiexpanded to extract the original features from the acoustic signal of a single-phase induction motor and classified it as normal, faulty bearing, or faulty bearing and shorted coils of auxiliary winding, using Nearest Neighbour classifier, Nearest Mean classifier, and

Gaussian Mixture Models [31]. In feature extraction, the spectrum was obtained using FFT and the differences in each state were calculated. The feature with the largest absolute value was used for learning.

Thus, statistical and frequency analysis methods are often used for fault detection and diagnosis in rotating equipment. As mentioned above, these methods are effective because of the periodic noise that occurs during rotating machinery faults, but many of these methods would be difficult to apply to STME, such as point machines, contactors, circuit breakers, and doors, that switch between two states by control signals, because its operation is not periodic. However, STFT and WT might be effective for STME because they include a time-varying component as a feature. In particular, WT performs scaling and translating of basis functions, which allows analysis over a wide frequency range. Also, because the window size can be varied, the computation time can be shorter than with ordinary time–frequency methods such as STFT, Wigner–Ville distribution, and instantaneous power spectrum, which require the window width to be fixed according to the frequency.

### 2.2.2 Point machines

A point machine is one type of STME, providing multiple routes for trains driving the switch rail from one position to another. The structure of a point machine is shown in Figure 3. The box of the point machine contains the motor and gears, which move the drive rod horizontally. The nut attached to the drive rod pushes or pulls the drive lug to move the stretcher bar to which the drive lug is attached. The stretcher bars are attached to the left and right switch rails and thus move both switch rails simultaneously. When the switching process is completed, the locking mechanism inside the box operates and the switch rail is locked. This prevents the switch rail from moving even under the impact of the train passing. When switching to another

direction, the switch rail is first unlocked, and then the drive rod starts to move. The detector rods are also attached to the left and right switch rails and thus can detect whether the switch rails have reached a specified distance. If the switch rail does not move the distance due to obstructions or loose nuts, the switch rail cannot be locked, and an alarm is triggered. The locking mechanism is adjusted when the point machine is installed. If there is a gap of 3.5 mm or greater between the switch rail and the stock rail, the switch rail will not be locked [20].

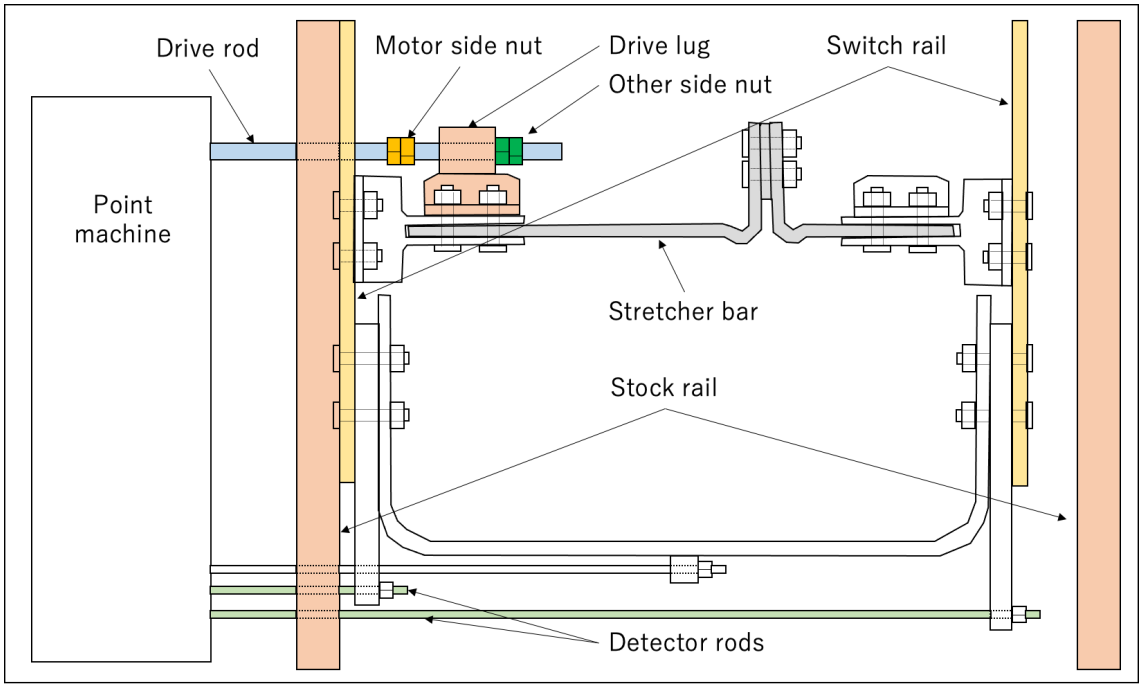


Figure 3. The structure of an HW point machine

Railway equipment is required to have a high level of safety and reliability. Therefore, most of it is designed redundantly. However, a point machine cannot be designed in this way. Due to the lack of redundancy, the failure of a point machine causes enormous disruption. The RSSB reported that point machine failures constituted 4.6% of total delay minutes in the year 2008/9 [32]. According to Network Rail, point machine failures accounted for only 0.56% of all incidents but totalled 3.5% of all delay minutes in the 12 months from 2015 to 2016 [33].

In the UK, many kinds of point machines are in use, depending on rail conditions, company policy, and so on. Figure 4 illustrates the number of point machines currently used in the UK. The total number of point machines is over 20,000, and the dominant systems in use are the HW and Clamplock [33]. Experiments in this study are carried out using the most common HW point machine.

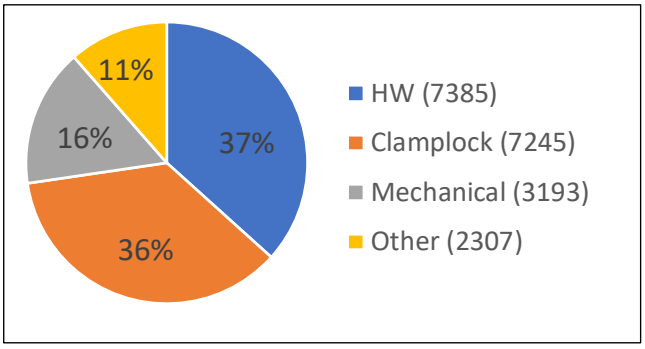


Figure 4. The number of point machines used in the UK

#### 2.2.2.1 Fault modes of point machines

According to Hassankiadeh's project, 2458 point machine failures happened in the UK in 2009 [34]. The number of each failure for each mode is shown in Table 1.

Table 1. The number of point machine failures in the UK in 2009

| Failure mode | Number of failures | Percentage [%] |
|---|---|---|
| Obstruction | 986 | 40.1 |
| Dry slide chair | 441 | 17.9 |
| Cracked/broken | 233 | 9.5 |
| Voiding (ballast) | 190 | 7.7 |
| Out of adjustment | 137 | 5.6 |
| Contamination | 136 | 5.5 |
| Plastic deformation/lipping | 127 | 5.2 |
| Wear | 93 | 3.8 |
| Loosed/missing (nuts) | 89 | 3.6 |
| Others | 26 | 1.1 |
| Sum | 2458 | - |

According to Network Rail's fault reporting database, a junction experienced 8253 minutes of delay due to a failure of a point machine in 42 months. Failures with a delay time of more than 5 hours are listed in Table 2. These failures account for 76.7% of the total delay minutes [35].

Table 2. Point machine failures from Network Rail's database

| Failure mode | Number of failures | Percentage [%] |
|---|---|---|
| Slide chair dry/seized | 15 | 12.4 |
| Drive rod out of adjustment | 8 | 6.6 |
| Facing point lockout of adjustment | 7 | 5.8 |
| Detector rod out of adjustment | 4 | 3.3 |
| Slide chair obstructed/contaminated | 3 | 2.5 |

East Japan Railway also listed the number of failures in the Tokyo area from 1996 to 2005 [36]. The number of failures for each mode is shown in Table 3. The percentage of each failure mode is mentioned, but the number of some failure modes is not given.

Table 3. The number of point machine failures in Japan from 1996 to 2005

| Failure mode | Number of failures | Percentage [%] |
|---|---|---|
| Obstruction | 154 | 31 |
| Signal equipment failure | - | 18 |
| Unknown | 85 | 17 |
| Dry slide chair | 46 | 9 |
| Improper sleeper position | - | 8 |
| Switch rail misadjustment | - | 6 |
| Locking misadjustment | - | 4 |
| Insulation failure | - | 3 |
| Track abnormal position | - | 2 |
| Over-tightening bolts | - | 1 |
| Accessories failure | - | 1 |

According to the fault management system records of S&C service affecting failures on Network Rail infrastructure from 2013 to 2018, failures listed in the Table 4 account for 80% of the delay costs [37].

Table 4. Point machine failures from Network Rail's FMS from 2013 to 2018

| Failure mode (2013-2018) | Delay cost (million pounds) |
|---|---|
| Cracked cast crossing | 23.4 |
| Null | 12.0 |
| Obstruction | 8.8 |
| Relay contacts HR | 8.2 |
| Dry slide chair / Contamination | 7.3 |
| Relay failure | 6.9 |
| Power supply failure (fuse blown) | 6.4 |
| No cause found | 6.4 |
| Rail position sensor faiure | 6.1 |
| Wear / Damage of switch rail | 5.6 |
| Locking blades out of adjustment | 5.2 |

Data from the UK and Japan shown in Table 1, Table 2 and Table 3 suggest that obstruction is the most common failure mode, and a dry slide chair is also common. Adjustment errors, loose nuts, over-tightened bolts or nuts, and contamination also occur in certain numbers. Looking at more recent data as shown in Table 4, it can be inferred that these failures continue to occur, given their substantial impact on delay costs. In addition to these faults, voltage drops, which have a high probability of occurring, are simulated faults used in the experiment of this study.

#### 2.2.2.2 Acoustic monitoring methods for point machines

Hamadache *et al.* summarised the fault detection and diagnosis methods and reviewed condition monitoring papers for point machines in 2019 [38]. At the time of writing, there have been 11 peer-reviewed papers on condition monitoring of point machines published since their survey. The results of their survey and subsequent published papers are summarised in Table 5 and Figure 5.

Many studies have monitored current, load force, voltage, and position, but few have used acoustic signals. When the faults described in the previous section occur, changes occur in the driving force (load) of the point machine. This is the reason why many researchers have monitored the force. However, force sensors need to be mounted directly on the point machine, and a sensor failure could adversely affect the operation of the point machine. To avoid this, point machines for Japanese high-speed trains calculate the load force from current, voltage, and motor speed [39]. The reason many researchers have monitored voltage and current is the ease of data acquisition and their close relationship to the load force. Usually, point machines get their power from a nearby power supply unit. Since these units are installed outside the track, data can be easily obtained by installing measurement equipment here. Since the current

is closely related to the load force, it is possible to monitor the operation of the point machine to some extent by monitoring the current. However, there are many cases where the power supply unit and the point machine are far from each other due to the layout of the tracks and space limitations. In such cases, the voltage and current of the power supply unit may not always be the same as that supplied to the point machine, since most point machines are installed outdoors and there is a possibility of voltage drops and leakage currents. The acoustic sensor does not need to be directly attached to the machine, nor does it need to consider the effects of voltage drop or leakage current, since it measures acoustic data directly from the machine. Although there are few examples, several previous studies of point machines have been conducted on fault detection and diagnosis using acoustic signals.

Table 5. The parameters of the point machines monitored in previous studies

| Monitoring parameter | Previous research | Number of studies |
|---|---|---|
| Current | [40-75] | 36 |
| Force | [40, 41, 43, 45, 51, 52, 54, 56, 68-70, 75-79] | 16 |
| Voltage | [40, 41, 43, 44, 49, 52, 54, 55, 61, 69, 70, 73-75, 80, 81] | 16 |
| Displacement | [41, 43, 45, 51, 69, 70, 75, 80, 81] | 9 |
| Speed | [41, 45, 70, 77, 78, 82-84] | 8 |
| Temperature | [61, 85-88] | 5 |
| Acoustic signal | [18, 19, 89-91] | 5 |
| Torque | [81-84] | 4 |

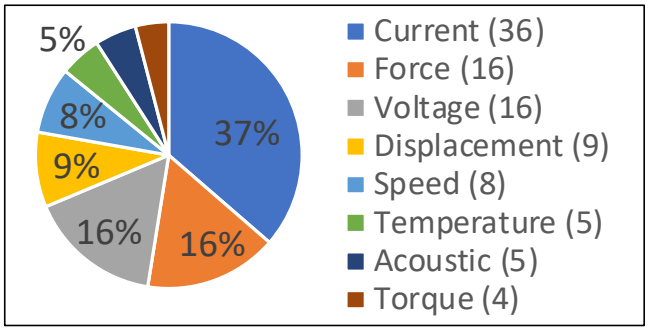


Figure 5. The parameters of the point machines monitored in previous studies

Lee *et al.* employed a bandpass filter from 300 Hz to 13 kHz for denoising, used MFCCs for feature extraction, and applied SVM to detect and diagnose failures from acoustic signals [18]. They collected 430 fault data (140 for 'ice obstruction', 140 for 'ballast obstruction', and 150 for 'slackened nut') and 150 normal data. The data were randomly split in half, with one half used as the training set and the other as the validation set. The length of each piece of data was not mentioned, but the waveform of the data seems to be about 5.5 seconds. The data were divided into 60 frames, and 12 MFCCs were calculated from each frame. These were classified using a multi-layer SVM, which diagnosed faults with 97% accuracy.

The MFCC is a weighted feature that considers the frequency perception characteristics of human hearing, and it is employed in the field of speech recognition and has been used in a wide variety of fields. It has the advantages of low computational cost, high discrimination capability, and good performance against noise. It is extensively used for automatic speech recognition and speech analysis due to these advantages [92-96]. It is also used for engine failure diagnosis [97], early classification of bearing failures [98], and quality assurance of voice signalling devices [99]. MFCCs are useful for feature extraction because they provide both time and frequency information. They also enable the handling of dynamic features as they extract both linear and non-linear properties of the signal. Unlike that of rotating machinery, the operating sound of STME is not steady, and if something goes wrong, there may be a gradual change in the intensity, length, and frequency of the sound. In such cases, MFCCs may perform very well as they capture minute changes in the characteristics of sounds.

SVM is a supervised machine learning method for pattern identification based on Vapnik's statistical learning theory [100]. It can be used for both classification and regression, but it is mostly used for classification tasks. It is a fast and reliable classification algorithm and

is expected to perform well with a small amount of data. In recent years, artificial neural networks (ANNs) have also attracted attention for their high accuracy. However, ANNs require a large amount of data to predict the response accurately and need a lot of time and computational resources to adjust the parameters, so SVM is more effective when the amount of data is small [101]. Santos *et al.* [101] compared SVMs and ANN to find the best classification method for wind turbine failure diagnosis and found that the linear kernel SVM is superior to other kernels and ANN in terms of accuracy, training and tuning times; 6551 pieces of data were used to check the performance and all classification methods had a high accuracy of over 96.8%. Considering only the accuracy of classification, both SVM and ANN were very useful, but when tuning time and training time were considered, it was concluded that SVM with a linear kernel was clearly the most suitable method for this case. The tuning time of SVM with linear kernels was less than half that of other SVMs, and the training time indicated at least 20% better performance. Comparing the performance of ANN and SVM, the tuning time of linear SVM was more than 100 times faster than that of ANN. Furthermore, ANN's parameter adjustments also required finding the optimal number of hidden layers, so the actual tuning time would be even longer. Therefore, the computational cost of SVM is small and the number of parameters that need to be optimised is small. It is also known to have a high classification accuracy for large dimensional data and is used for failure detection in various industrial equipment.

Although the degree of nut looseness in Lee *et al.*'s experiment [18] is not stated, the combination of MFCCs and SVM may be able to detect slight changes in STME operation because it can detect the looseness of nuts. It would be meaningful to investigate how much looseness change can be detected by this combination.

Sun *et al.* and Cao *et al.* conducted experiments using a Chinese point machine to verify the effectiveness of the acoustic monitoring method. They simulated nine types of failures: 1. no load, 2. indication circuit error due to poor contact, 3. large resistance during the switching process, 4. obstacles that are too large to finish the switching process, 5. gears meshing loosely in the retarder, 6. gear teeth pitting resulting from an uneven mesh surface (level 1), 7. gear teeth pitting resulting from an uneven mesh surface (level 2), 8. gears meshing tightly in the retarder (level 1), 9. gears meshing tightly in the retarder (level 2). Sun *et al.* used ten time-domain and three frequency-domain statistical parameters as features to detect failure [89]. They applied binary particle swarm optimisation (BPSO) to select optimal features, and 13 features were reduced to 3 to 4. One-against-one SVM was used to detect the failure and found that accuracy was over 99%. They also proposed a method that combines empirical mode decomposition (EMD), multi-scale fractional permutation entropy (MFPE), and particle swarm optimisation support vector machines (PSO-SVM). They used EMD to reduce the noise and calculated MFPE. MFPE is a new feature they proposed that solves the problem of fractional permutation entropy without considering the values of the time series. A One-Nearest Neighbour classifier, Random Forest, and Naive Bayesian classifier (NB) were used as comparators to demonstrate the superiority of PSO-SVM. PSO-SVM was the most accurate of all methods, with an accuracy of over 99%. Cao *et al.* used Wavelet Packet Decomposition Entropy (WPDE), statistical time-domain and frequency-domain parameters as features to diagnose failure [19]. They applied EMD to get intrinsic mode functions (IMFs) from acoustic data. Time-domain parameters, frequency-domain parameters and WPDE were calculated from each IMF. They used ReliefF and BPSO to select optimal features from them; 330 features were reduced to 18 to 37. They compared accuracy using SVM, NB, k-nearest neighbour (KNN),

linear discriminant analysis (LDA), and decision tree with the CART algorithm and found that all methods except LDA and CART achieved an accuracy of more than 90%.

Among their methods, features that use WPDE seem to be effective. Wavelet analysis decomposes a signal into shifted and scaled versions of wavelets as Fourier analysis decomposes it into sine waves. WT can be broadly classified into two types: continuous wavelet transforms (CWT) and discrete wavelet transforms (DWT). CWT is suitable for analysing slowly changing behaviour and transient behaviour but has the disadvantage of being computationally time-consuming. DWT discretises the scale more coarsely than does CWT and can be used for compression and denoising while preserving important features of the data [102]. However, the frequency resolution is not enough for practical problems, especially in a high-frequency range, and insufficient treatment of the high frequency of bearing faults has been reported [103]. Wavelet packet decomposition improves on the time–frequency resolution of DWT, has sufficient frequency resolution, and is computationally more efficient than CWT. Wavelet packet decomposition is a signal processing technique that breaks down a signal into a tree structure of wavelet packets, each representing a unique combination of time and frequency information, by recursively decomposing the signal into frequency sub-bands and analysing each sub-band using WT. During the wavelet packet decomposition, wavelet packet coefficients are generated, which represent the signal in each sub-band of the decomposition. However, due to the large number of coefficients, WPDE is used instead of coefficients, as it can provide useful information on signal complexity and can detect changes that may indicate a fault. The use of WDPE reduces the input data dimensionality, making it more manageable for processing and analysis.

Analysing the same experimental data with both MFCC and WPDE will show which is best for fault classification using acoustic data.

It has been shown that high accuracy can be obtained using several classifiers. Among these methods, KNN has the advantage of a short computation time. KNN is a supervised classification method which can predict unknown data by calculating the distance between the training data and unknown ones. The unknown data are categorised to their majority class among the nearest k neighbours. As with the comparison of feature extraction methods, the best classifier can be found by using multiple classifiers.

Unlike that of rotating machinery, the motion of a point machine is not constant or periodic, so previous studies have used time-varying components such as MFCC and WPDE. Their results show that it is possible to diagnose failures in a point machine by acoustic signals, but these faults seem to be serious ones. As described in section 2.2.2, the point machine is adjusted so that if a gap of 3.5 mm or more is created between the switch rail and the stock rail due to a large obstruction or loose nut, the detector rod detects it, and an alarm is triggered. In the event of a contact failure in the internal circuit, the controller will trigger the alarm because the switching process completion signal has not been received. Although the severity of the faults was not clearly described in Lee *et al.*'s experiment (MFCC and SVM) [18], the photographs show that the size of the obstruction seems to be large enough to be detected by the detector rod. However, the ability to detect the difference between ice and ballast is likely to be useful for fault classification. There is no detailed description of the loosened nuts either; it would be worthwhile to verify how much looseness can be detected by this method. Since Sun *et al.*'s and Cao *et al.*'s methods can detect no-load and increased resistance, they may be able to detect changes in the load on the machine, such as the drying of the slide chairs.

There is little benefit in diagnosing failures using acoustic methods if they can be diagnosed by elements of the system itself, such as the detector rod or the controller signal. It is also of little use for failures that are unlikely to occur in practice, such as gear failures. If faults with a high probability of occurring, described in section 2.2.2.1, can be diagnosed from the initial state, this would be a useful condition monitoring method. It is significant to validate some of their research methods, as they are likely to be effective against initial faults of the point machine. In this study, initial faults that are not detectable by the detector rod or the controller signal will be made and it will be verified how well they can be detected by the methods in the previous studies. In the case study section, MFCC and WPDE are used as features, and SVM and KNN are used as classifiers.

### 2.2.3 Contactors

Contactors and circuit breakers are one of the types of STME. Contactors are electric power devices that open and close the circuit when there is no current flowing or when the rated current is flowing. However, these devices alone do not cut off an accidental current more significant than the rated current in the case of a short circuit or earth fault. Unlike a circuit breaker, they cannot cut off an accidental current, but are highly durable against opening and closing operations. Both the contactor and circuit breaker have a moving contact (electrode), which engages with or detaches from the fixed contact (electrode) to connect or disconnect the circuit. The structure of a contactor is shown in Figure 6. Both mechanical structures are similar, but a circuit breaker has a mechanism to extinguish the arc and can cut off an accidental current. The moving parts are moved very quickly using the force of solenoid coils or springs.

These machines are a type of STME, like point machines, but they differ from point machines in terms of operating speed. These machines operate very quickly, in less than a

second, whereas point machines move slowly, taking several seconds. Because of the similarity in motion but the difference in speed, the two types of machines will be used as case studies in this research. A point machine as a slow STME and a contactor as a fast STME are used in the experiments in this study.

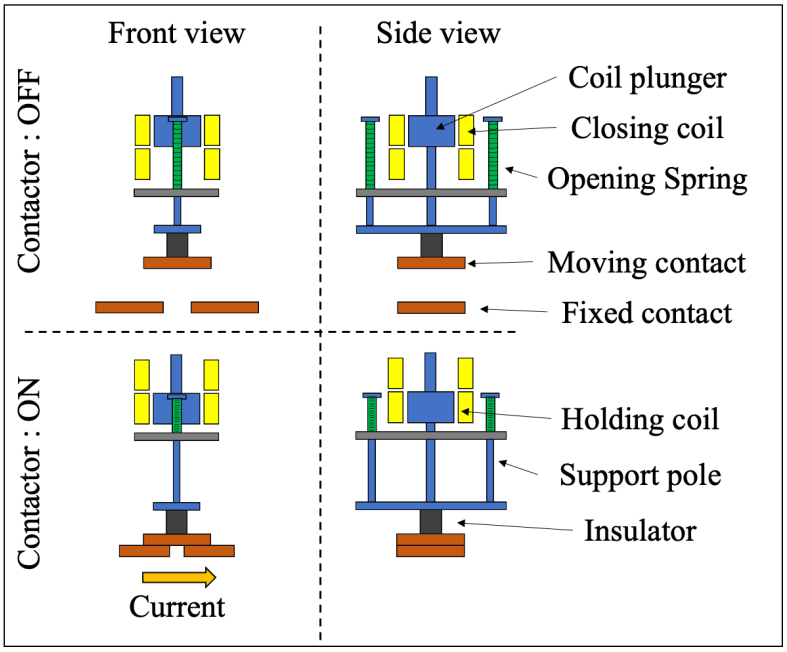


Figure 6. The structure of a contactor

### 2.2.3.1 Fault modes of contactors

Contactors are widely used where circuits are frequently switched on and off, such as in blast furnaces in steel mills, power factor correction capacitors in high-voltage distribution networks, and high-speed railways. In the field of railways, they are used in the changeover section of Japanese bullet trains and the opening and closing of the propulsion coils of Maglev trains [104-106]. A changeover section is a section that separates different power systems. In Europe, voltage is not applied here, and it is called a neutral section. In a Japanese high-speed railway, this section is connected to one of the next sections by a contactor, and voltage is

always applied. This eliminates the need for the train to coast while passing through the section. When the train completely enters the section, the contactors are operated, and the power system is switched quickly. Therefore, the contactors are operated every time a train passes [106]. Due to the high frequency of operation, mechanical failures are the most frequent faults. An international study of more than 70,000 circuit breakers in use in 22 countries has shown that 54.4% of severe failures and 49.3% of minor failures are due to mechanical causes [107]. Another study of more than 281,000 circuit breakers in use in 83 countries has shown that 43.5% of failures are related to mechanical problems [108]. Unlike the failures of the point machine described in section 2.2.2.1, detailed information on how many failures of what type have occurred is rarely published in the case of electrical power equipment such as contactors and circuit breakers. However, as mechanical failures account for about half of the failures, damaged parts, improper parts installation and obstruction are considered in this study. In addition to these faults, a lack of grease and spring weakening, which are expected to be more likely to occur, are also considered.

#### 2.2.3.2 Condition monitoring methods for contactors

A wide range of research has been carried out on condition monitoring of circuit breakers and contactors, largely utilising voltage, current, and vibration analysis techniques [109-116]. These approaches, however, require direct access to the monitored systems, which presents a safety risk, and the nature of the environment means that the risk of sensor failures is also increased. For contactors and circuit breakers, little previous research using acoustic signals have been carried out. On the other hand, vibration analysis for circuit breakers has been widely studied.

Hou *et al.* proposed a fault diagnosis method for a 12 kV circuit breaker [117]. The method calculates the WPDE of the vibration and acoustic signals of the circuit breaker and SVM is used for classification. In their work, they obtained 30 normal data and two fault data (insufficient lubrication of the crank arm, mechanism falling off in moving). Three data from each state were used as training data, and the remaining 21 data were used for validation. The results showed that the combination of vibration and acoustic data could diagnose faults with an accuracy of more than 90%. Although the classification accuracy of this study was high, only 10 data were obtained for each state, and the number of data needs to be increased to check the generality.

Huang *et al.* proposed a method to extract the EMD energy entropy from the vibration data of a 72.5 kV SF6 gas circuit breaker and to classify the faults using a multi-layered SVM [118]. In this verification, the following three faults were considered: 'loosening the base screw', 'invalid overtravel of the buffer spring', and 'time-delay vibration event caused by the inadequate lubrication for the operating mechanism'. Twenty-five data for each fault and 25 normal data were collected. To demonstrate the effectiveness of EMD and SVM, several features and classifiers were combined, and their accuracy was compared. The characteristics used were EMD and wavelet packet transform energy entropy, and the classifiers were SVM and a back-propagation network. The combination of EMD and SVM was shown to have a classification accuracy of 95% for all faults.

Huang *et al.* proposed a fault diagnosis method using variational mode decomposition (VMD) and a multi-layered SVM for circuit breaker vibration data [119]. They proposed a fault diagnosis method using VMD and multi-layered SVMs for three faults: 'jam fault of the iron core', 'looseness of the base', and 'insufficient lubrication of the connecting lever'. The

characteristic is extracted from the vibration of the circuit breaker. Twenty data of each fault and normal operation were used for training, and 20 data were used for validation. The results showed that the classification accuracy was 100% when using a multi-layered SVM. They also validated for the detection of the new faults that were not in the training data. When the classifier was not trained on the connecting lever's lubrication fault, the single SVM could not determine the fault. Still, the multi-layer SVM could detect and diagnose the fault as an unknown one with 100% accuracy. In actual condition monitoring, it may be difficult to obtain all types of fault data in advance, and unexpected faults may occur; therefore, the ability to detect and diagnose unknown faults can be very practical.

Yang *et al.* proposed a fault classification method for 12 kV circuit breakers [120]. The Morphological Correlation Coefficient was used to detect faults, and the ensemble empirical mode decomposition Hilbert marginal spectrum energy entropy (EEMD-HMSEE) obtained from vibration data was used to train the SVM for classification. Fifty normal data and 50 of each of the three simulated faults, 'Oil Damper Failure', 'Operating Mechanism Jamming', and 'Insulation Rod Loosening', were taken, and 60% were used for training and 40% for validation. In the validation, EMD-HMSEE-SVM using EMD as a feature and EEMD-HMSEE-KNN using KNN as a classifier were also validated, and it was found the proposed method's accuracy was the best for classification. Even when EEMD-HMSEE-KNN was used, the classification accuracy was over 96%. To validate the practicality of the proposed method, five data were obtained from three circuit breakers of the same type in actual use. Obtained data were analysed by the same method and the actual fault of oil damper failure was found by this analysis. The verification also found a fault that was not investigated in the laboratory (loosening of the transmission shaft). Furthermore, 20 data were obtained from each phase of different types of 252 kV circuit breakers and analysed by the same method. As a result, it was

found that there was an anomaly in one of the phases. The maintenance staff investigated and discovered that a layer of dirt accumulated on the surface of the filter in the oil cylinder had caused an abnormality in the brake of the operating mechanism. This abnormality disappeared after removing the dirt. These results showed that the proposed method is practical for several types of circuit breakers and effective for faults that are not in the training data.

Most of the studies analysed vibration, but Hou *et al.* also used WPDE from acoustic data for classification [117]. WPDE was also used by Cao *et al.* for point machine fault diagnosis [19], so it is worthwhile to use this method for contactors to confirm its performance. In addition to this, MFCC has also been shown to be effective in diagnosing failures in acoustic data of point machines [18], therefore, it is important to as certain this method is also effective for contactors. Although SVM has been widely used in studies of circuit breakers, KNN has also been used with high accuracy in previous studies, therefore, SVM and KNN are used for contactors.

## 2.3 Background noise level

In this study, experiments were carried out using a point machine and contactors to obtain data. The experiments were carried out in as quiet a place as possible, as the acoustic data were measured, but usually, point machines are installed outdoors and contactors both outdoors and indoors, so there might be noise such as environmental noise or another machine's operating sound in the data if considering a practical situation. Therefore, noise was artificially added to the acquired data in the analysis. This section describes the type and sound pressure level (SPL) of the added noise.

It is known that the frequency distribution of wind and rain noise is not constant and differs depending on the intensity [121-123]. The operating noises of other machines in buildings also vary widely, such as that of compressors or the humming noise of a transformer, so it is undesirable to add only specific noises for evaluation purposes. Hence, in this study, white noise was added to the acquired data to evaluate the effect of general noise on classification accuracy.

The SPL of the operating sound of other machines in a building varies depending on the type and its distance from the target, and most pneumatically operated machines have been replaced by electric ones, so little of the equipment installed in substations generates loud noise like compressors do [124-127]. If there is special equipment which is water-cooled, a pump may generate noise, but if the equipment is indoors, it is easier to deal with the noise compared with the noise of rain, such as by installing a sound barrier between the monitoring target and the noise source or moving the measuring microphone closer to the object to be monitored. Because point machines and contactors are installed near railway tracks, there may be a loud noise when trains pass nearby, but because they usually operate before or after trains pass, it is unlikely that the noise of trains passing would affect monitoring.

In this study, the SPL of the noise to be added is considered based on noise outside such as wind and rain. Although the sound of the wind is not negligible, it does not continue compared with the rain. In addition, since the STME is not always in motion and operates only when changing the course of a train or switching on and off power equipment, it is considered less likely that strong winds are blowing every time the STME operates. On the other hand, it keeps raining during the rainy season and may continue to rain when STME operates every

time. For these reasons, the sound of rain is likely to influence the acoustic measurement of the STME. Therefore, the SPL is considered based on the sound of rain.

According to the UK climate report, in 2020, there were 170 days with over 1 mm of rain per day and 40 with over 10 mm/day [128]. Rainfall is similar in Japan, which has high railway usage, with 107 days with more than 1 mm/day and 49 days with more than 10 mm/day [129]. Dubout recorded the volume intensity of natural rainfall on an unlined low-slope steel-trough roof deck, and the resulting SPL in a room beneath it [130]. According to his equation, the SPL of 10 mm/hour of rain falling is 72.1 dB, and that of 1 mm/hour is 54.8 dB. Steel roofs are known to produce louder rainfall noise, and it has been observed that different materials produce 18 dB less sound [131]. In fact, Griffin conducted a 20 mm/h artificial rainfall experiment using a 6 mm glass roof and showed the SPL to be about 50 dB [132]. Rain causes the roof shingles to vibrate and reverberate, resulting in loud noise indoors; on the other hand, outdoors, the rain is expected to be quieter than it is indoors because the impact of the rain is weakened by vegetation. If the SPL of rain outdoors is about 18 dB less than with a steel roof, it would be 54.1 dB at 10 mm/h and 36.8 dB at 1 mm/h. In this study, 55 dB is used for the SPL of heavy rain and 37 dB for the SPL of light rain. The noise of rain inside may be louder than outside, but buildings such as substations where contactors and circuit breakers are installed are constructed with reinforced concrete to protect the equipment from storms and earthquakes. In such buildings, the sound of rain can hardly be heard.

## 2.4 Proposed method

According to previous research, some fault diagnosis algorithms extract features from the acquired data and input them into a classifier. This method seems to be effective, but it is not clear which feature extraction methods and classifiers are best for STME. Although the

same algorithm is used in this study, multiple feature extraction techniques and classifiers are used to compare the accuracy. The features used in this study are MFCC and WPDE which are also used in the point machine. KNN and SVM, which have been frequently used in previous research, are used as classifiers.

Previous researchers tested with a single microphone, but this method does not reveal which position is best for acoustic monitoring. In this study, multiple microphones were placed at different locations to acquire data, and the same algorithm was used to verify which location data were best for analysis.

In this study, normal and simulated fault data were acquired from STME to train the fault diagnosis model. This method is called supervised learning, but it is necessary to verify the transferability of the model to use this method in industry. Transferability is the ability of a model trained by acquired data from one machine to diagnose faults in other machines. Since it is difficult to obtain simulated fault data from all the machines used in the industry, it is necessary to obtain simulated fault data from several machines, train the model with the data, and monitor all the machines with the model. The transferability of the model is essential to realise this. An image of the transferability of the model is shown in Figure 7.

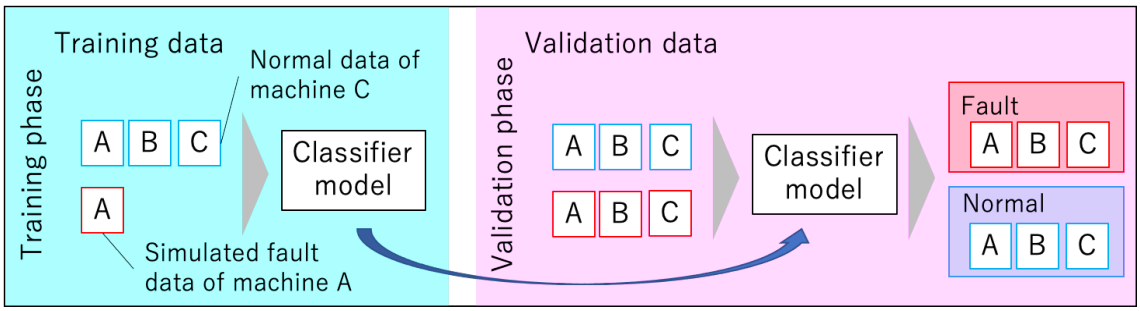


Figure 7. Transferability of the model

The microphone doesn't have to be in front of the machine because the sound is spread around the machine. If data from multiple machines could be collected from a single microphone, it would be possible to conduct condition monitoring at a low cost. In this study, a fixed microphone was installed in a building which has multiple contactors to acquire data from multiple machines from a fixed position and accuracy using these data was verified.

# CHAPTER 3 METHODOLOGY

## 3.1 Introduction

As discussed in Chapter 2, a fault diagnosis algorithm, which extracts features from the acquired data and inputs them into a classifier, seems to be effective for STME from previous studies, but it is not clear which features and classifiers are the best. Although the same algorithm is used in this study, multiple features and classifiers are used to compare the accuracy. This chapter explains the fault diagnosis algorithm, features, classifiers, and the evaluation method of the fault diagnosis model used in this study. The most suitable combination of features and classifiers for fault diagnosis of STME will be verified by combining features and classifiers which have been shown to be highly accurate in previous studies. The features used are the Mel Frequency Cepstral Coefficient (MFCC) and Wavelet Packet Decomposition Energy (WPDE), and the classifiers are the Support Vector Machine (SVM) and K-Nearest Neighbour (KNN).

The algorithm for detecting and diagnosing STME faults in this study is shown in Figure 8. The data from the experiments were split into two parts: one for training the fault classification model and one for validation. K-fold cross-validation was used and 90% of all the data was used for training and the remaining 10% for validation. Data were measured in as quiet a place as possible so that only acoustic data from the machine were measured. Therefore, the analysis algorithm provides a function to add additive white Gaussian noise so that the effect of noise on classification accuracy can be verified. It also includes a bandpass filter, which enables investigation of the frequency bands in acoustic data that are important for classification. Since the dimensionality of the raw data is large, features useful for classification were

extracted from the data and used to train the model. Diagnostic results were obtained by the model classifying the validation data. The data analysis was conducted using MATLAB R2021b.

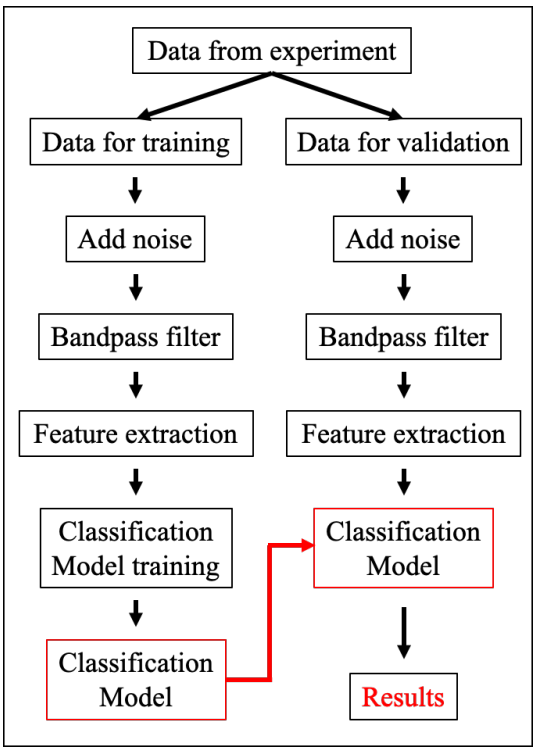


Figure 8. Algorithm for diagnosing STME faults

## 3.2 Features for classification

In recent years, with the spread of inexpensive sensors, the amount of data acquired by condition monitoring has become large. This requires methods to extract features and get a compact representation from large amounts of data. Acoustic data contain a lot of redundant information, and it takes a lot of computation to analyse it. It is possible to extract useful feature vectors from the data, which reduces the dimensionally of the data, shortens the analysis time, and reduces storage requirements. Reducing irrelevant and redundant information enables improves predictive performance and the ability to generalise models.

### 3.2.1 Mel Frequency Cepstral Coefficient (MFCC)

The MFCC is a weighted feature that considers the frequency perception characteristics of human hearing. It provides both time and frequency information and enables the handling of dynamic features as it extracts both linear and non-linear properties of the signal. It can be expected to perform very well in the diagnosis of STME faults as it captures minute changes in the characteristics of sounds. Veteran maintenance staff sometimes detect faults from the operating sound of machines, and it is conceivable that a difference in the MFCC occurs when a fault occurs. Although it is possible to analyse sounds outside the audible range of humans using special high-performance microphones, most of the operating sounds of point machines and contactors are within the audible range (below 20 kHz), as shown in the spectrogram in the figure in Chapter 1. In addition, the frequency range that can be acquired by most commercially available microphones is within the human audible range, and it is important to find effective features within the audible range in order to develop a fault detection method that can be realised at a low cost. Since the MFCC can capture the fine features of sound in the audible range, it is expected to be effective for fault detection. In fact, it has been used to detect failures of point machines. The process of calculating the MFCC is as follows. Firstly, acoustic data are processed frame by frame in the time domain, similar to the Short-Time Fourier Transform (STFT). Pre-emphasis filtering is applied to emphasise high-frequency components of the signal since the power of sound attenuates at higher frequencies. Window processing is applied to minimise discontinuities on both sides of the frame. This process lowers the high frequency on both sides and emphasises the main signals of the centre of the frame. The Fast Fourier Transform is used to convert signals from the time domain into the frequency domain and obtain the amplitude spectrum. The obtained amplitude spectrum is multiplied by the mel filter bank to obtain the mel frequency spectrum. This is called filter bank analysis, one of the

methods to reduce the dimensionality of the spectrum. It is based on the idea of aggregating the values of the frequency components over a certain range. The mel filter bank is a multiple overlapping triangular bandpass filter in which a frequency axis is taken on a mel scale [133] and a filter is allocated to it so that the width of the filter becomes equal. The mel scale, commonly used in speech recognition, is a perceptual frequency scale designed to replicate the non-linear characteristics of human hearing. It represents frequency bands perceived by the human ear as equally spaced. It exhibits logarithmic spacing, indicating that the frequency intervals between points on the scale increase as the frequency increases. The mel filter bank analysis converts the scale of the frequency from linear scale to mel scale. Then, the logarithm is taken from the results. Finally, the mel spectrum is converted to the time domain by a discrete cosine transform and the low-dimensional component of the cepstrum obtained is the MFCC.

The following parameters were used for the calculation of MFCC in this study. A frame length of 20–40 milliseconds (ms) with a 50% overlap is commonly used for speech and speaker recognition tasks. Shao *et al.* used a frame size of 20 ms and a 10 ms overlap for calculating MFCCs for speaker recognition [134]. Jurafsky *et al.* mentioned that the frame width is often set to 20–30 ms and the overlap length is around 50% to 75% of the frame width [135]. According to Rabiner *et al.*, the Hamming window is the most commonly used window function in speech processing [136]. In this study, the frame length was set to 30 ms and the overlap length was set to 20 ms, and the Hamming window was applied. If the dimensionality of the MFCC is increased, the more delicate components of the mel frequency spectral envelope can be represented; however, since the dimensionality of the feature vector increases making the calculation time long, an MFCC with fewer than 20 dimensions [18, 96, 137, 138] or an MFCC and logarithmic energy are often used [94]. The MFCC and its time-varying component delta MFCC, and the time-varying component of delta MFCC, delta delta MFCC, are

sometimes used [95, 138-140]. Nelwamondo *et al.* tested the accuracy of bearing failure detection by varying the number of MFCCs [98]. The results showed that if the number of MFCCs was less than 13, the detection rate increased as the number of MFCCs increased, although the detection rate remained almost the same when more than 13 MFCCs were used. It is common to use 13 MFCCs in the acoustic monitoring field, and the first coefficient is called the DC component which is related to the overall loudness of the signal. In this study, 12 of 13 coefficients, excluding the first coefficient, the DC component, were used as features to avoid classifying conditions by the loudness of the signal. The window frame length is 30 ms, the overlap length is 20 ms, and the number of MFCCs is set to 12, so if the data length is 1 second, 1176 features are calculated per datum.

### 3.2.2 Wavelet Packet Decomposition Energy (WPDE)

WPDE is a measure of signal complexity that is calculated using the Wavelet Packet Decomposition (WPD) technique. WPD decomposes a signal into sub-bands of different frequencies, and WPDE calculates the entropy of each sub-band to provide a multiscale measure of signal complexity that is sensitive to changes in signal structure. WPDE has been used as a feature in various applications, including speech recognition, image processing, and biomedical signal analysis. Therefore, WPDE is a valuable tool for analysing signals that may undergo changes in complexity over time, and its applications are widespread in the field of signal processing. By analysing the WPDE values, it is possible to detect the presence of faults in machinery. WPDE is an effective feature for condition monitoring because it is sensitive to changes in signal complexity that may be indicative of machinery faults. Since WPDE is also used for fault detection of point machines and circuit breakers, it is expected to be an effective feature for fault detection of STME [18, 117, 141].

Wavelet analysis decomposes a signal into shifted and scaled versions of wavelets whereas Fourier analysis decomposes it into sinusoids of specific frequencies. Wavelet transforms can be broadly classified into two types: continuous wavelet transforms (CWT) and discrete wavelet transforms (DWT). CWT is a time–frequency transform and is ideal for analysing non-stationary signals. A signal being non-stationary means that its frequency domain representation changes over time. CWT uses a variable-size window to tile the time–frequency plane whereas the STFT uses a fixed window for local frequency analysis. In signal processing, a wide window width is suitable for analysing the low frequency range and a narrow window is appropriate to find out fast changes in the signal. Therefore, CWT is ideal for the analysis of non-stationary phenomena such as transient behaviour, rapidly changing frequencies, and slowly changing behaviour, that contain frequency changes in the time domain, as it allows the window width to be varied whereas STFT requires several calculations for changing the window width appropriately. DWT discretises the scale more coarsely than does CWT; therefore, DWT is useful for signal and image compression and denoising while preserving important features. A potential drawback of using CWT is that it is computationally time-consuming. Although DWT can perform time–frequency decomposition of a signal, it is generally believed that the degree of frequency resolution in DWT is not sufficient for practical analysis. As a compromise between CWT-based and DWT-based methods, WPD is computationally efficient and has sufficient frequency resolution.

WPD offers better time–frequency resolution than does DWT for non-linear and non-stationary signal analysis, and it has been proven to perform better than DWT [142]. It extends the capabilities of DWT: both the approximate and detail coefficients are decomposed into new coefficients, whereas DWT does that only for the approximate one. The detail coefficients store information lost between two successive approximations, but DWT does not reanalyse the

detail coefficients. The advantage of WPD is that it allows for a more selective and fine-grained analysis of the signal, as the user can choose which sub-bands to retain and which to discard, based on the information content of the signal. WPD of a discrete-time signal *x(t)* is defined as:

$$C_{j,n}(k) = 2^{\frac{j}{2}} \int x(t)\, \psi_n\left(2^j t - k\right) dt$$

where *j* is the level of decomposition, *k* is the node index in the binary tree of wavelet packets, $\psi_j$ is the wavelet function, and $C_{j,n}(k)$ is the wavelet packet coefficient. Wavelet packet coefficients can represent the original signal in detail, but as input data for machine learning, they have the disadvantage of having a large number of features. In fault detection, certain frequency components may strongly appear in the signal at the time of failure. WPDE is used to capture this with a small number of features instead of wavelet packet coefficients. WPDE can be calculated by the following procedure. First, calculate the energy of each sub-band by

$$E_{j,n} = \sum\nolimits_k \left|C_{j,n}(k)\right|^2$$

Next, compute the total energy of WPD by

$$E_{total} = \sum\nolimits_n E_{j,n}$$

Relative energy can be expressed by

$$p_{j,n} = \frac{E_{j,n}}{E_{total}}$$

WPDE can be obtained by

$$H = -\sum p_{j,n} \ln p_{j,n}$$

In this study, WPDE is also used as a feature to compare it with MFCC. In the WPD of circuit breaker data, some previous researchers used Daubechies wavelets as mother wavelets with a decomposition level of 3 to the vibration data [117, 141]. While many studies have analysed circuit breaker vibration data, Hou *et al.* calculated WPDE from acoustic data as well. They applied level 3 decomposition WPD with Daubechies 2 as the mother wavelet and showed that insufficient lubrication and mechanism fall-off can be detected by using WPDE as a feature. Since those faults can happen in various STMEs, in this study, Daubechies 2 is used as the mother wavelet and the decomposition level is set to 3.

## 3.3 Classification

### 3.3.1 Support Vector Machine (SVM)

SVM is a widely used supervised machine learning algorithm based on Vapnik's statistical learning theory [100]. The basic idea of SVM is to find a hyperplane that maximally separates the data into different classes. SVM has many advantages over other classification algorithms, such as high accuracy, robustness to outliers, and the ability to handle high-dimensional data. SVM is a fast and reliable classification algorithm that requires optimisation of a small number of parameters. It is a popular method for the detection of failures in various types of industrial equipment. SVM is a powerful tool for binary classification and has been extended to handle multi-class classification. In multi-class classification, SVM can be implemented using either a one-vs-one or one-vs-all approach. In the one-vs-one approach, a binary classifier is trained for every pair of classes, and the final prediction is made by majority voting. In the one-vs-all approach, a binary classifier is trained for each class to distinguish it from all the other classes. SVM has been used for fault detection and classification of STMEs such as point machines and circuit breakers and has been shown to be able to classify them with

high accuracy. Although it can be expected to obtain good results, there is no previous research using SVM to classify initial faults based on acoustic measurement, so accuracy needs to be investigated.

SVM classifies *n*-dimensional data into *n* – 1-dimensional separating hyperplanes. The SVM theory is as follows: The hyperplane to classify *N* data can be expressed by the following equation.

$$W^T X_i + b = 0 \quad (i = 0,1,2, \dots N)$$

The data belonging to group 1, $G_1$, and the data belonging to group 2, $G_2$, satisfy the following equation.

$$W^T X_i + b > 0 \quad (X_i \in G_1)$$

$$W^T X_i + b < 0 \quad (X_i \in G_2)$$

Using the label function *t*, the above equation can be expressed as follows:

$$(W^T X_i + b) > 0 \quad (i = 0,1,2, \dots N)$$

$$t_i = \begin{cases} 1, & (t_1 \in G_1) \\ -1, & (t_2 \in G_2) \end{cases}$$

The distance between a point in *n*-dimensional space and a hyperplane can be expressed by the following equation.

$$d = \frac{|W^T X_i + b|}{\|w\|}$$

The condition of maximising the margin can be expressed by the following formula.

$$max_{w,b} M, \qquad \frac{t_i(W^T X_i + b)}{\|w\|} \geq M \quad (i = 0,1,2, \dots N)$$

In general, the hyperplane is invariant if both sides of the hyperplane equation are multiplied by any real number, so the condition for margin maximisation can be expressed as follows:

$$t_i(W^T X_i + b) \geq 1 \quad (i = 0,1,2, \dots N)$$

For data on the hyperplane, the equation $t_i(W^T X_i + b) = 1$ is satisfied, and the margin *M* can be expressed as $M = 1/\|w\|$. Therefore, the margin maximisation problem can be described by the following equation.

$$\begin{cases} \min\limits_{w} \dfrac{1}{2}\|w\|^2 \\ t_i(W^T X_i + b) \geq 1 \quad (i = 0,1,2, \dots N) \end{cases}$$

The kernel function in SVM maps the input data into a high-dimensional feature space, where a linear decision boundary can be used to separate the data into different classes. The choice of kernel function can have a significant impact on the classification performance of SVM, as different kernel functions are suited for different types of data. The linear kernel function is useful because it simplifies the decision boundary, making it easier to interpret and understand. This can be especially useful when the goal is to gain insights into the relationship between the input features and the output labels. When considering which features are useful for classification, simple boundaries may be helpful in understanding the distribution of the features. Therefore, a linear kernel is used in this study.

The Box Constraint is a hyperparameter in SVM that determines the degree to which misclassifications are allowed. It is a regularisation parameter that determines the trade-off between maximising the margin of the decision boundary and minimising the classification error on the training data. In SVM, the Box Constraint parameter controls the penalty for misclassifying training data and constrains the magnitude of the coefficients for the decision boundary. A higher Box Constraint value leads to a narrower margin and a more complex decision boundary allowing fewer misclassifications, while a lower value leads to a wider margin and a simpler decision boundary allowing more misclassifications. In practical applications, it is important to find a balance between the number of misclassifications and the complexity of the model. Without setting a Box Constraint, SVM may overfit the training data and fail to generalise well to unseen data. Thus, it is crucial to set an appropriate Box Constraint to achieve a good balance between model complexity and accuracy. A common practice is to set the Box Constraint to 1, which allows for some misclassifications while still keeping the margin reasonably large. This value is often used because it strikes a balance between overfitting and underfitting, and it is a widely accepted default value in many SVM

implementations. This is particularly useful when dealing with real-world datasets, where the data may contain noise or outliers. In this study, the Box Constraint is set to 1.

When performing multi-class classification, choosing between the one-vs-all and one-vs-one methods depends on several factors. One-vs-all builds one binary classifier for each class, treating all other classes as a single class, whereas one-vs-one trains one binary classifier for every pair of classes. While one-vs-all is more straightforward to implement and can handle large numbers of classes, it may suffer from imbalanced data, where some classes have few examples, and also from ambiguities between classes that are difficult to separate. On the other hand, one-vs-one directly models the interactions between each pair of classes, which can lead to higher accuracy than one-vs-all in some cases, especially when the data are imbalanced or the classes are overlapping. In this study, the one-vs-one method for multi-class classification was applied, as it offers several advantages over one-vs-all. Specifically, a dataset from a condition monitoring system might contain multiple classes that are not well balanced, with some fault classes having much fewer samples than normal or other common faults, and one-vs-all may struggle to achieve satisfactory results for these classes, as the model has to rely on a few examples only. On the other hand, one-vs-one can leverage the similarities and differences between classes more effectively, leading to better classification accuracy overall. Furthermore, the computational cost of one-vs-one is manageable by choosing only serious fault classes. Therefore, one-vs-one is expected to be a promising approach for our multi-class classification task.

### 3.3.2 K-Nearest Neighbour (KNN)

The KNN algorithm is very simple and has the advantage of shortening the learning time. It is a non-parametric machine learning algorithm that can be used for both binary and multi-class classification. KNN is based on the idea that similar data points should have similar labels. The algorithm works by comparing the distance between a new data point and the data points in the training set to find the *k* nearest neighbours. The predicted class of the new data point is determined by a voting scheme among the *k* nearest neighbours. It is also used for fault classification of point machines and circuit breakers so it is expected that this would also be effective for STME [19, 120]. KNN is also used and its accuracy is compared with SVM to validate which classifier is suitable for fault classification. The algorithm for KNN for multi-class fault classification is as follows:

First, given a training dataset and its corresponding class labels, and a test dataset, for each test data point, calculate the distance between the test data point and each data point in the training set. A commonly used distance metric is Euclidean distance, and it was used in this study. Select the *k* closest data points to the test data point based on the calculated distances. Determine the class of each of the *k* nearest neighbours and use a voting scheme to determine the predicted class label for the test data point. One common voting scheme is simple majority voting, where the predicted class label is the class label that appears most frequently among the *k* nearest neighbours. Reducing the number of *k* increases the likelihood of overlearning. In addition, when performing multi-class classification, it is preferable that *k* is larger than the number of classes because the number of training data around the test data is used for classification. The value of *k* was set at 10 in this study.

## 3.4 Validation

There are several evaluation metrics for machine learning, including Accuracy, Precision, Recall, F1 score, ROC curve, and AUC [143]. Accuracy is the percentage of correct results out of all predictions. It is the number of correct answers divided by the total number of data. Precision is the percentage of positive predictions that are positive. It is the number of true positives divided by the total number of data predicted to be positive. Recall is the ratio of predicted positives to actual positives. It is the number of true positives divided by the total number of actually positive data. The F1 score is a harmonic mean of Precision and Recall, with a higher score indicating better performance. The ROC curve plots the True Positive Rate (TPR) against the False Positive Rate (FPR) for different thresholds. It is a useful visualisation tool for comparing the performance of different models and selecting the optimal operating point. AUC is the area under the ROC curve. It summarises the overall performance of a binary classifier across all possible thresholds.

The failure of industrial equipment causes significant service impact and damage, so maintenance and replacement are performed before the equipment fails. Therefore, most of the condition monitoring data from industrial machinery are normal data, with only a small amount of failure data, resulting in an imbalanced dataset. When dealing with an imbalanced dataset, Accuracy, ROC curve, and AUC may not be appropriate evaluation metrics for machine learning models. This is because Accuracy does not take into account the imbalanced nature of the data, and may lead to high accuracy due to the model's ability to accurately predict the majority class while performing poorly on the minority class. Similarly, the ROC curve and AUC are based on TPR and FPR, which may be biased towards the majority class and may not provide an accurate assessment of the model's performance on the minority class. Precision, Recall, and F1 score are better suited for evaluating the performance of models on an

imbalanced dataset as they take into account both the TPR and FPR of the minority class. Additionally, Precision and Recall are especially useful for identifying models that have high precision in detecting the minority class. Therefore, when evaluating machine learning models on imbalanced datasets, it is important to carefully select appropriate evaluation metrics that accurately capture the model's performance on the minority class.

Precision, Recall, and the F1 scores are expressed by the following equation using True Positive (TP), False Negative (FN), and False Positive (FP). The relationship between TP, FN, FP, and True Negative (TN) is shown in Table 6 as a confusion matrix.

$$Precision = \frac{TP}{TP + FP} \tag{3}$$

$$Recall = \frac{TP}{TP + FN} \tag{3}$$

$$F1\ score = \frac{2TP}{2TP + FP + FN} \tag{4}$$

Table 6. Confusion matrix

| | Predicted fault | Predicted normal |
|---|---|---|
| Actual fault | TP | FN |
| Actual normal | FP | TN |

FP is the number of normal data diagnosed as a fault. FP means a diagnostic result is wrong but as the equipment is fine there is no risk of an accident, but the more FPs there are,

the less confidence the maintenance engineers have in the system. FN means that faults are missed, increasing the probability of accidents and this is known as a wrong-side failure in the railway field [144, 145]. The most important thing when considering condition monitoring of industrial machines is not to miss any faults as the damage caused by a failure is significant. TP and FN are more important than FP; therefore, in the condition monitoring of industrial machines, a fault detection model should be evaluated by Recall rather than Precision. However, if the models are evaluated only by Recall, a model that diagnoses all data positively will also be evaluated as having high performance, so in this research, Recall will be used for evaluation, and the F1 score also will be used to check the balance of the model.

## 3.5 Summary

This chapter explains the fault diagnosis algorithm, features, classifiers, and evaluation method of the fault diagnosis model used in this study. The algorithm used in this study is shown in Figure 8. Of the data acquired in the experiment, 90% of the total is used for training and 10% is used for validation by k-fold cross-validation. When evaluating the effect of noise, additive white Gaussian noise is added. Additionally, for investigation of the crucial frequency range in the analysis, a bandpass filter is employed to obtain data from the required range.

The MFCC and WPDE, which are features used in this study, and SVM and KNN, which are classifiers, have been previously explained in this chapter. In summary, the MFCC is calculated using the MATLAB mfcc function. For the calculation, a window frame length of 30 ms is employed with an overlap length of 20 ms, and a Hamming window is used. Twelve MFCCs are used, excluding the first coefficient which is the DC component. The WPDE is calculated using the modwpt function, Daubechies 2 is used as the mother wavelet, and the decomposition level is set to 3. For SVM classification, the templateSVM and fitcecoc

functions are used, and the Box Constraint is set to 1. For KNN classification, the fitcknn function with Euclidean distance is used and $k$ is set to 10.

Although these methods have been used in point machines and circuit breakers in previous research, their accuracy has been investigated only for serious failures or an insufficient amount of data have been verified. In this study, a sufficient amount of initial fault data is acquired to verify how accurately the combination of these techniques can diagnose faults. Accuracy is verified by Recall and F1 score. In the condition monitoring of industrial machinery, it is important not to miss a fault, because missing a fault causes a large amount of damage. Recall is a suitable metric to evaluate a model for how accurately it can diagnose faults. However, since a model that diagnoses all data as faults is also highly evaluated when evaluation is performed only by Recall, the balance of the model is also investigated using the F1 score.

In the next chapter, experiments on a point machine and contactors will be described. The features of data obtained from experiments will be extracted and classified by the method described here, and their accuracy will be compared.

# CHAPTER 4 EXPERIMENT WITH SLOW STME: POINT MACHINE

## 4.1 Introduction

To confirm the effectiveness of the proposed method, two types of STME were used to acquire data and investigate the diagnostic accuracy of the proposed method. As mentioned in Chapter 1, STME is categorised into two types: one is slowly operated and generates sound in the low-frequency range, such as point machines or doors, and the other is operated at high speed and generates sound in the high-frequency range, such as contactors or circuit breakers. To investigate whether the proposed method is effective for general STME, this study uses both types of STME, slow STME and fast STME. This chapter describes the details of the experiment and results for slow STME. A point machine is used as the first experimental target. A point machine is a type of STME that moves a set of points to change the route of a train. It uses motor or hydraulic power to move the rails over a period of several seconds. The sound of the movement is long and mostly in the low-frequency range. In the experiment, normal and simulated fault data were obtained. Classification accuracy was compared to determine the optimal feature extraction and classification method for fault diagnosis. Since the data were acquired indoors and the effect of background noise is small, white noise was added to the acquired data to simulate an outdoor environment to investigate the effect on the classification accuracy.

## 4.2 Experiment using a point machine

To investigate the accuracy of mechanical fault diagnosis by using acoustic data, tests were conducted using an HW point machine. The structure of the HW point machine is shown in Figure 9. The point machine contains the motor and gears, which move the drive rod, and the motor side nut or the undriven side nut attached to the drive rod pushes or pulls the switch rails. When the switching process is completed, the locking mechanism inside the point machine operates and the switch rail is locked. When switching to another direction, the switch rail is first unlocked, and then the drive rod starts to move. In this experiment, the direction in which the switch rail moves away from the point machine was defined as Normal to Reverse (NR), and the direction in which the switch rail approaches the point machine was defined as Reverse to Normal (RN), as shown in Figure 9.

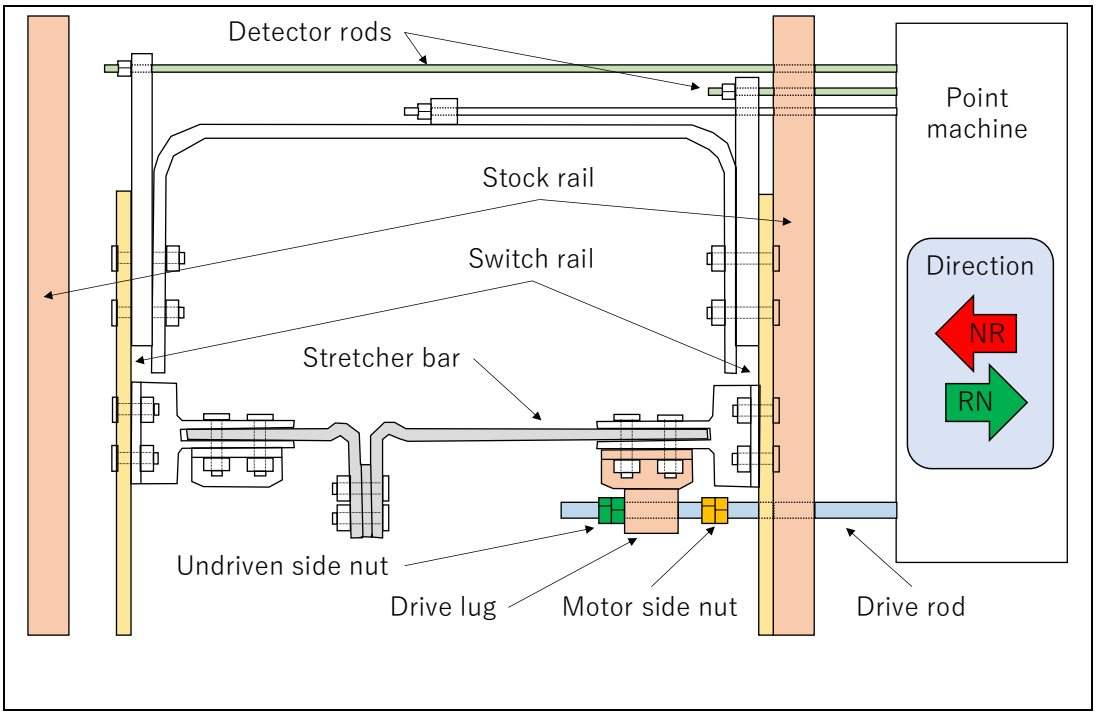


Figure 9. Structure of HW point machine

Acoustic data were collected from the HW point machine in a laboratory at the University of Birmingham. Two microphones were used for data acquisition, one (mic point) placed next to the point machine and the other (mic track) placed in the track. Microphone positions are shown in Figure 10. Table 7 shows the measuring equipment used in this test. As described in Chapter 2, obstruction is the most common failure of point machines, and a dry slide chair is also common. Contamination and adjustment errors such as loose nuts and over-tightened bolts or nuts also occur in certain numbers [34-36]. In addition to these faults, voltage drops have a high probability of occurring. Therefore, obstruction, dry slide chair, contamination, loose nut, over-tightened nut, and voltage drop were used as simulated faults in the experiment of this study.

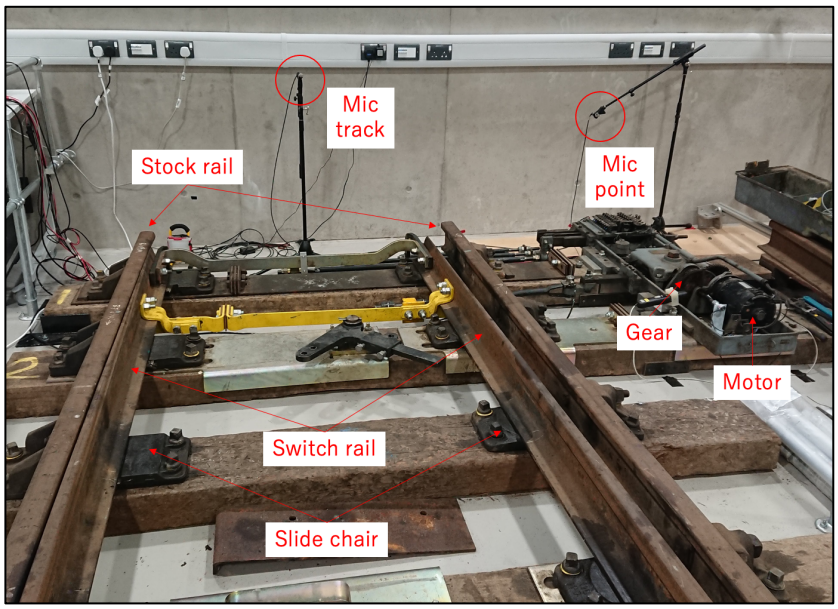


Figure 10. Location of microphones

Table 7. Measuring equipment

| Measuring equipment | Model | Range |
|---|---|---|
| Microphone | GRAS 46E | 3.15 Hz ~ 20 kHz |
| Current sensor | Current transducer HTR 50 | −50 A ~ 50 A |
| Force sensor | Rail pin | −17 kN ~ 17 kN |
| Displacement sensor | SLS 190 | 0 ~ 250 mm |

The point machine was operated every 10 seconds and the data were acquired. Each piece of data was collected for 4.5 seconds from 0.5 seconds before the current supply to the motor exceeded 10 A. Data were obtained for each direction ‘NR’ and ‘RN’. The test schedule is shown in Table 8.

Table 8. Test schedule

| Data type | Number of data NR | Number of data RN |
|---|---|---|
| Contamination | 125 | 129 |
| Dry slide chair | 495 | 499 |
| Normal | 849 | 851 |
| Obstruction (motor side) | 167 | 167 |
| Obstruction (undriven side) | 317 | 313 |
| Voltage drop | 87 | 88 |
| Loose nut (motor side) | 144 | 147 |
| Loose nut (undriven side) | 73 | 74 |
| Over-tightened nut (motor side) | 137 | 133 |
| Over-tightened nut (undriven side) | 240 | 242 |

Since the point machine had not been used for many years, rust and dust had stuck on the slide chair. A slide chair is a component of a rail track and is placed underneath the rail, providing a flat surface for the rail to sit on and distributing the weight of the train more evenly. The position of the slide chair is shown in Figure 10. It also helps the movement of the switch rail as grease is applied to it. Some point machines used in industry are stained by iron powder from rails and rusted, and this condition is called contamination. In the experiment, this

condition was defined as a contamination and data were obtained under this condition. After data acquisition, all slide chairs were cleaned up and dried to make the condition of dry slide chairs. A dry slide chair is a condition in which the grease on the slide chair is washed away by rain, and the switch rail movement becomes impaired. In this condition, the resistance of the switch rail and the slide chair increases and may cause failure. In this study, the condition after cleaning the slide chair was defined as dry slide chair and data were collected. After that, grease was applied, and normal data were obtained. Each condition of the slide chair is shown in Figure 11.

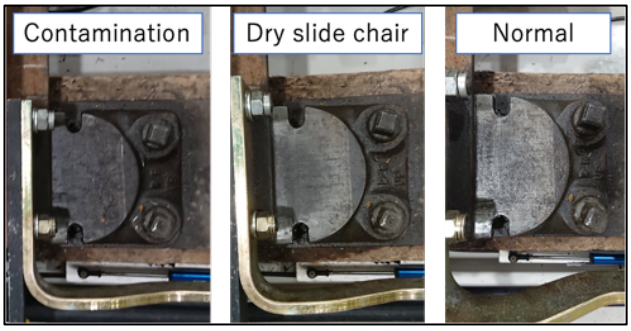


Figure 11. Condition of the slide chair

To simulate obstruction, thin metal plates were applied to make a gap between the switch rail and the stock rail. The gap made by a metal plate is shown in Figure 12. Since many point machines are installed near train stations, rubbish falls from the platform onto the tracks and sometimes gets stuck between the rails. In rural areas of Japan, turtles sometimes wander onto the track from a level crossing, move along to the point machine, and get caught between the rails of the point machine [146]. In the case of a large obstruction, it is immediately removed by maintenance staff because an alarm is triggered due to incompletion of the point machine operation; however, in the case of a small obstruction or one crushed by the force of the point machine, there is no interference with the operation and there may be a delay in noticing the

presence of the obstruction. If it is a small obstruction, the point machine tries to move the switch rail completely and keeps applying the force, which will continue to apply greater force than designed and may cause a failure. In this study, the gap was set to less than 3.5 mm as detector rods can detect gaps over 3.5 mm [20]. The gap was made on both the motor side and the undriven side. The case with obstruction on the point machine side is called 'obstruction motor side', and the case on the opposite side is called 'obstruction undriven side' in this study.

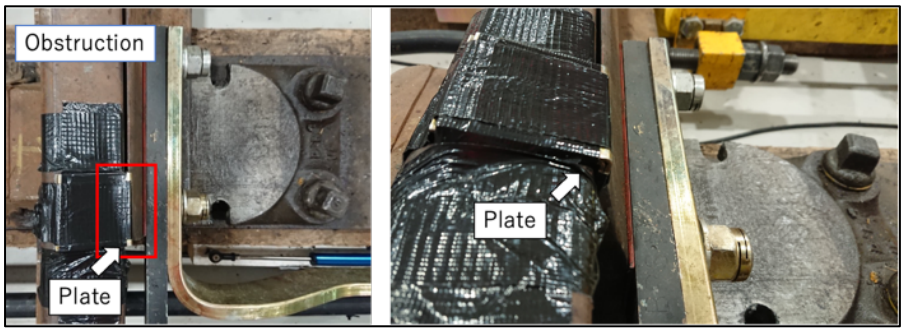


Figure 12. Obstructions between switch rail and stock rail

To simulate a voltage drop, the voltage supplied to the point machine was reduced from the standard voltage of 110 V to 105 or 100 V. There are many cases where the power supply unit and the point machine are far from each other due to the layout of the tracks and space limitations. In such cases, the voltage and current of the power supply unit may not always be the same as that supplied to the point machine, since most point machines are installed outdoors and there is a possibility of voltage drops and leakage currents. Since the power supply unit is equipped with a voltage sensor, the voltage at the unit can be measured, but if a leakage occurs in the cable between the unit and the point machine, the unit's sensor cannot detect a voltage drop. If the acoustic data of the point machine are changed by a voltage drop and it can be detected, the voltage sensor of the unit can be reduced.

To simulate loose nuts and over-tightened nuts, the nuts attached to the drive rod were loosened and over-tightened. The nuts adjusted in this experiment were the motor side nut and the undriven side nut shown in Figure 9. Loosening the nuts of a point machine can cause serious accidents such as derailment [3]. Nuts that are not properly tightened are known to loosen more quickly than those that are properly tightened. A loose nut sometimes happens because nut tightening requires a particular technique [147]. Past railway accident investigations have confirmed that some maintenance staff were not adequately trained or familiar with the correct procedure for tightening nuts [3]. Therefore, it is regularly checked by maintenance staff, but because there are many opportunities for adjustment, it is possible that inappropriate maintenance such as loosening or excessive tightening may occur when checks are performed by staff with inappropriate knowledge. The case with the nut on the motor side loosened is called ‘loose nut motor side’, and the case with the nut on the undriven side loosened is called ‘loose nut undriven side’. Over-tightening cases are called in the same way ‘over-tightened motor side’ and ‘over-tightened undriven side’.

Example time-domain representations and power spectrograms for both normal and fault data are shown in Figure 13. Comparing the signals, no clear difference can be seen, but the dry slide chair produces low-frequency sound after 4 seconds. Also, the operation time is slightly longer for the voltage drop and over-tightened nut. Low-frequency sound is generated after around 3.5 seconds in normal data, but it cannot be confirmed in over-tightened nuts. No observable differences can be seen clearly in the other fault data; therefore, it needs investigation using a feature extraction method to identify differences.

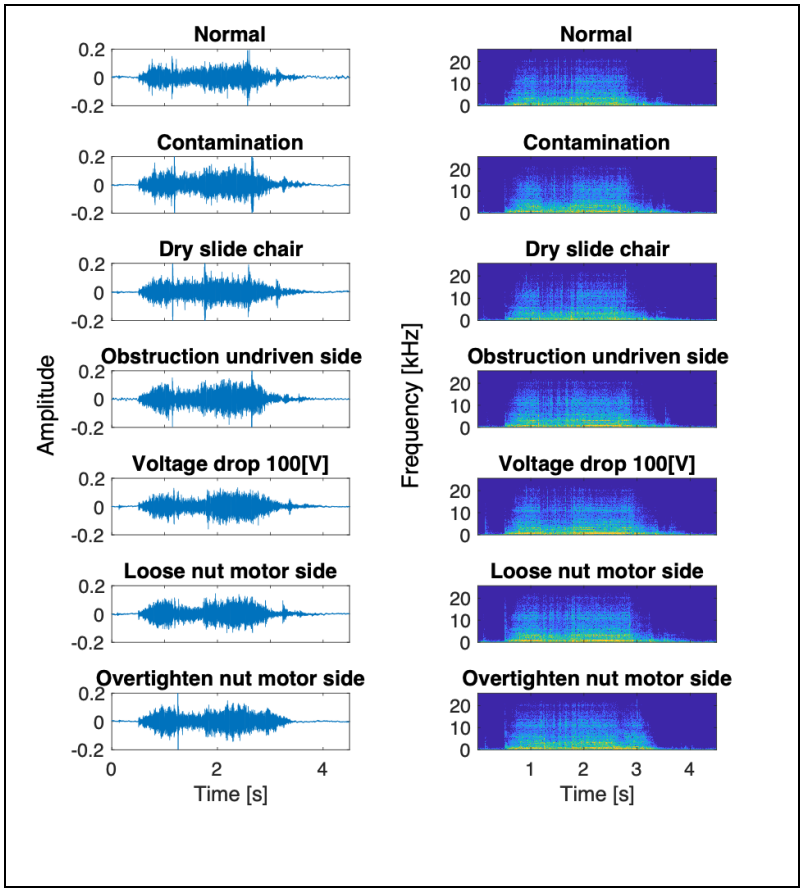


Figure 13. Spectrograms for each condition of signal and power (NR direction)

## 4.3 Classification accuracy

Accuracy was evaluated by Recall and F1 score metrics as described in Chapter 3. MFCC and WPDE were used as features and SVM and KNN were used as classifiers. Details of these methods are also described in Chapter 3. Table 9 shows the Recall and F1 score for the classification of all faults by each feature extraction method and classifier. When MFCC was used as the feature, it was found that both Recall and F1 scores were more than 99% regardless of the classifier. On the other hand, the use of WPDE was found to be impractical due to a considerable drop in accuracy.

Table 9. Recall of the fault diagnosis

| Feature extraction | Classifier | Mic | NR | | RN | |
|---|---|---|---|---|---|---|
| | | | Recall [%] | F1 score [%] | Recall [%] | F1 score [%] |
| MFCC | SVM | Point | 99.6 | 99.8 | 99.2 | 99.6 |
| | | Track | 99.3 | 99.7 | 98.9 | 99.4 |
| | KNN | Point | 99.6 | 99.6 | 99.6 | 99.8 |
| | | Track | 99.6 | 99.7 | 99.4 | 99.7 |
| WPDE | SVM | Point | 49.0 | 61.5 | 42.1 | 57.8 |
| | | Track | 16.7 | 27.2 | 30.4 | 45.5 |
| | KNN | Point | 79.9 | 82.7 | 77.1 | 81.8 |
| | | Track | 63.5 | 69.1 | 67.0 | 74.8 |

### 4.3.1 Classification accuracy using MFCC

When MFCC was used as the feature, NR data seemed to be diagnosed slightly more accurately than RN data. To investigate the results further, confusion matrices were created , as shown in Figure 14 and Figure 15. Each figure has four matrices, which are the results of classifying the data in the NR direction obtained from ‘mic point’, the data in the RN direction obtained from mic point, the data in the NR direction obtained from ‘mic track’, and the data in the RN direction obtained from mic track. The top two matrices are for data acquired from the mic point and the bottom two are data from the mic track. The two on the left are for data

in the NR direction, and the ones on the right are for data in the RN direction. Figure 14 shows the classification of these four sets of data by SVM and Figure 15 shows the result using KNN as a classifier. From all the figures, it can be seen that most faults were diagnosed accurately as well as detected. However, some faults appear to have been diagnosed as normal, especially when SVM was used as the classifier. These are called False Negatives (FN), and when RN data are used, there seem to be slightly more FN, reducing the Recall. When using KNN, the number of FN is smaller than when using SVM, but the number of False Positives (FP) is larger than that for SVM.

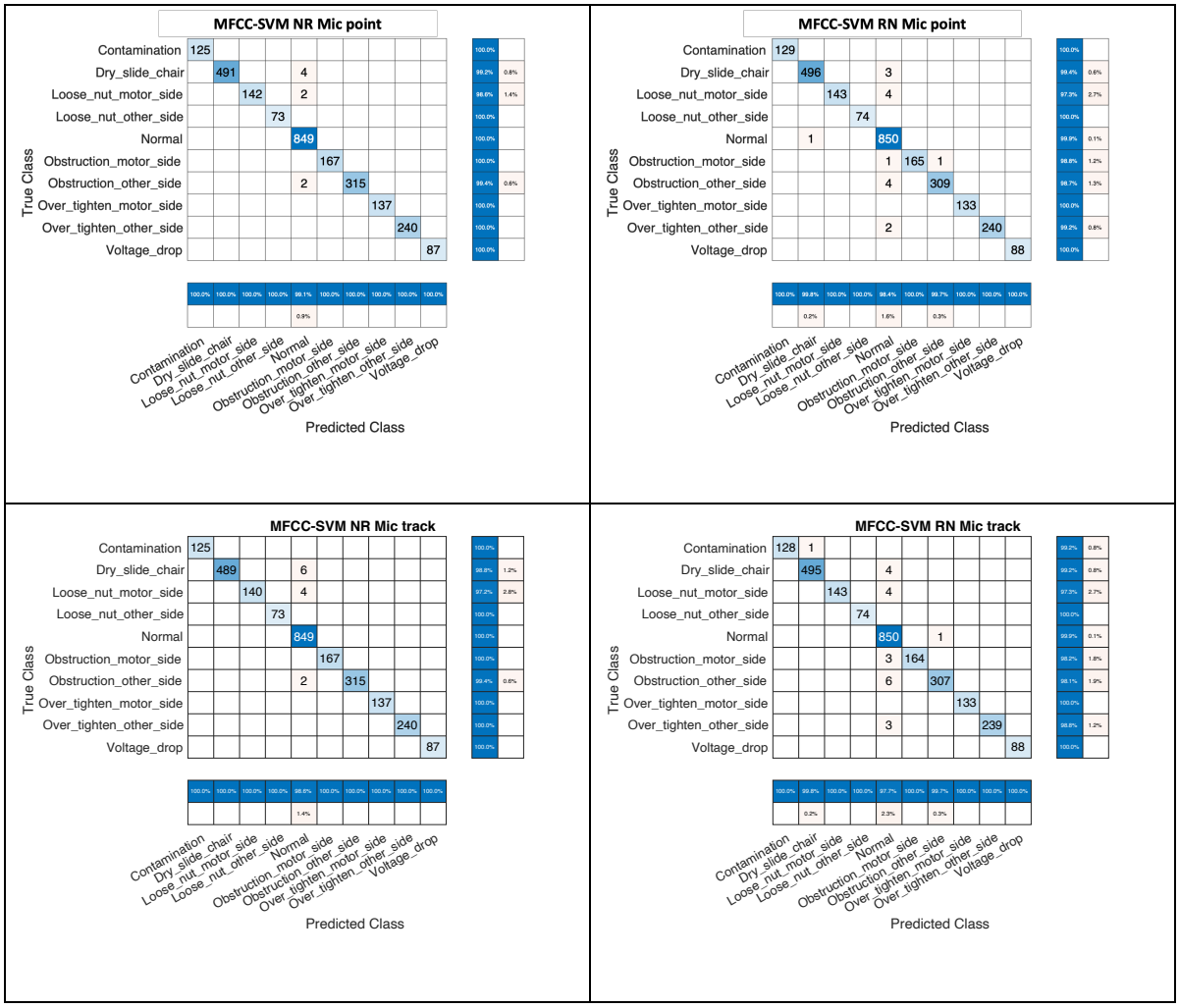


Figure 14. Diagnostic results by MFCC-SVM

In the case of ‘obstruction motor side’, ‘obstruction undriven side’, and ‘over-tightening undriven side’, the results of the NR data are better than those of the RN for both classifiers. As for ‘obstruction motor side’, since the obstruction was placed on the motor side, it was thought that the RN direction operation would produce a louder collision sound of the rail and the object, and would be able to classify the fault more accurately; however, the NR data were more accurately diagnosed. The accuracy of both NR data of ‘obstruction motor side’ and RN data of ‘obstruction undriven side’, where the switch rail did not hit the object, were expected to be low as there wasn’t a collision sound in the data; however, both faults can be diagnosed with high accuracy. This suggests that there is a more important factor to diagnose

an ‘obstruction’ rather than collision sound. It is probable that the initial position of the rail changes due to the presence of the obstruction, which changes the sound of locking and unlocking the switch rail. Figure 16 shows the amplitude of operating sound of ‘obstruction motor side’ for each direction. The NR data from both microphones turned out to be louder than those of RN side, especially for the unlocking phase. The NR data of the mic point is over 17% louder (greater SPL) than the RN, and the unlocking phase of the data is over 30% louder. The SPL of the unlocking phase of NR was higher than that of RN, and it is thought that the higher accuracy could be obtained because the clear difference of features was captured. The SPL seems to be a factor in the higher accuracy of the analysis result of ‘mic point’ than that of ‘mic track’. The mic point data is over 90% louder than mic track data, and it is considered that the difference in the characteristics became clear.

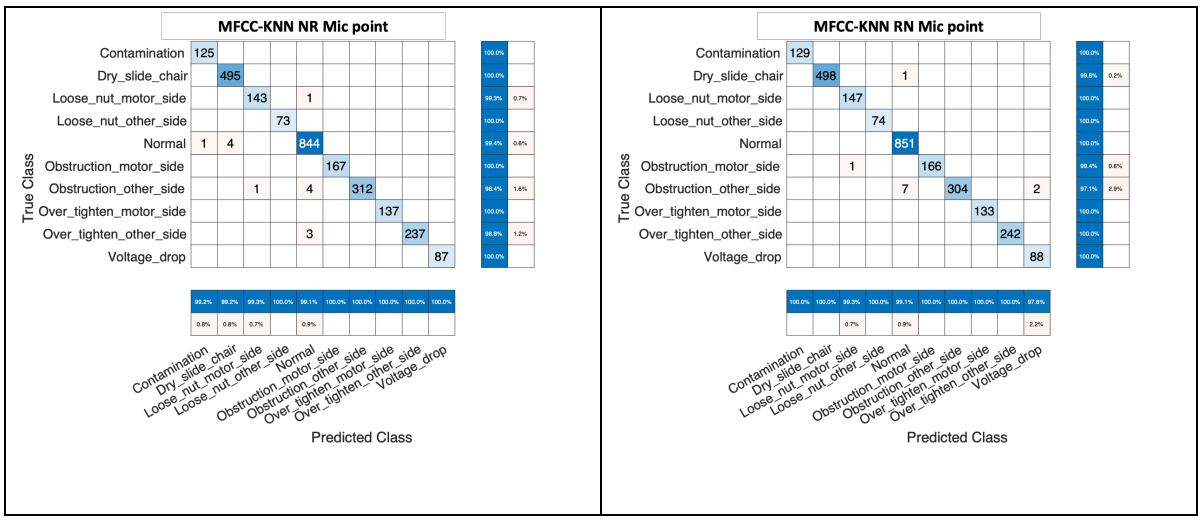

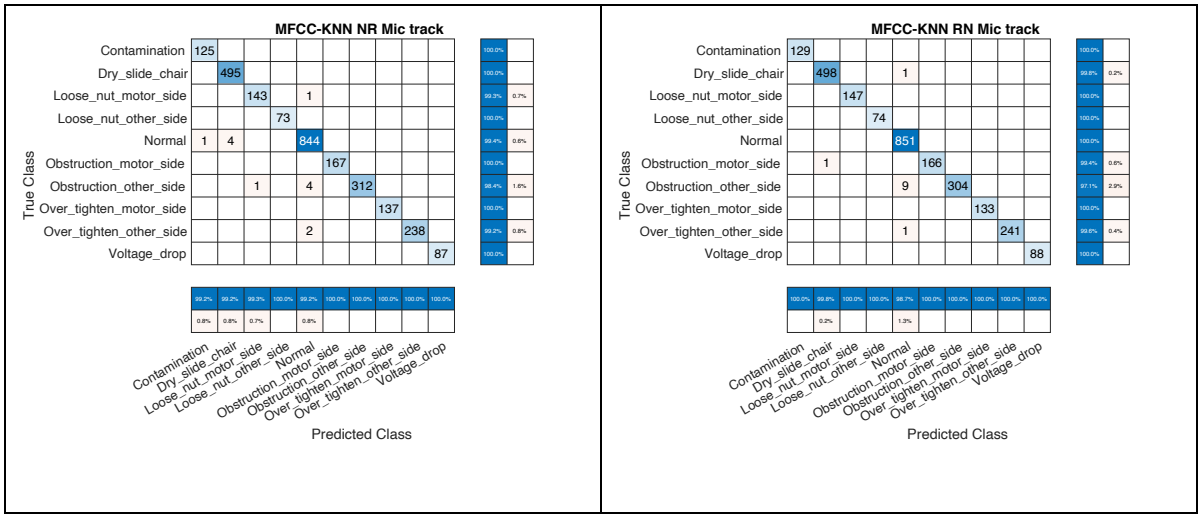


Figure 15. Diagnostic results by MFCC-KNN

The same phenomenon seems to occur during over-tightening. When the undriven side nut is over-tightened, it makes sense that RN data are diagnosed correctly as the nut would move the switch rail earlier than usual and push the switch rail more against the stock rail than usual, resulting in a significant difference in the operating sound. However, since the data in the NR direction were also classified without error, it is conceivable that excessive tightening of nuts causes a change in the locking mechanism and a large difference in the sound at the time of unlocking.

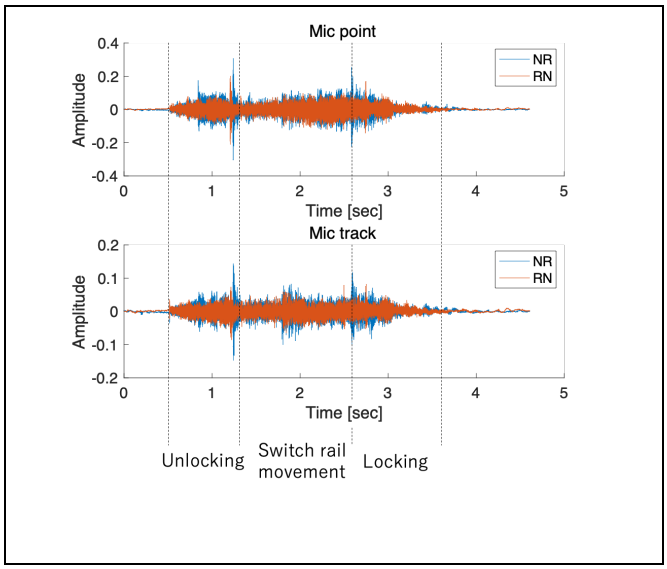


Figure 16. Amplitude of operating sound for each direction

In the case of ‘loose nut motor side’, KNN can accurately diagnose data in either direction, although SVM misdiagnosed several data as normal. When the nut on the motor side is loosened, it is assumed that a large difference occurs in the NR direction as the nut cannot push the switch rail enough, and little difference occurs in the RN direction since the nut is unlikely to directly affect the movement of the switch rail. However, as RN data were also classified accurately, it is conceivable that when the nut on the motor side is loosened, the force pushing the switch rail against the stock rail becomes weak and the position of the switch rail changes more on the motor side than usual. This changes the sound of unlocking, and the RN data were accurately classified.

Both SVM and KNN could diagnose a voltage drop with 100% accuracy. Although the voltage was only changed by about 4.5~9%, it is considered that the differences in the MFCC appeared due to the changes of the motor rotation speed by lowering the voltage. The voltage of a point machine installed outdoors is likely to drop due to electric leakage, and many point machines have voltage sensors. If the microphone eliminates the need for voltage monitoring sensors, it can be expected to reduce the maintenance cost of point machines.

When ‘dry slide chair’ was classified by SVM, there were more FNs in the NR direction, but when using KNN, only one FN was present in the RN direction and NR data were diagnosed with 100% accuracy. When comparing the difference in accuracy between microphones when using SVM, the accuracy of mic point is higher even though the state of the slide chair was changed. This suggests that the sound from the point machine is more important than the rail when diagnosing faults. Overall, diagnostic performance appears to be higher when using KNN as a classifier for all faults.

Diagnostic performance depending on the position of the microphone was investigated and it was found that the data acquired by the microphone near the point machine had higher diagnostic accuracy regardless of which classifier was used. The spectrograms for mic point and mic track are shown in Figure 17. The SPL of mic point is larger when unlocking from 0.5 to 1.2 seconds and locking from 2.5 to 3.5 seconds. This is because there is a locking mechanism in the point machine. On the other hand, the SPL of the track microphone becomes larger for the sound of the switch rail moving on the slide chair between 1.2 and 2.5 seconds. Before the analysis, it was thought that the abnormal condition could be detected from sound changes of the rail moving on the slide chair due to the large noise of the rail colliding with obstruction, contamination, and the dry condition; however, considering the analysis results, it was concluded that locking or unlocking the switch rail is more effective for diagnosing the abnormal condition. Since locking and unlocking sounds are effective in diagnosing abnormalities, it is considered that the diagnostic accuracy of mic point increased with a larger SPL of the sound in those parts.

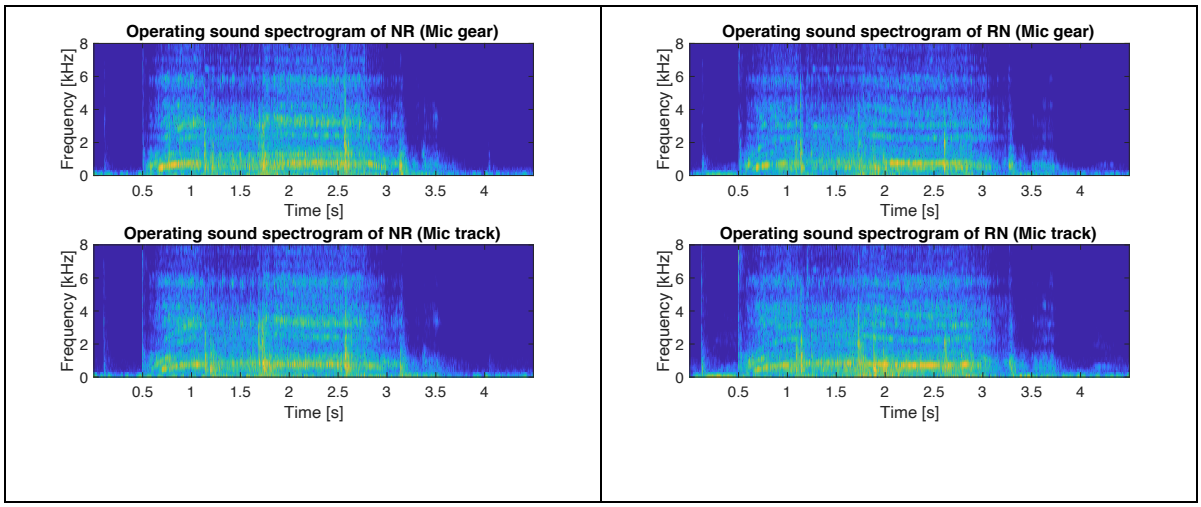


Figure 17. Sound spectrogram for each microphone

### 4.3.2 Summary of accuracy using MFCC

The analysis described in section 1.2.1 revealed that it is possible to diagnose point machine faults with high accuracy using either SVM or KNN classifiers when MFCC is used as the feature. SVM results in more FN, while KNN results in more FP, and KNN was found to be slightly more accurate than SVM. A detailed analysis of the classification accuracy shows that the sounds of locking and unlocking are important factors when classifying faults. The reason why the accuracy of the RN data for many faults was high is that because the sound of unlocking was larger than that of the NR data, and the clear difference of features could be calculated. At first, in the case of an obstruction or lack of grease, it was expected that the sound of a rail colliding with an obstruction or the sound of a rail moving on a slide chair with insufficient grease would be important for the diagnosis; however, data from mic point with a high SPL of unlocking were classified with higher accuracy than data from mic track with a high SPL of moving rail sound. This also supports the importance of the sound of unlocking. Furthermore, the higher accuracy of mic point for most faults is probably due to the larger SPL of the unlocking than for mic track. For these reasons, when using an MFCC, it is important to acquire the sound of the unlocking at a high SPL, and a mic point that can achieve this is the most suitable position for diagnosis.

### 4.3.3 Classification accuracy using WPDE

When WPDE was used as the feature, the Recall was drastically reduced compared to MFCC. Figure 18 and Figure 19 show classification accuracy using WPDE. It is revealed that most of the data were accurately diagnosed when MFCC was used, but when WPDE was used, most could not be diagnosed correctly. When SVM was used as the classifier, most of the fault data except for ‘over-tightened undriven side nut’ were misclassified as normal. As detection accuracy of ‘over-tightened undriven side nut’ is high, when this fault occurs, a distinct noise

is generated, which makes a large difference in WPDE. Most of the other faults, that were almost accurately diagnosed by MFCC, were not accurately diagnosed by WPDE, suggesting that there is little difference in each frequency band, although there are some differences in the time component of the operating sound data.

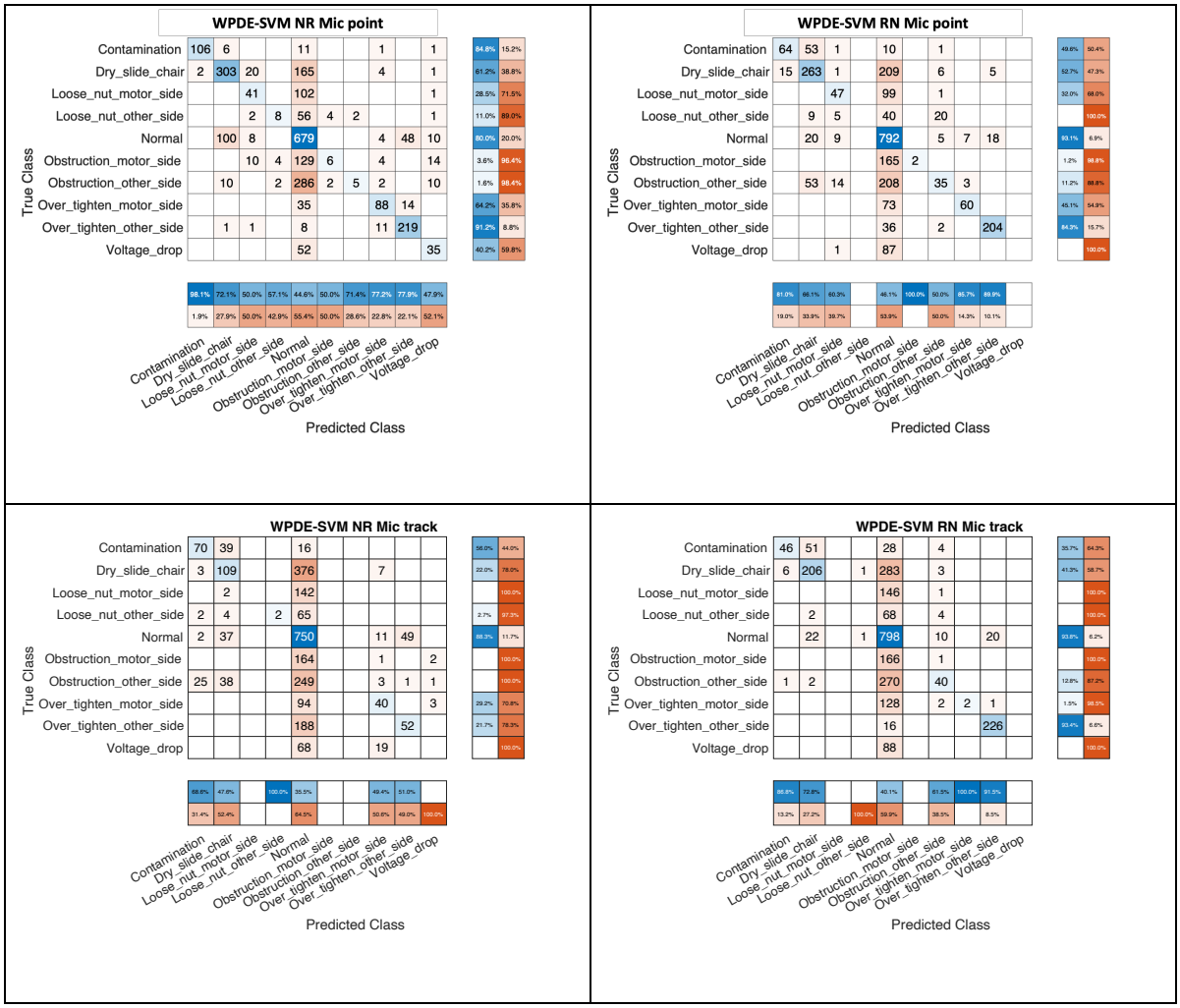


Figure 18. Diagnostic results by WPDE-SVM

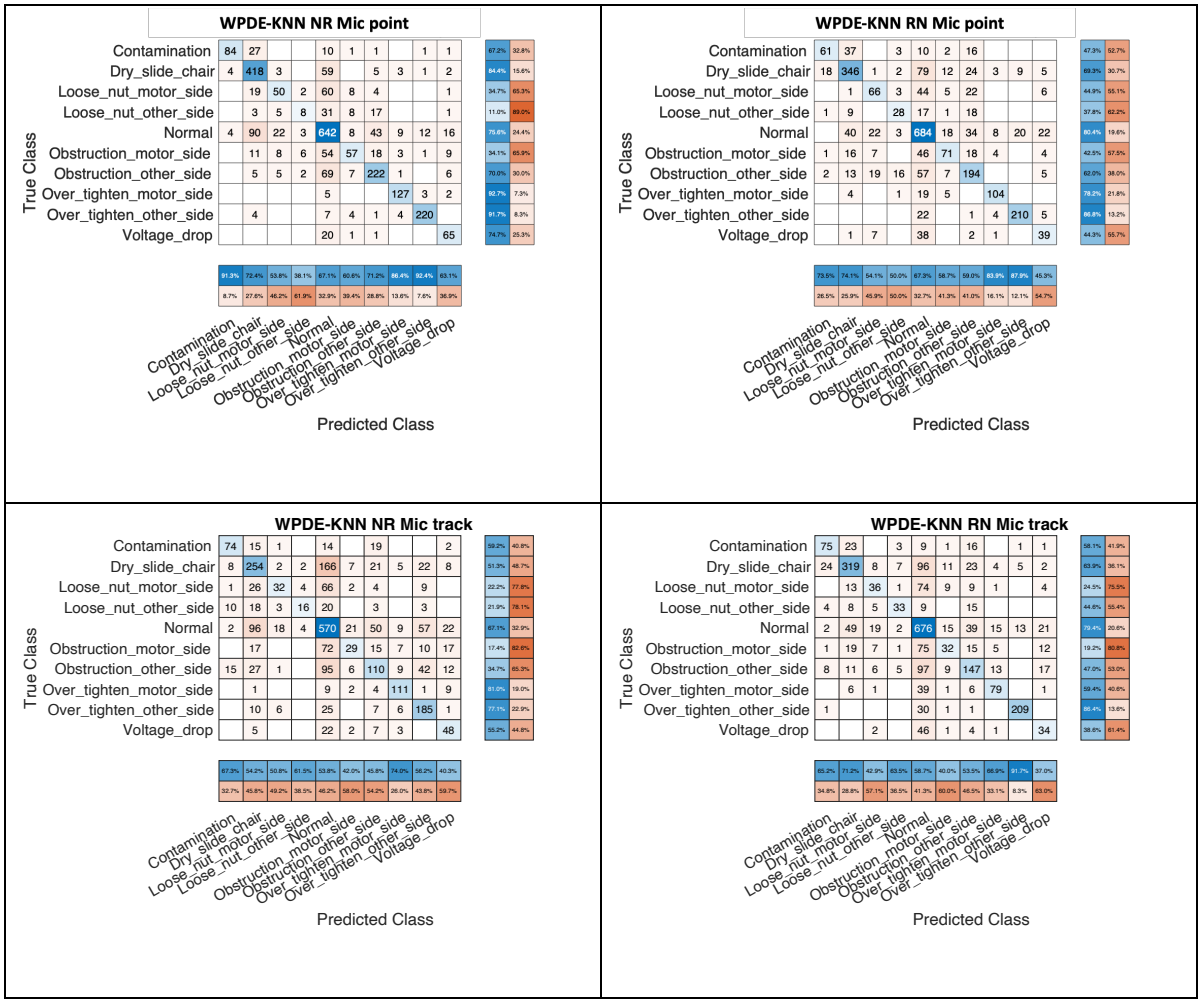


Figure 19. Diagnostic results by WPDE-KNN

When the voltage dropped, the frequency of the motor rotation sound, which constituted most of the data, changed, and it was expected that the WPDE would be able to detect abnormalities, but the accuracy was considerably low. The small range of voltage changes prevented a significant difference in WPDE. The reason MFCC was able to detect voltage drops is related not only to changes in frequency components, but also to delays in operation time. A voltage drop changes the speed of the motor, which in turn increases the operating time of the point machine. While MFCC can detect changes in the time component as a feature, WPDE cannot detect the voltage drop because it is difficult to detect minute

changes in the time component and this should be the reason WPDE cannot detect a voltage drop.

Although the sound of rail movement due to contamination and dry slide chairs should also cause changes in the frequency component, the combination of WPDE and SVM seems to have had difficulty in diagnosing abnormalities.

Noise during locking and unlocking is also expected to occur when there is an obstruction or a loose or over-tightened nut, but the detection rate of these faults was low. The reason for this is that the operating sound data of the machine itself are longer than the length of the abnormal noise and the difference of WPDE becomes small. However, the use of KNN as a classifier improved the accuracy a little. In particular, the dry slide chair and over-tightened nut of the NR data acquired from mic point could be diagnosed with a certain degree of accuracy. In the case of the dry slide chair, as was the case with the MFCC, the mic point data had better diagnostic accuracy, suggesting that when a fault occurs, there is a change in the operating sound of the point machine rather than the operating sound from the rail. For the same reason, an over-tightened nut should also generate noises in the point machine. The reason why SVM could not detect this might be related to the distribution of features. SVM cannot classify with high accuracy unless the distribution of features is linearly separable. KNN is relatively adaptive to data with non-linear boundaries because it classifies based on the distance between data points. This may have allowed KNN to classify them with a certain degree of accuracy.

The reason why ‘loose nut’ could not be detected by WPDE is that it does not generate much abnormal sound compared to ‘over-tightened nut’. Initially, it was assumed that the abnormal sound was generated by the locking mechanism because the position of the switch rail changes as the position of the nut changes. The lock rod has a cutout, and the locking bar

enters the cutout to lock the point machine so that the switch rail does not move after switching the position. The structure of the locking mechanism is shown in the red frame of Figure 20. When the nut of the drive rod is loosened or over-tightened, it changes the position of the switch rail, and also the position of the lock rod, as it is connected to the switch rail. This may make the locking bar and lock rod, which normally do not touch each other, rub together to produce an abnormal sound. When the undriven side nut is loosened, the switch rail cannot achieve its proper position and neither can the lock rod, locating the position more to the undriven side than usual. This makes the locking bar touch the motor side of the lock rod cutout.

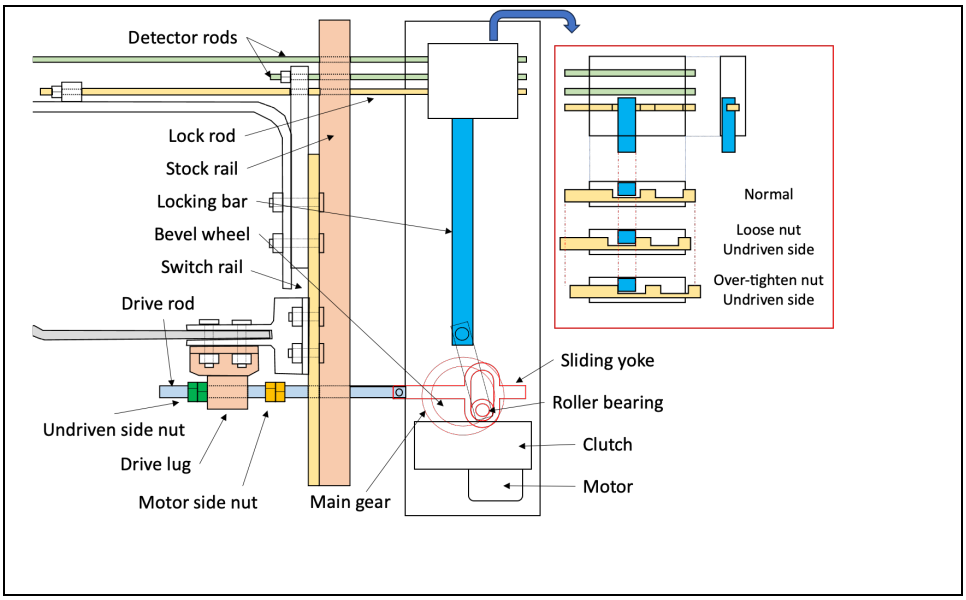


Figure 20. Structure of the point machine

If so, the detection rate for both ‘over-tightened nut’ and ‘loose nut’ cases should be high. However, the high detection rate for ‘over-tightened nut’ and the low detection rate for ‘loose nut’ suggest that the abnormal sound is not only generated from the locking mechanism but also generated from other parts or components. Spectrograms were made to investigate the abnormal sound generated during the locking phase of ‘loose nut’ and ‘over-tightened nut’. The generated spectrograms are shown in Figure 21.

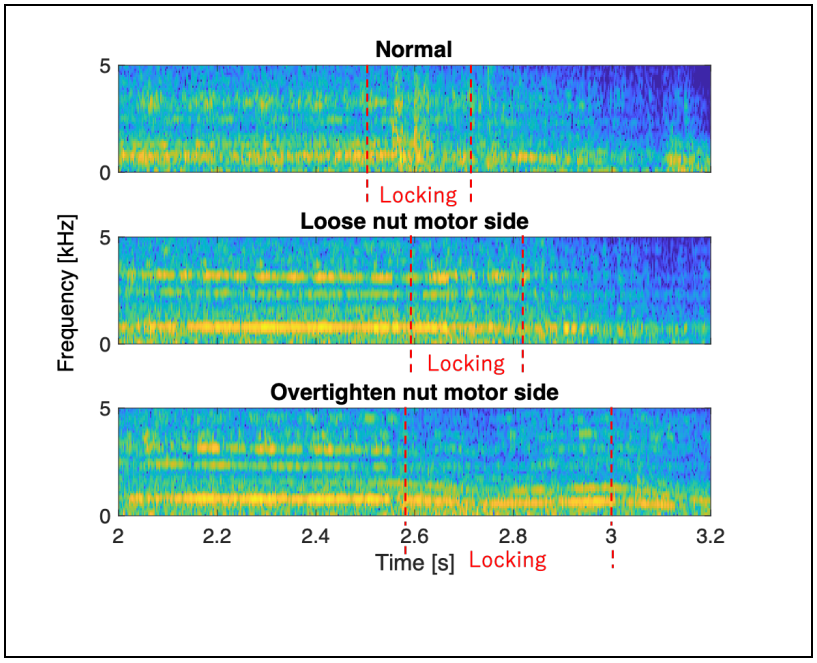


Figure 21. Sound spectrograms for over-tightened and loose nuts (NR direction)

Spectrogram investigation revealed that there was no significant noise in the locking phase when the nut was loosened. In both cases of 'loose nut' and 'over-tightened nut', the abnormal sound from the motor before locking was found to be larger than normal. This is caused by a load on the motor that is different from the normal load due to the different position of the nut. In addition, it was confirmed that the timing of the locking was changed by changing the position of the nut. The reason why both 'loose nut' and 'over-tightened nut' could be diagnosed with high accuracy using MFCC is that it captures the characteristics of the abnormal sound of the motor and the difference of the timing of the locking. On the other hand, WPDE failed to capture these features, which may have reduced the accuracy of identifying 'loose nut'. However, for over-tightening, it was found that low-frequency sound is generated during the locking phase. As it is possible to diagnose 'over-tightened nut' using WPDE, it suggests that WPDE captures this feature to classify the data.

This abnormal sound occurs in a frequency band almost equal to the rotation speed of the motor (500 Hz), and it is highly possible that it occurs near the motor. In addition, since it

is caused by excessive nut tightening, it seems to be caused by the fact that the switch rail meets the stock rail and the motor tries to keep running even though there is no more space to move. In such a case, the clutch is activated to prevent excessive load on the motor.

The abnormal sound happening in the case of 'over-tightened nut' is thought to be due to clutch slipping. The clutch is a mechanical device used to transmit or shut off the power of a motor to the main gear. It allows for smooth starting and stopping of gears without stopping the motor. The clutch consists of a pressure plate, a friction plate, and a flywheel. When the clutch is engaged, the pressure plate presses the friction plate against the flywheel, transmitting power from the motor to the gear. When the clutch is disengaged, the pressure on the friction plate is released, disconnecting the motor power from the gear. If an unexpected or excessive load is applied to the motor while the clutch is engaged, clutch slipping happens. This means that the friction plate is unable to effectively grip the flywheel, resulting in a loss of power transmission to the wheel and the production of a squealing sound or a grinding noise as the friction plate slips against the flywheel. If the nut is over-tightened, the switch rail is already attached to the stock rail, but the motor tries to keep turning and clutch slipping occurs. The movement of each component when the nut is over-tightened is described as follows.

The drive rod to which the nut is attached is connected to the sliding yoke in the point machine. The structure of the point machine is shown in Figure 20. The part shown in red is called the Scotch yoke mechanism, which converts the rotational motion of the motor into horizontal motion. The gear in the clutch connected to the motor rotates the main gear, and the rolling bearing attached to the main gear pulls the sliding yoke and changes the direction of motion. When the drive rod nut is over-tightened, the switch rail contacts the stock rail early. Normally, as soon as the switch rail touches the stock rail, the machine is locked and stops

operation. However, if the nut is excessively tightened, the machine tries to continue to operate even after the switch rail contacts the stock rail, and the switch rail is subjected to a large reaction force from the stock rail. The reaction force from the stock rail also exerts excessive force on the drive rod through the drive lug. This force may cause excessive load on the motor through the sliding yoke and main gear, resulting in clutch slipping and an abnormal sound. When the nut is loosened, the motor is not overloaded because the motor is not subjected to excessive force from the stock rail. This could be the reason for the low fault detection accuracy for 'loose nut' but a high rate for 'over-tightened nut' by WPDE.

### 4.3.4 Summary of accuracy of using WPDE

It was found that classification accuracy is significantly reduced when WPDE is used compared with MFCC. While MFCC can capture fine sound changes, WPDE seems to capture only large changes. Only over-tightening could be detected with relatively high accuracy. On the other hand, because loose nut was not detected with high accuracy, it could be that WPDE can capture the abnormal sound of the motor generated only during over-tightening. Considering the results of section 1.2.2, it was found that the MFCC is the best method for diagnosing faults using acoustic data.

## 4.4 The effect of noise

Since point machines are usually installed outdoors, noise such as wind and rain is mixed in when taking the acoustic data of the point machine. To examine the effect of noise on the proposed method, white noise was added to the data. The SPL of added noise was 37 dB and 55 dB corresponding to light and heavy rain, respectively [130, 131]. Table 10 and Table 11 show the results of adding noise. Considering fault detection and diagnostic accuracy, it is better to use MFCC as a feature: when using MFCC, even if noise equivalent to heavy rain is

added, it was found that it has little effect on accuracy. The results for mic point and mic track also show that mic point is more accurate. This is because the data from mic point are over 90 % louder than the track one and therefore, less affected by noise. It can be expected to detect and diagnose a point machine fault with high accuracy without being affected by noise in an actual outdoor field.

Table 10. Recall of fault diagnosis with 37 dB noise

| Feature extraction | Classifier | Mic | NR | | RN | |
|---|---|---|---|---|---|---|
| | | | Recall [%] | F1 score [%] | Recall [%] | F1 score [%] |
| MFCC | SVM | Point | 99.6 | 99.8 | 99.1 | 99.5 |
| | | Track | 99.6 | 99.8 | 98.9 | 99.5 |
| | KNN | Point | 99.7 | 99.7 | 99.6 | 99.8 |
| | | Track | 99.3 | 99.4 | 99.4 | 99.7 |
| WPDE | SVM | Point | 49.0 | 61.5 | 41.9 | 57.6 |
| | | Track | 16.9 | 27.3 | 30.1 | 45.2 |
| | KNN | Point | 79.4 | 82.3 | 77.3 | 81.9 |
| | | Track | 63.5 | 68.9 | 66.6 | 74.8 |

Table 11. Recall of fault diagnosis with 55 dB noise

| Feature extraction | Classifier | Mic | NR | | RN | |
|---|---|---|---|---|---|---|
| | | | Recall [%] | F1 score [%] | Recall [%] | F1 score [%] |
| MFCC | SVM | Point | 99.6 | 99.8 | 99.3 | 99.6 |
| | | Track | 99.3 | 99.7 | 98.7 | 99.3 |
| | KNN | Point | 99.7 | 99.7 | 99.1 | 99.5 |
| | | Track | 99.6 | 99.7 | 99.3 | 99.6 |
| WPDE | SVM | Point | 49.0 | 61.3 | 46.7 | 62.3 |
| | | Track | 46.6 | 60.8 | 37.5 | 53.4 |
| | KNN | Point | 78.6 | 81.5 | 77.7 | 82.4 |
| | | Track | 71.7 | 76.3 | 71.7 | 78.9 |

## 4.5 Important frequency range of operating sound

It is conceivable that the operating sound of the point machine includes various sounds such as the rotating sound of the motor, the sound of the rail being dragged, and the sound of the locking mechanism. To investigate which frequency band affects the diagnostic accuracy, the MFCC was calculated from operating sound data after applying bandpass filters, and the calculated accuracy was compared by using SVM. Each accuracy was calculated by varying the lowest and highest frequencies of the bandpass filters. The lowest frequency tested was 20

Hz and the highest was 20 kHz. Two hundred and 10 bandpass filters were investigated, with the lowest and highest frequencies of the bandpass filters varying by 1000 Hz. Since it takes time to calculate the accuracy using all the data, it was calculated by randomly selecting 10 sets of data for each condition. The results are shown in Figure 22. The top 10% of accuracy is shown in red and the bottom 10% in blue. The results revealed that the accuracy of the data increased when including sounds around 11 kHz. On the other hand, if sounds around 3 kHz are included, the accuracy decreases. From this result, it was found that the frequency range around 11 kHz is important for diagnosing the condition. On the other hand, since the accuracy decreases when 3 kHz sounds are included, it is considered that this frequency range contains noise and sound unrelated to condition diagnosis. By using a bandpass filter to acquire important frequency bands, the effect of noise can be reduced, and accuracy can be enhanced.

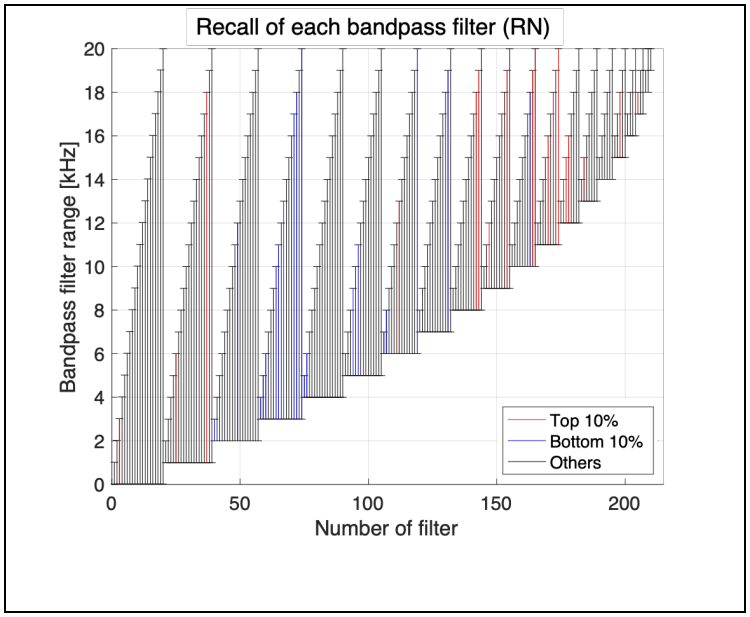


Figure 22. Recall of each bandpass filter

## 4.6 Summary and findings

In Chapter 1, the hypothesis that it is possible to diagnose the initial faults of STME, such as point machines, from acoustic data was described. The investigation in this chapter proved that initial faults can be detected and diagnosed with high accuracy for a point machine. The answers to the following research questions in the same chapter were found by this analysis.

- Which algorithm is most appropriate?

It was found that the combination of MFCC and SVM (MFCC + SVM) and of MFCC and KNN (MFCC + KNN) enables fault detection and diagnosis with high accuracy. Accuracy for both is sufficiently high, but MFCC + KNN was found to be slightly more accurate than MFCC + SVM. It was also found that WPDE can diagnose faults to some extent with accuracy for some types of faults, but many misdiagnoses occur. This may be because the difference of each frequency band did not increase even when the fault occurred, and the WPDE was not capable of capturing minute time-varying components such as MFCC.

- How accurate is the system and does that vary by fault?

When the MFCC was used as a feature, it was found that all faults could be detected and diagnosed in more than 95% of cases. Most faults can be accurately classified, but some misclassification of ‘loose nut’ and ‘obstruction’ occurs. However, it can be said that the diagnostic performance of all faults is sufficiently high.

- How tolerant is it to noise?

It was found that the proposed method has little effect on classification accuracy even when the data are mixed with noise at heavy rain levels. Even if there is noise, it can diagnose the condition of the target, so practical application is expected.

- Which microphone position is most appropriate?

For all faults, the analysis accuracy of the data acquired by the microphone near the point machine was the highest. It was found that the microphone should be placed close to the point machine because the sound generated from the point machine can be used to detect and diagnose faults with high accuracy. Since the point machine is slightly away from the centre of the track, installing a microphone near the point machine is expected to reduce the risk rather than installing a microphone inside the track.

# CHAPTER 5 EXPERIMENT WITH FAST STME: CONTACTORS

## 5.1 Introduction

This chapter describes the details of the second experiment to verify whether STME faults can be diagnosed by acoustic data and the results of the data analysis. The second experimental target is a contactor. A contactor is a switch used to turn an electric circuit on and off and uses a solenoid coil or spring force to move a moving blade. Most contactors operate in less than one second, a shorter operation compared to point machines. Since the moving and fixed blades collide with each other at high speed, the operating sound has a wide frequency range. To investigate the diagnostic accuracy for impulse sounds containing high frequency bands, normal and simulated fault data are obtained from the machines as in Chapter 4. Features are extracted from the data and the accuracy is calculated with each feature and classifier to find the best combination. As with the point machine, since the data were acquired indoors to capture only the acoustic data from the target, white noise was added to the acquired data to simulate other machines' sound, and the effect on classification accuracy was also investigated.

## 5.2 Experiment using contactors

To investigate the accuracy of mechanical fault diagnosis by using acoustic data, tests were conducted using 6.6 kV contactors. The structure of a contactor is shown in Figure 23. The contactor has two moving parts, one at the top and the other at the bottom. The electrode connected to the moving part engages with and detaches from the fixed electrode to connect

and disconnect the circuit. Figure 24 shows the movement of the components when the contactor is opened and closed. The following procedure switches the contactor on and off.

1. The plunger is accelerated by the current flowing through the solenoid coil. This causes the upper and lower moving parts to move downwards and upwards.
2. The opening springs are shortened, and the moving contact (electrode) contacts the fixed contact, thus forming a circuit.
3. After the circuit is formed, the current flows through the holding coil, which attracts the plunger and continues to form the circuit.
4. The holding coil's current is stopped, and the opening spring force returns the moving part to its original position.

This mechanism is designed to ensure that the circuit is safely opened in a power failure.

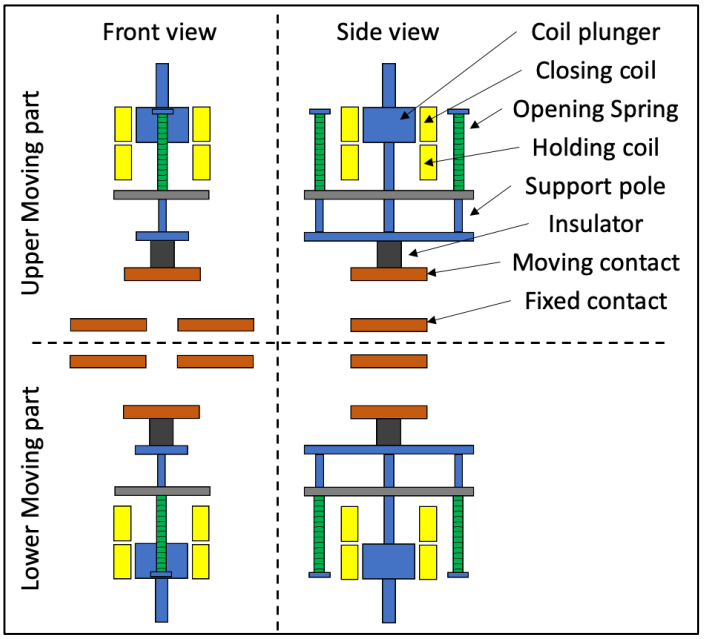


Figure 23. Structure of the contactor

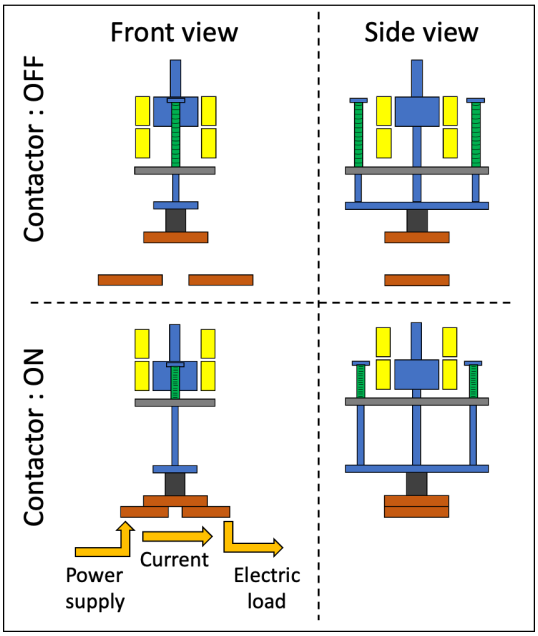


Figure 24. Movement of contactor components through opening and closing

In the test, one normal contactor and one damaged contactor were used. The damaged contactor (contactor B) had a broken bolt in the lower moving part, although it could be opened and closed. All contactors were installed in the same cabinet. As described in Chapter 2, most failures of circuit breakers are related to mechanical problems [107, 108]. Similar failures are likely to occur with contactors that are similar in structure to circuit breakers. Since contactors operate more frequently than circuit breakers, a lack of grease in moving parts, weakening of springs that are repeatedly compressed, improper position of components, and loosening nuts can also be considered. Since operating the contactor with the nut loosened can cause the machine to break, obstruction was simulated in this study as loosened nuts may come off and get caught between the moving parts. Metal powder may be generated by wear of the moving part due to long periods of operation. It is also conceivable that metal powder and dust may accumulate as an obstruction between the moving parts.

In this study, the following multiple faults shown in Table 12 were considered to have happened and data for those simulated faults were obtained from contactor A. A lack of grease is quite likely to occur because of the frequent use of machines. When the grease runs out, it is expected that the friction of the sliding surface increases, making an unusual high-frequency sound, and the operating time increases. It is also conceivable that the spring may become weak due to frequent use. As the spring weakens, the initial position of the moving blade changes, which appears to make a difference in the sound when the blade starts moving. Since many parts move frequently, the parts wear out and metal powder may be generated. Not only metal powder but also dust can accumulate, and there is a high possibility of such kinds of objects being caught between moving parts. It is conceivable that a nut or some parts may come off due to high-frequency operation and be caught in a moving part as well. If obstruction happens, an abnormal sound is expected to occur as the blade hits the object. Pins connecting parts may also shift from their normal position due to frequent operation. If a pin slips and the connection between the components becomes weak, the balance of power may be changed, and the timing of the operating sound may change.

Table 12. Simulated fault modes

| Fault number | Fault mode |
|---|---|
| Fault 1 | Lack of grease |
| Fault 2 | Spring weakening |
| Fault 3 | Obstruction |
| Fault 4 | Improper pin position |

Table 7 shows the measuring equipment used in this test. Since the contactors were installed inside the cabinet, one microphone (mic inside) was placed next to the contactor inside the cabinet, and other microphone (mic door) was placed in front of the contactor outside the cabinet. Microphone positions are shown in Figure 10 and Figure 26. Two acceleration sensors were installed, one for each of the upper and lower solenoid coils, and four current sensors were installed to measure the closing and holding current of the upper and lower coils.

Table 13. Measuring equipment

| Measuring equipment | Model | Range |
|---|---|---|
| Microphone | RION UC59 | 10 Hz ~ 20 kHz |
| Accelerometer | RION PV91C | 1 Hz ~ 15 kHz |
| Current sensor | HIOKI CT9691 | - |
| Data recorder | HIOKI MR8847A | - |

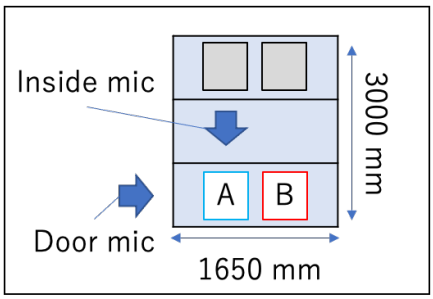


Figure 25. Location of measuring equipment and contactors

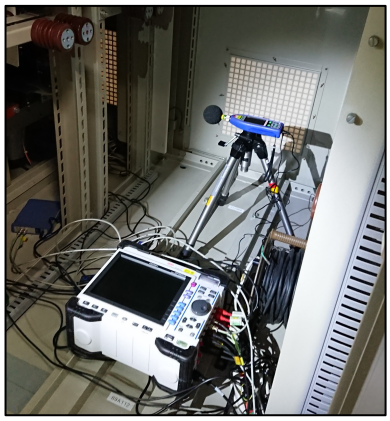

Figure 26. Measuring equipment (inside mic and data recorder)

A damaged contactor was used, which had been damaged in an endurance test carried out in the past to check its durability. Periodic maintenance was carried out every 60,000 cycles in the test, and after 1.8 million cycles, the bolt leading to the bottom moving part was found to be broken. The structures of the normal and damaged contactors used are shown in Figure 27. In the damaged contactor, the bolt connecting the bottom plunger and the moving part was broken. The system continued to operate despite the plunger and moving part being separated from each other as the accelerated plunger would contact the moving part to carry it upward. When holding current is stopped, the components would fall separately.

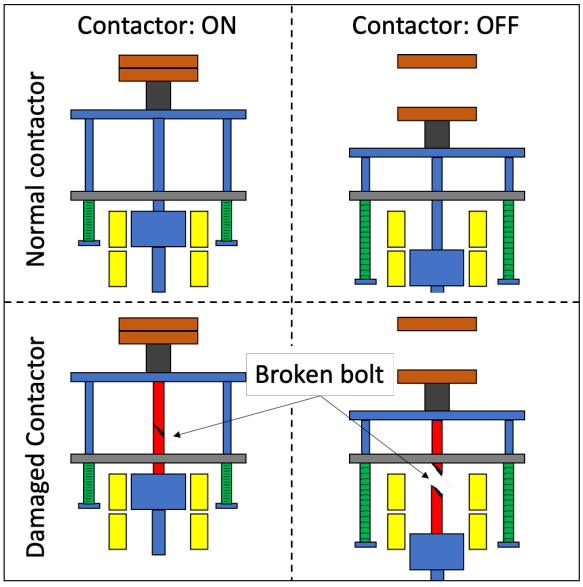


Figure 27. Structure of normal and damaged contactors

Details of each simulated fault are shown in Figure 28, Figure 29, Figure 30, and Figure 31. In simulated fault 1 (lack of grease), the grease applied to the sliding parts of the contactor was removed. The greased areas are highlighted in Figure 28.

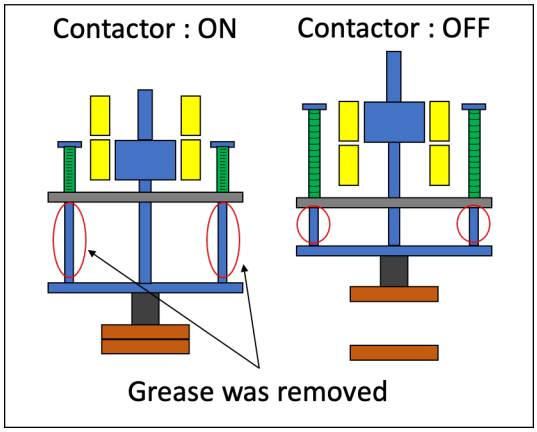


Figure 28. Simulated fault 1: lack of grease

In simulated fault 2 (spring weakening), a weakening of the upper opening spring was simulated. If a spring is used frequently, it is expected that it will be compressed over time, and the force will be weakened. To shorten the spring, a tape was applied between the fixed part and the damper. Although it is desirable to replace the normal spring with a spring with a small spring coefficient to create an actual fault condition, the fault was simulated by shortening the spring because it takes time and effort to prepare and replace a proper spring. By using the tape, the behaviour at the time of opening is different from that in the actual fault but the length of the spring can be shortened arbitrarily, and the gradual change can be observed; therefore, tape was applied. The thickness of the tape was varied between 1, 3, 5, and 20 mm, and the data for each case were obtained. In the actual fault, repeated operation shortens the spring length and weakens its force. Using tape to simulate this situation shortens springs that are not actually shortened, so the force of the springs is stronger than in the actual fault. However, the spring length of the contactor used in this study is more than 110 mm and the force of the solenoid coil is also powerful because the blade is opened and closed at high speed. Therefore, the effect of increasing spring force by compression of about 1~5 mm is small, and in the case of 1~5 mm, it is considered that the actual fault can be accurately simulated. In the case of 20 mm compression, applying tape cannot accurately simulate actual fault conditions, so it was not used to calculate classification accuracy, but only to investigate important features for fault detection discussed in Chapter 6. In this simulated fault, the motion of closing is the same as that of the actual fault, but the motion of opening is different from that of the actual fault. Normally, the moving part is pulled up by the force of the spring and in contact with the damper. If the force of the spring is weakened, the moving part can no longer be pulled up completely, and the position of the moving part becomes lower than its normal position, creating a gap between the fixed parts and damper. In the actual fault, when the holding state ends, the moving

part goes back and through the initial position and goes up and down repeatedly from the initial position, and then gradually decays and returns to the initial position. However, in the case of the simulated fault, the moving part cannot go up beyond the initial position because the tape is attached, and the speed instantly becomes zero or rebounds at the initial position. For this reason, only closing data were used in the verification of the fault diagnosis.

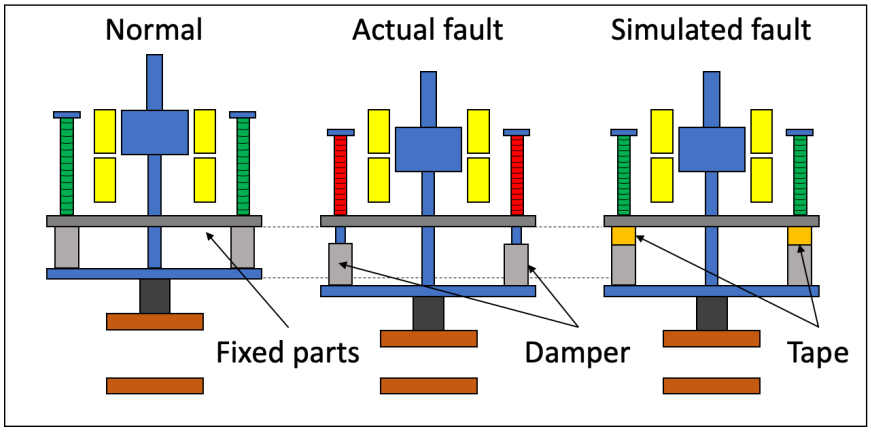


Figure 29. Simulated fault 2: spring weakening

In simulated fault 3 (obstruction), objects were placed between the moving contact and the fixed contact. The placed objects were a piece of cloth (1 mm thick), a piece of tape (1 mm thick), a piece of rubber (5 mm thick), and a piece of wood (20 mm thick). The reason for using a piece of cloth was to simulate dust accumulating on the blade. Contactors have many frequently moving parts that wear out and this produces metal powder, and in addition this, metal powder from the rails and dust from the ballast sometimes lie thick on the blades, requiring the filter of the cabinet to prevent dust and regular cleaning of the contactors. If dust accumulates faster than expected due to faulty filters or poor maintenance, resistance between the blades is likely to increase and malfunction may occur, and there is currently no way to detect this fault. When dust accumulates, it is considered that the high frequency range of the impact sound of the blade is attenuated, and this is why cloth was used to simulate this condition.

It is also conceivable that high-frequency operation may cause the obstruction of some components which have come off due to loosened screws, stress concentration, or fatigue. The parts that are likely to get caught are dampers that continue to exert force and screws and nuts that are likely to become loose. If these are caught between the blades, the impact sound itself may be reduced, or conversely, increased. To simulate this condition, rubber similar to the damper and wood that generates a loud noise when the blade is struck, as well as screws and nuts, were used as obstruction materials.

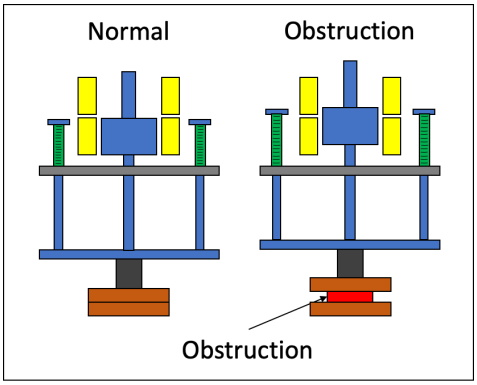


Figure 30. Simulated fault 3: obstruction

In the case of simulated fault 4 (improper pin position), the pin of the lower part connecting the coil plunger and the moving part was displaced from its proper position. Even if the pin was displaced, the contactor could be opened and closed.

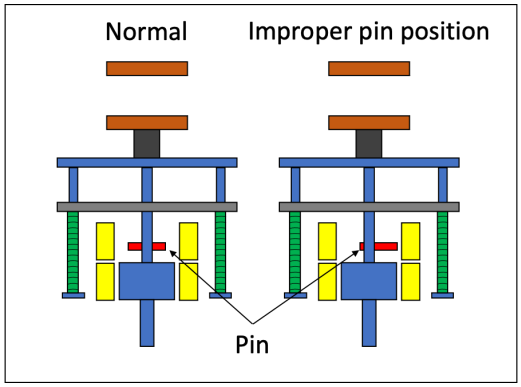


Figure 31. Simulated fault 4: improper pin position

Example time-domain representations and power spectrograms for both normal and fault data are shown in Figure 13. The fault data of broken bolt, lack of grease, and obstruction have an observable abnormal sound before the blade impact. No significant difference can be seen in the other fault data, and it seems to require investigation to identify differences that are not easily observable. Although it is difficult to tell the differences in these data by conventional analytical methods, it is possible to calculate the difference of the distribution of each frequency component and the time change by using WPDE and MFCC, and it is expected to have some clear differences. It can be expected to find useful differences by analysing many data using KNN and SVM, even if the differences are small. In this study, each feature is calculated from the data obtained from the machine, and the classification accuracy of the classifier is calculated and evaluated. Which coefficients of the calculated features contribute to the classification accuracy will be discussed in Chapter 6.

To prevent the solenoid coil from overheating, the contactor operation was performed once in every 15 seconds. In this way, opening and closing data were acquired once every 15 seconds. The test schedule is shown in Table 8. First, to verify whether fault detection by acoustic data is possible, data were acquired in September 2020 using contactors A and B,

which have large differences in operating sound. Then, an algorithm for fault detection was prototyped, and since it was expected to be accurate to some extent, and to investigate the diagnosis performance, the data of the fault with a small sound difference were also acquired from contactor A in February 2021.

Each set of data was collected for one second from 0.05 seconds before the control signal voltage exceeded 50 V. Data were obtained for each switching on and off. In the building where the contactor is installed, equipment other than the contactor is also installed, and the pump for cooling runs irregularly, so some of the data include the sound of the pump and its interference loudness was over 75 dB. Since both normal and fault data contain this sound, data containing noise were also used in the analysis to simulate a more realistic situation.

Table 14. Test schedule

| Date | Data type | Contactor | Number of data<br>Closed | Number of data<br>Open |
|---|---|---|---|---|
| Sep 2020 | Normal | A | 118 | 117 |
| | Broken bolt | B | 341 | 341 |
| Feb 2021 | Normal | | 99 | 95 |
| | Lack of grease | | 333 | 331 |
| | Obstruction | A | 106 | 110 |
| | Spring weakening | | 276 | 241 |
| | Improper pin position | | 71 | 79 |

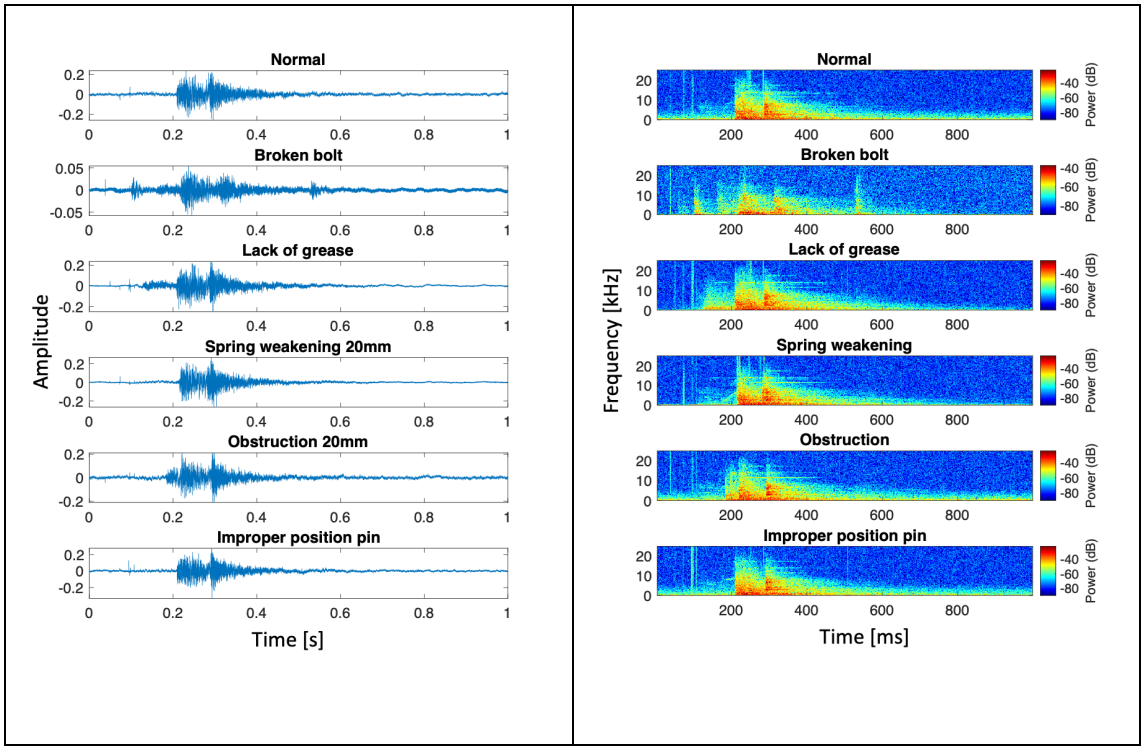


Figure 32. Spectrogram for each condition of signal and power

## 5.3 Classification accuracy

Table 9 shows the Recall and F1 score for normal and abnormal classification by each feature and classifier. It can be confirmed that all features and classifiers can classify faults with high accuracy over 95%.

Table 15. Recall of the fault diagnosis

| Feature | Classifier | Mic | Closed | | Open | |
|---|---|---|---|---|---|---|
| | | | Recall [%] | F1 score [%] | Recall [%] | F1 score [%] |
| MFCC | SVM | Inside | 99.6 | 99.4 | 98.6 | 97.9 |
| | | Door | 99.5 | 99.3 | 98.4 | 97.9 |
| | KNN | Inside | 100.0 | 98.7 | 100.0 | 97.6 |
| | | Door | 99.7 | 98.7 | 99.9 | 96.3 |
| WPDE | SVM | Inside | 99.7 | 95.0 | 99.8 | 94.8 |
| | | Door | 98.5 | 94.9 | 98.8 | 94.4 |
| | KNN | Inside | 98.3 | 94.3 | 98.3 | 94.4 |
| | | Door | 96.5 | 94.3 | 98.4 | 93.9 |

As a trend of the analysis results, when MFCC is used, it seems that the closed data can be diagnosed more accurately than the open data when the Recall and F1 score are considered. As mentioned in the above paragraph, which explains the details of the simulated fault, spring weakening is not included in the result of open data. When the contactor is closed, the plunger is accelerated by the coil and the moving part moves at high speed and collides with the fixed blade, whereas when the contactor is opened, it returns to its original position at a slower speed by the spring force than when it is closed. If there is an abnormality or difference in the state of the contactor, it is likely that the acoustic data will be more different in the closing

phase, as the moving part moves at high speed and may make a loud abnormal sound. This may be one of the reasons why the analysis results for the closed data were better than for the open data. Comparing the results of the inside and door microphones, the inside microphone has better classification accuracy. The signal-to-noise ratio (SNR) might be the reason for this result and SNR might be another factor that can affect the accuracy of analysis results. Accurate analysis might be carried out if only the acoustic data from the target can be measured, but as a matter of fact, the acoustic data from equipment other than the target will also be mixed in, reducing the accuracy. The better performance of the inside mic is thought to be due to the SNR being higher than that of the door one; as the inside mic is located inside the panel, it measures less noise from other equipment compared to the door one. The performance of the classifiers was found to be highly accurate in diagnosing faults, regardless of whether SVM or KNN was used. However, when considering the F1 score, KNN had a higher number of FPs than did SVM, resulting in a lower F1 score. When WPDE is used, Recall is high, but the F1 score is lower than in the case of MFCC. The difference in accuracy depending on the mic location is the same as in the MFCC case, with the inside mic providing better accuracy. SVM seems to be superior to KNN as a classifier.

It is thought that one of the reasons for the lower accuracy of WPDE compared to MFCC is its ability to capture changes in the time component as a feature value. MFCC divides one second of data into 98 pieces in the calculation process in this analysis and calculates the feature values for each analysis window. Therefore, if there is a large difference at a certain time in the acoustic data, the feature values of that analysis window will change significantly. For example, in the case of a broken bolt or obstruction, there is a possibility that an abnormal sound is generated at a certain time, and in the case of lack of grease, spring weakening, or improper pin position, there may also be a delay in operation. In the case of MFCC, such

detailed differences can be captured in the feature values. While MFCC is based on the decomposition of a signal into overlapping time windows and the calculation of cepstral coefficients for each window, WPDE decomposes a signal into sub-bands of different frequencies using wavelet packet decomposition and then calculates the entropy of each sub-band. WPDE calculates the entropy of each sub-band by summarising the changes in each frequency band, which may result in a loss of fine-grained temporal information and does not capture the temporal dynamics of the signal explicitly.

Figure 33, Figure 34, Figure 35, and Figure 36 show the diagnostic results of each method. It is revealed that most of the data were accurately diagnosed when MFCC was used, but when WPDE was used, there were many cases of FP and misdiagnosis of different faults.

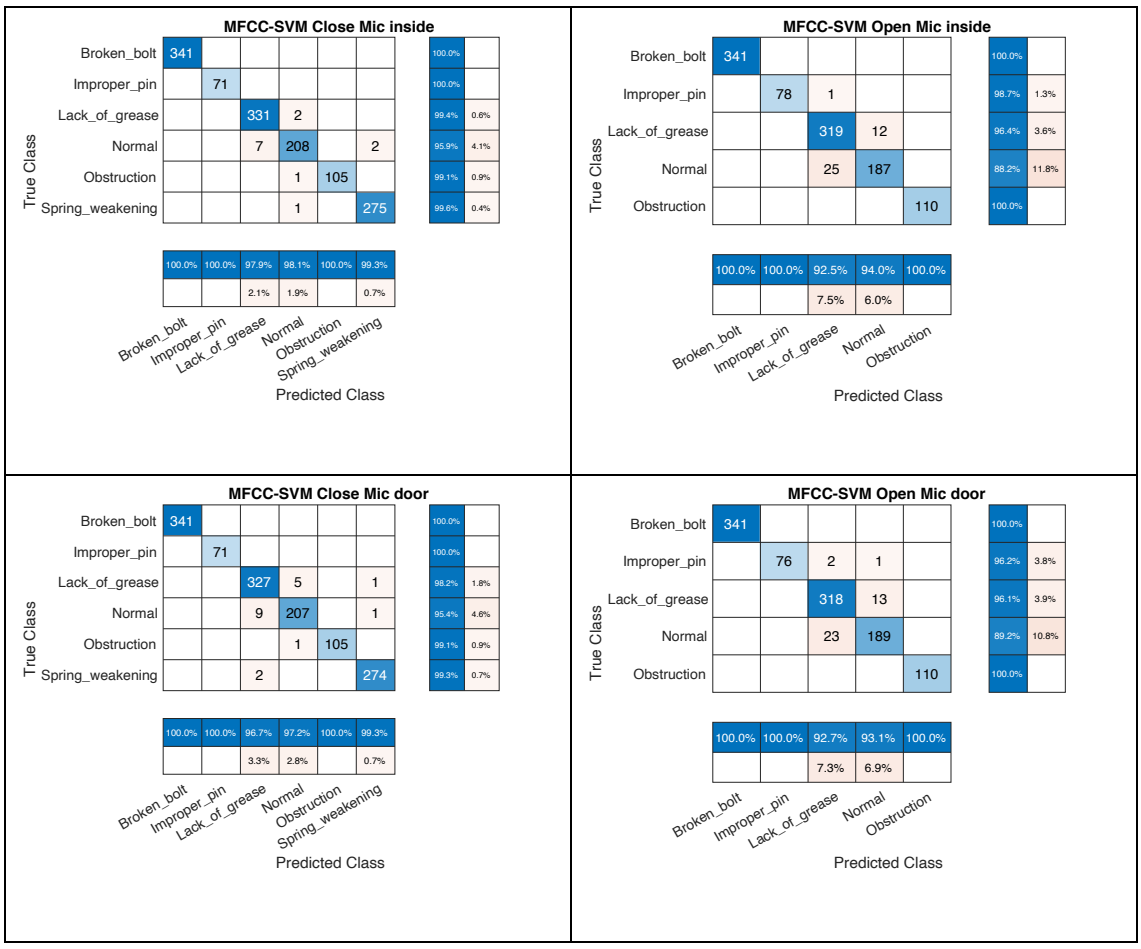


Figure 33. Diagnostic results by MFCC-SVM

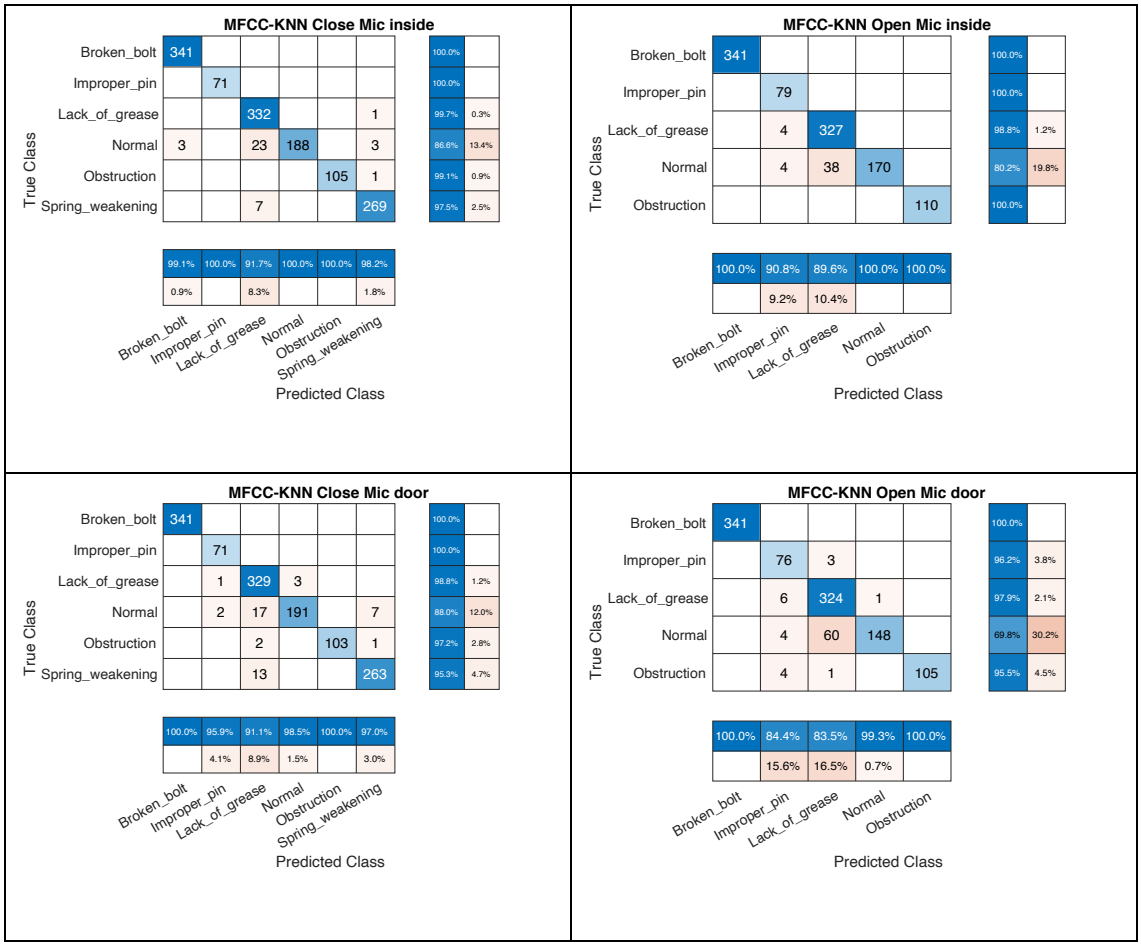


Figure 34. Diagnostic results by MFCC-KNN

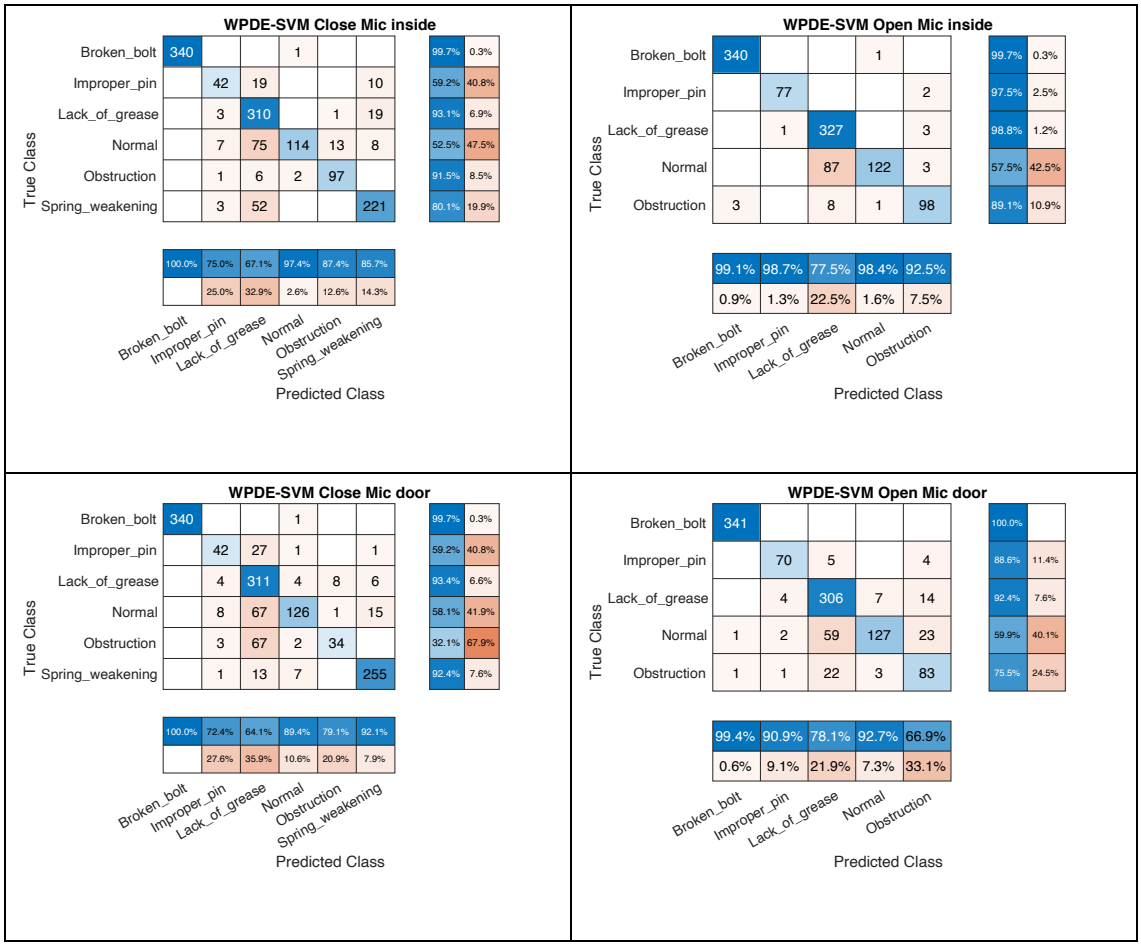


Figure 35. Diagnostic results by WPDE-SVM

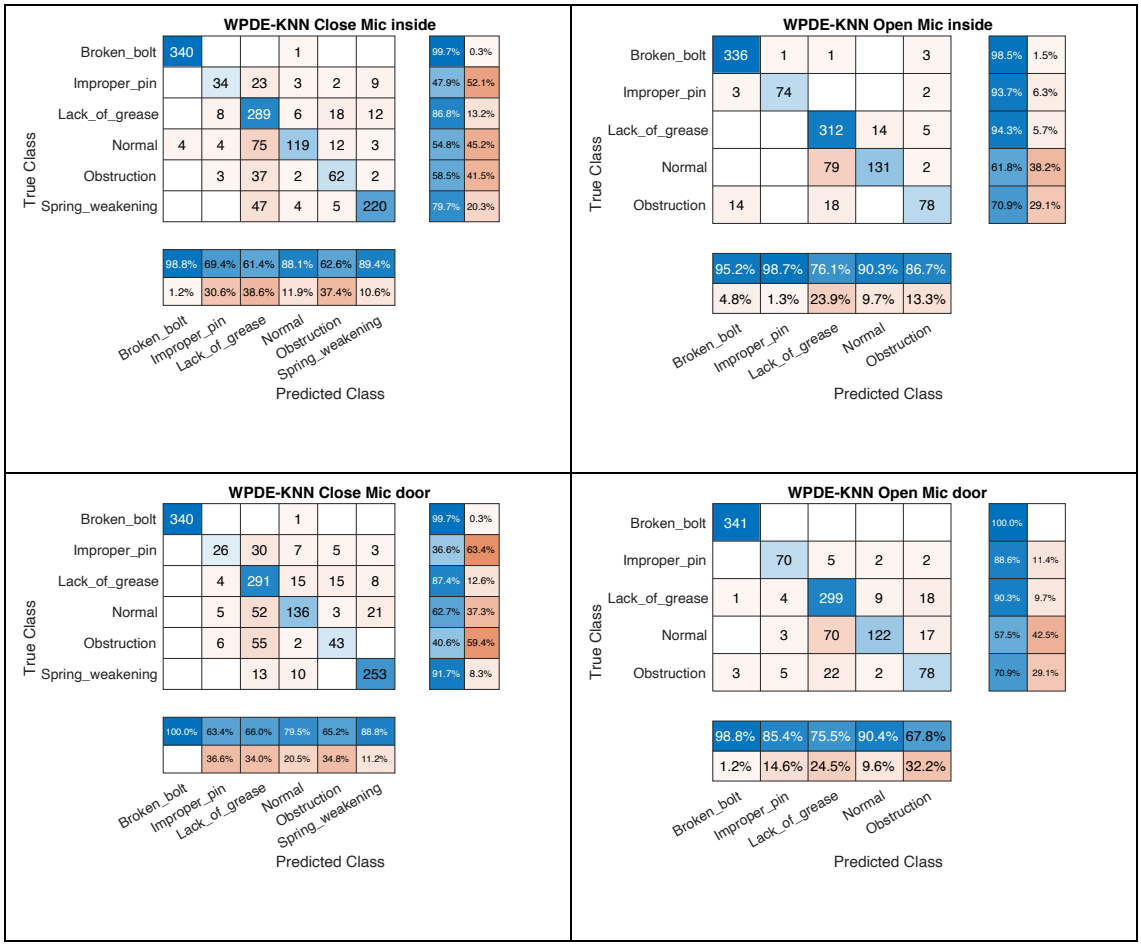


Figure 36. Diagnostic results by WPDE-KNN

Whichever feature is used, there is misdiagnosis of the normal state, lack of grease, and spring weakening, suggesting that the operating sound of these cases may be similar. For lack of grease, open data have a higher number of misdiagnoses. This is probably related to the SNR mentioned above, and in addition to this, the grease itself is used to smooth high-speed movement when the contactor is closed; the closed data seem to have a greater effect in acoustic data without grease. In the case of improper pin position and obstruction, there are many misdiagnoses with WPDE but few with MFCC. Frequent misdiagnosis using WPDE indicates that there is little difference in each frequency band, although there is some difference in the time component. Since the MFCC classified it accurately, it is inferred that a subtle abnormal noise or delay occurred. Even in the analysis of WPDE, the inside mic data have fewer

misdiagnoses, which supports the fact that the inside mic can detect minute differences. In the case of a broken bolt, the diagnostic accuracy is almost 100%, suggesting a clear difference in the operating sound. In this study, each piece of operation data was verified one by one. Since spring weakening and lack of grease faults progress gradually, it is highly likely that the data before and after the test data are also fault data. A higher fault detection accuracy can be expected by verifying multiple data (3 to 5 operations) instead of diagnosing data one by one.

## 5.4 The effect of noise

To investigate the effect of noise, white noise was added to the acoustic data acquired by the microphone. Since the frequency of noise generated around the target is not constant, white noise uniformly distributed over the whole frequency range was used to investigate the effect of general noise. The SPL of the noise to be added were 37 dB and 55 dB, which corresponds to light and heavy rain, respectively. Table 10 and Table 11 show the results of adding noise. No combination of features and classifiers significantly reduced the accuracy of the diagnosis when 55 dB of noise equivalent to heavy rain was added. In the case of MFCC-SVM, the Recall accuracy was reduced by up to 0.9% and the F1 score accuracy by about 0.8%, but it could be said that the classification accuracy was sufficiently high even when there was noise. In the case of MFCC-KNN, it was found that the addition of noise had no effect on the Recall rate or F1 score. MFCC-SVM was the most accurate when there was no noise, but MFCC-KNN was more accurate when there was heavy rain-level noise. WPDE-SVM was found to have little impact on accuracy even when there was noise. In the case of the closed data of WPDE-KNN, the Recall was reduced by 0.4% and the F1 score was also reduced by 0.3% by the addition of noise. A review of these results shows that noise does not significantly

affect diagnostic results. To investigate the further effect of noise, the accuracy was investigated by adding more than 55 dB noise.

Table 16. Recall of fault diagnosis with 37 dB noise

| Feature | Classifier | Mic | Closed | | Open | |
|---|---|---|---|---|---|---|
| | | | Recall [%] | F1 score [%] | Recall [%] | F1 score [%] |
| MFCC | SVM | Inside | 99.4 | 99.1 | 99.0 | 98.3 |
| | | Door | 99.5 | 99.1 | 97.9 | 97.6 |
| | KNN | Inside | 98.9 | 98.9 | 99.9 | 97.8 |
| | | Door | 98.5 | 98.5 | 99.8 | 96.0 |
| WPDE | SVM | Inside | 99.7 | 95.0 | 99.6 | 94.7 |
| | | Door | 98.4 | 94.8 | 98.7 | 94.3 |
| | KNN | Inside | 98.0 | 94.1 | 98.5 | 94.4 |
| | | Door | 96.2 | 94.0 | 99.1 | 94.2 |

Table 17. Recall of fault diagnosis with 55 dB noise

| Feature | Classifier | Mic | Close | | Open | |
|---|---|---|---|---|---|---|
| | | | Recall [%] | F1 score [%] | Recall [%] | F1 score [%] |
| MFCC | SVM | Inside | 99.0 | 98.6 | 99.0 | 98.3 |
| | | Door | 98.6 | 98.5 | 98.0 | 97.5 |
| | KNN | Inside | 100.0 | 98.9 | 100.0 | 97.8 |
| | | Door | 99.6 | 98.6 | 99.9 | 96.1 |
| WPDE | SVM | Inside | 99.7 | 95.0 | 99.6 | 94.7 |
| | | Door | 98.4 | 94.8 | 98.7 | 94.4 |
| | KNN | Inside | 97.9 | 94.1 | 98.5 | 94.4 |
| | | Door | 96.1 | 94.0 | 99.1 | 94.2 |

For noise louder than 55 dB, the SPL was determined by referring to the sound of passing trains, since STME is often used for railway facilities. In Japan, there is an upper limit on the noise generated by the Shinkansen bullet train. The standards for regulating the environmental conditions of Shinkansen noise are established to preserve the living environment and contribute to protecting people's health [148]. According to this standard, the noise generated by the Shinkansen should be 70 dB or less in residential areas and 75 dB or less in other areas, including commercial and industrial areas, where the normal living conditions shall be preserved. Zannin *et al.* measured the noise of trains passing through residential areas

in large Latin American cities. According to their measurements, the noise levels in the proximities of the rail line varied from 68 to 80 dB [149]. In this study, noise of 80 dB was added on the assumption that the equipment was installed beside a railway. The diagnostic results with noise of 80 dB are shown in Table 18.

The closed data result with noise of 80 dB showed improved accuracy in most combinations compared to the one with noise of 37 dB, and 55 dB. On the other hand, in the case of open data, it was found that the accuracy was degraded in most combinations, except WPDE-SVM. Figure 37 shows the variation in diagnostic result when noise was added; the evaluation was performed by multiplying the Recall and F1 score by the root, so that both Recall and F1 score values can be considered.

Table 18. Recall of the fault diagnosis with 80 dB noise

| Feature | Classifier | Mic | Closed | | Open | |
|---|---|---|---|---|---|---|
| | | | Recall [%] | F1 score [%] | Recall [%] | F1 score [%] |
| MFCC | SVM | Inside | 99.6 | 99.2 | 98.3 | 97.9 |
| | | Door | 99.0 | 98.8 | 97.8 | 97.5 |
| | KNN | Inside | 100.0 | 98.9 | 99.9 | 97.5 |
| | | Door | 99.9 | 99.0 | 99.8 | 95.4 |
| WPDE | SVM | Inside | 99.7 | 95.4 | 99.8 | 94.8 |
| | | Door | 99.2 | 95.2 | 100.0 | 94.8 |
| | KNN | Inside | 97.9 | 94.4 | 98.7 | 94.4 |
| | | Door | 96.5 | 93.9 | 98.5 | 93.9 |

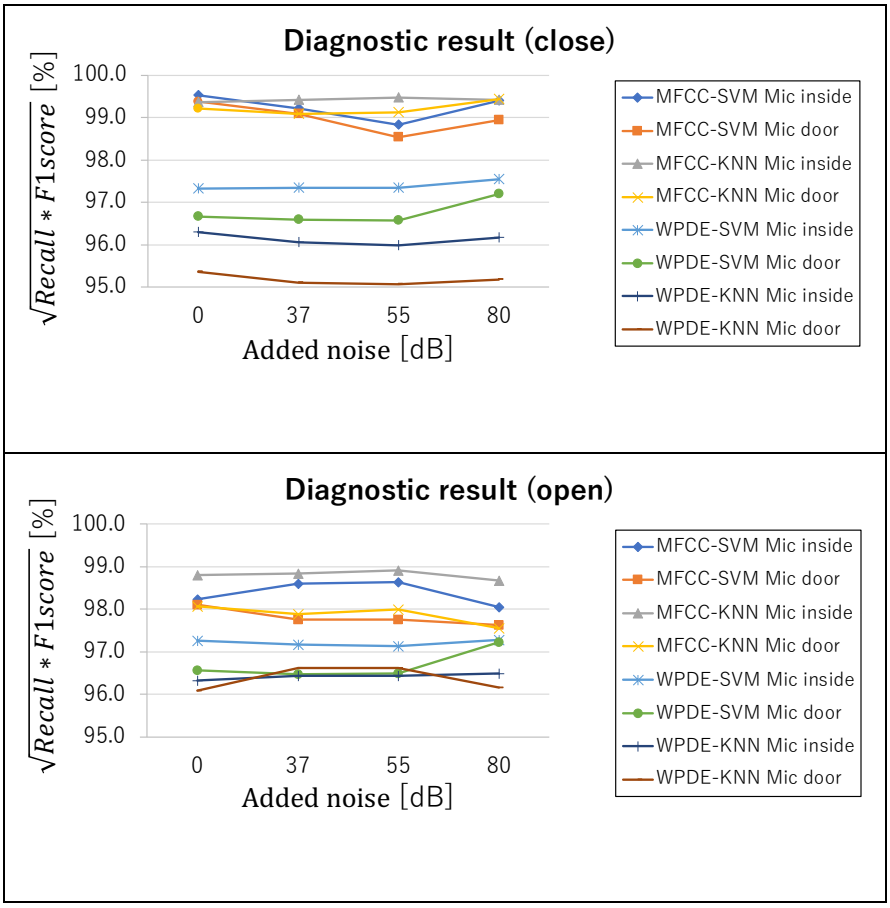


Figure 37. Variation in diagnostic accuracy with noise (up to 80 dB)

When noise is added, the accuracy is expected to decrease as the noise is louder, but the opposite phenomenon occurred in the closed data. When 37 and 55 dB noise was added, the accuracy decreased, but when 80 dB noise was added, the accuracy increased. The reason for this may be that the added noise made a difference in the features used for diagnosis. Since the SPL of the contactor is large, the addition of 37 dB or 55 dB may not be enough to mask its acoustic data. Instead, it is likely that acoustic data of other machines are drowned out by the white noise. When acoustic data are collected by a microphone, sounds from equipment other than the target machine are also collected. Although these sounds did not originally contain useful information to diagnose the condition of the target, they may have influenced the classification. When there was no noise, high diagnostic accuracy was obtained in this study, which might be due to the use of subtle noise changes as feature values other than changes in

the acoustic data of the target device. To give a specific example, if a machine other than the target is operating during the acquisition of normal data of the target and the machine is not operating during the acquisition of simulated fault data of the target, the normal data contain the operating sound of the machine as features. The classifier may also use its operating sound features for classification. By adding white noise, those fine noises were masked, and accuracy might become decreased. Figure 38 shows the spectrograms of the signals with 37 dB and 55 dB noise. Since the SPL of the operating sound of the contactor is large, it can be seen that white noise hardly affects the acoustic data of the contactor.

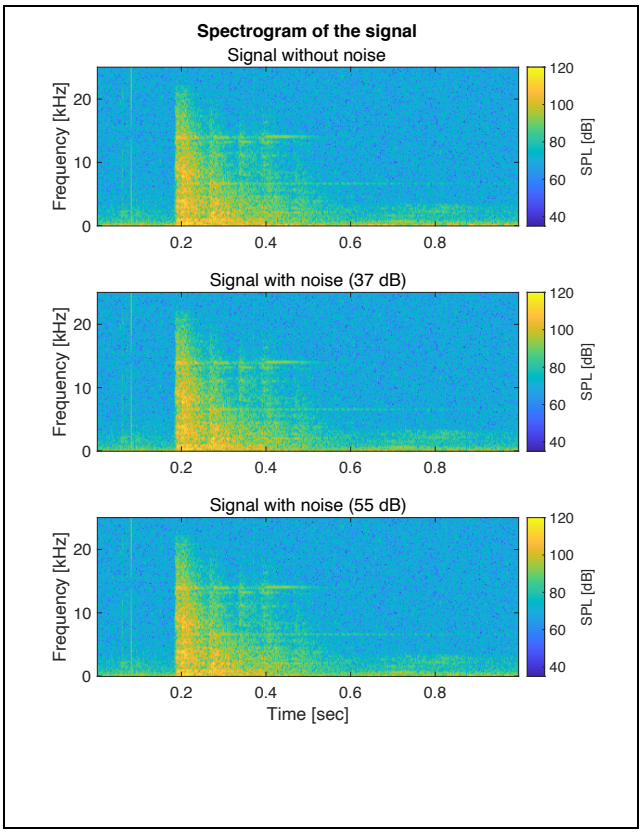


Figure 38. Spectrogram of the signal with noise (Closed data, 37 dB and 55 dB)

The reason for the increased accuracy when 80 dB noise was added might be that part of the acoustic data that are not necessary for fault classification was masked. When the SPL of an important part for fault classification is large and the SPL of an unrelated part is small, it

is considered that the 80 dB noise drowns out the unrelated part and increases the accuracy. The spectrogram with 80 dB noise is shown in Figure 39. It can be confirmed that the operating sound of low frequency, less than 500 Hz, at around 0.0~0.2 seconds and the sound at around 0.5~0.9 seconds were drowned out a little bit by the white noise. On the other hand, there seems to be no significant effect on the waveform at around 0.2~0.4 seconds. This can be seen more clearly when 100 dB noise is added. A spectrogram with 100 dB noise is also shown in Figure 39. All but the strongest sound in the 0.2~0.4 second interval is drowned out by noise. Even when 100 dB of noise was added, Recall and F1 score were greater than 95% when MFCC was used as a feature; therefore, it can be said from this analysis that the data in this area is highly important in diagnosing the condition of the contactor.

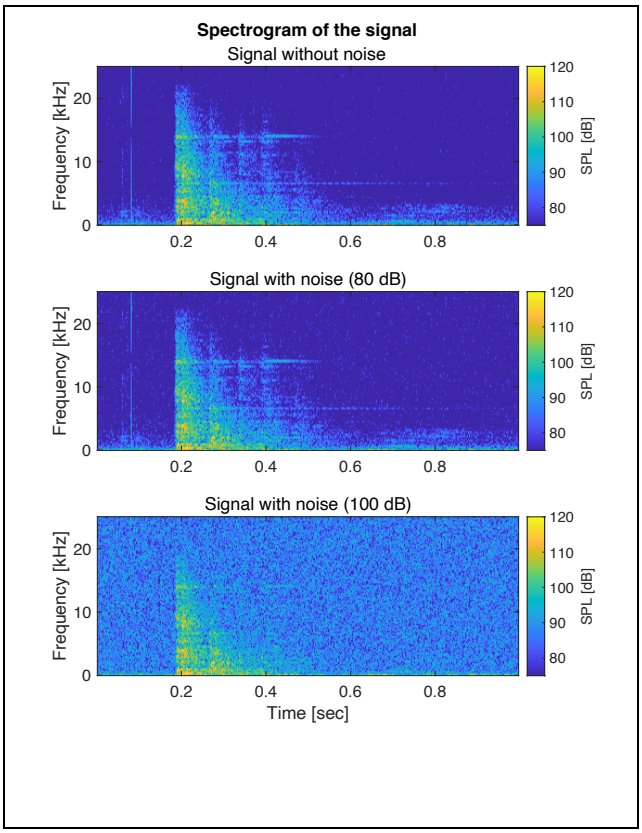


Figure 39. Spectrogram of the signal with noise (Closed data, 80 dB and 100 dB)

According to the results of the analysis above, the classification accuracy increases because the addition of noise with a certain SPL can drown out acoustic data that are not important for classification. However, if a louder noise is added, even important parts are drowned out, which is expected to reduce the accuracy. To test this hypothesis, further investigation of the trend was done by adding more noise. If the hypothesis is correct, adding a certain amount of noise will drown out the parts that are not necessary for classification and increase the accuracy, but the effect of noise will appear from a certain point as an important part is drowned out, and decrease the accuracy. The SPL of added noise were 70 dB, 90 dB, and 100 dB. Figure 40 shows the transition of classification results when noise was added.

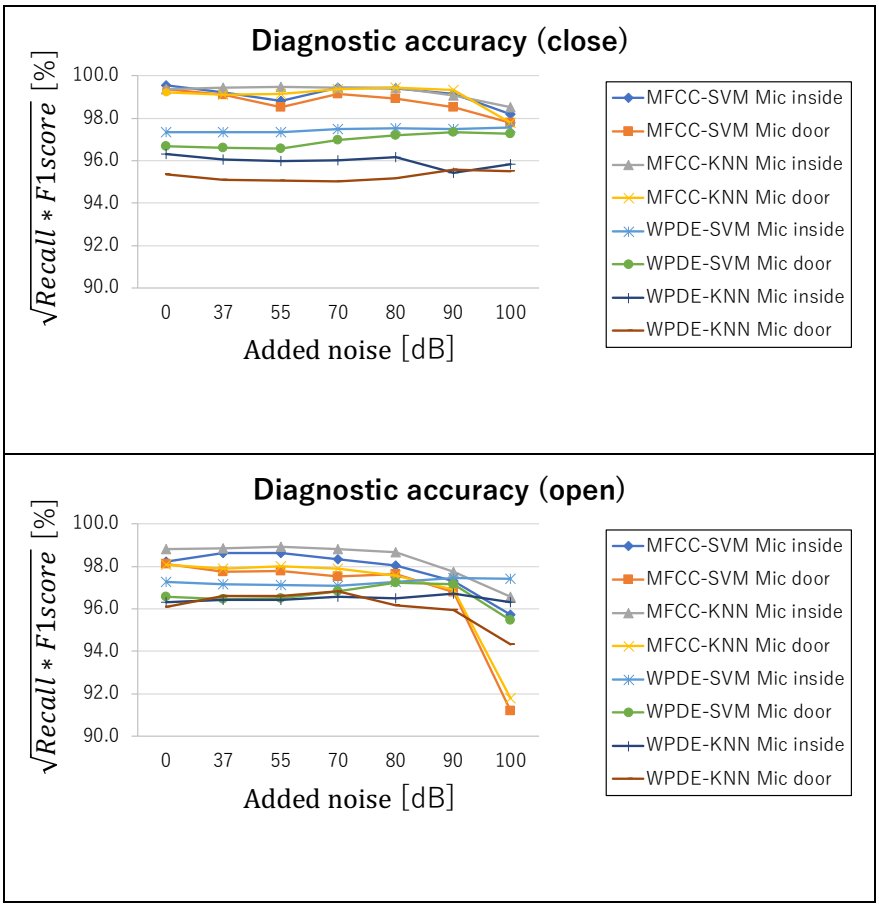


Figure 40. Variation in diagnostic accuracy with noise (up to 100 dB)

As mentioned above, in the case of closed data, adding a small noise slightly increased the accuracy, and adding a large noise seemed to affect the parts that were important for classification and decreased the accuracy. The phenomenon where the accuracy increased by adding a small amount of noise could not be confirmed in open data, but the accuracy decreased rapidly by increasing the SPL of the noise. This is probably because the noise drowned out most of the acoustic data of the contactor. Although a sharp drop has not been confirmed in the closed data, it is expected that adding noise of more than 100 dB reduces the accuracy as it does for the open data.

This analysis shows that the proposed method is highly resistant to noise. Both closed and open configurations can diagnose the condition with high accuracy, but closed data can diagnose the condition with greater accuracy. It was found that MFCC was more accurate than WPDE, but in the case of MFCC, the accuracy decreased as the noise increased. However, when closed data are used for analysis, the accuracy of WPDE exceeds MFCC when the noise exceeds 100 dB. Since it is unlikely that noise exceeding 100 dB would be mixed in with data under a monitoring environment (if noise exceeding 100 dB is mixed in with the monitoring data, measures such as installing a sound barrier between the noise source and the microphone or installing the microphone closer to the target should be taken), it can be said that using MFCC as a feature can diagnose the condition with the highest accuracy. The above analysis proves that the method proposed in this study can accurately diagnose the condition of the contactor. It was also found that high accuracy can be maintained even when there is noise such as rain.

## 5.5 Summary and findings

The hypothesis, described in Chapter 1, is that even in the case of an initial fault, the operating sound of STME changes due to damage or deformation of the parts, making it possible to detect and diagnose the faults by acoustic data. In the case study of this chapter, it was clarified that the contactor's faults could be diagnosed with high accuracy even in the initial condition. Answers to the following research questions were also able to be obtained.

- Which algorithm is most appropriate?

The verification shows that the combination of MFCC and KNN (MFCC + KNN) is the most accurate for fault detection. The combination of MFCC and SVM (MFCC + SVM) also gives sufficient accuracy, being found to be only slightly less accurate than MFCC + KNN. MFCC + KNN is the most accurate combination for classifying normal and abnormal states, but it also misdiagnoses some faults as other ones. On the other hand, MFCC + SVM is more accurate than MFCC + KNN in diagnosing faults. It can be said that the combination of MFCC and SVM is the best overall. Using WPDE, it was found that faults could be diagnosed with some degree of accuracy for some faults, although the accuracy was lower than that of MFCC.

- How accurate is the system and does that vary by fault?

When the MFCC is used as the feature for closed data, faults can be detected with more than 99% accuracy and all faults can be diagnosed with an accuracy of more than 95%, but some normal data are misdiagnosed as lack of grease, and the diagnostic performance of normal data falls below 90%. The diagnostic accuracy of the closed data is higher than that of the open data. Diagnostic performance for all faults is high, but the accuracy for a lack of grease is low compared with the others, and there are some misdiagnoses with normal, suggesting that there

are small differences between a lack of grease and normal data. It was found that the use of KNN as a classifier also reduces the diagnostic performance of spring weakening.

- How tolerant is it to noise?

Noise was added to the data to investigate the effect on the system of noise. The results showed that the addition of noise equivalent to heavy rain (55 dB) had little effect on diagnostic accuracy. It was also found to be tolerant to the level of noise of trains passing through (90 dB). Adding noise slightly improved the diagnostic accuracy. This may be because the added white noise drowned out other noise recorded by the microphone unrelated to the condition diagnosis, and only high SPL sounds important for diagnosis were used for classification.

- Which microphone position is most appropriate?

The investigation results showed that the microphone inside the cabinet was more accurate than was the door one. One of the reasons for this is that the SPL of the contactor is higher because the inside microphone is closer to the contactor compared to the door one, and it is placed inside the cabinet so there is no barrier between the microphone and target. Another possible reason is that while the door microphone outside the cabinet was directly affected by the operating noise of other machines, the inside microphone was located inside the cabinet, making it difficult for noise from other machines to mix in. The results show that it is desirable to set the microphone as close to the observation target as possible and acquire the target data at a high SPL. It was also found that when the object is placed inside the cabinet, placing the microphone inside the cabinet makes it less susceptible to external noise and is ideal.

# CHAPTER 6 TRANSFERABILITY

## 6.1 Introduction

From the validation in Chapters 4 and 5, it became clear that it is possible to diagnose the condition of STME from acoustic data. However, the fault diagnosis model must have transferability to be used in practical deployment. Transferability is the ability of a model, trained by data acquired from one machine, to diagnose faults in other machines. Since it is difficult to obtain simulated fault data from all the machines used in the industry, it is necessary to obtain simulated fault data from several machines, train the model with the data, and monitor all the machines with the model. Transferability of the model is essential to realise this. Image of the transferability of a model are shown in Figure 41 and Figure 7. To monitor machines in operation, it is necessary to acquire simulated fault data from several machines and make the model with normal data from many machines in operation as shown in Figure 41. This model should be used to monitor many machines in operation. Normal and simulated fault data were acquired from contactors A and C in this study. In the investigation of transferability, a model was created using normal data from both contactors and simulated fault data from one contactor in the training phase as shown in Figure 7. The transferability was investigated by determining whether the model can detect other fault data that are not in the training data set.

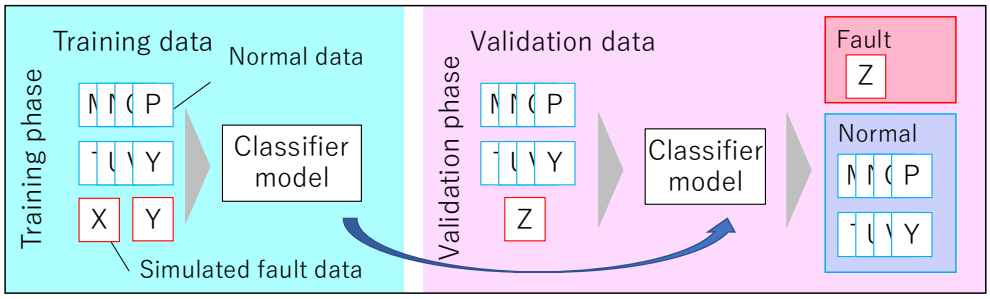


Figure 41. Transferability of the model in practical development

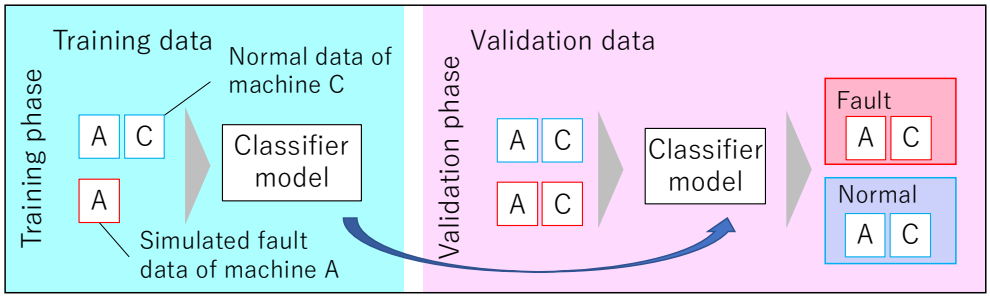


Figure 42. Transferability investigation of this study

## 6.2 Transferability experiment

Additional experiments were conducted to investigate the transferability in this study. In this section, the same method used in Chapter 5 was used for contactors to investigate the transferability at first. As a result of the analysis, it was not possible to obtain high performance by using same method, so additional investigation was needed for improvement. Details of the improvements are described in the next section.

In this experiment, the target is the contactor, and the MFCC, which proved to have the best fault diagnosis performance, was used as the feature. As for classifiers, both SVM and KNN, which showed high performance, were used to compare the accuracy and to validate which is more suitable for practical use. The contactor used in this experiment was contactor C, installed inside the same cabinet as contactors A and B, used in Chapter 5. As in the experiment

described in Chapter 5, one microphone was installed next to the contactor in the cabinet (mic inside) and another in front of the cabinet door (mic door), and the type of microphone was the same as that used in Chapter 5. Microphone positions are shown in Figure 10. The data of mic inside were used for transferability analysis as the diagnostic results were better than those of mic door. The simulated faults were also the same as in Chapter 5 (lack of grease, spring weakening, improper pin position and obstruction) and the level of spring weakening and obstruction was set to 1 mm in this case. About 50 data were acquired for all faults. Since more than 50 normal data could not be acquired in the December 2022 experiment, normal data acquired in January 2021 were also used for validation. The test schedule is shown in Table 8.

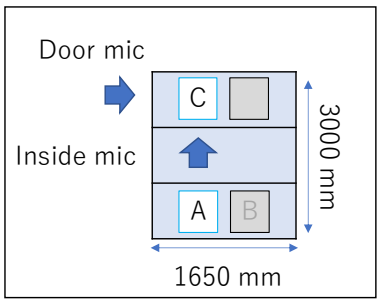


Figure 43. Location of measuring equipment and contactors

Table 19. Test schedule

| Date | Data type | Contactor | Number of data<br>Closed | Number of data<br>Open |
|---|---|---|---|---|
| Sep 2020 | Normal | A | 118 | 117 |
| Jan 2021 | Normal | C | 234 | 241 |
| Feb 2021 | Normal | A | 99 | 95 |
| | Lack of grease | | 333 | 331 |
| | Obstruction | | 106 | 110 |
| | Spring weakening | | 276 | 241 |
| | Improper pin position | | 71 | 79 |
| Dec 2022 | Normal | C | 25 | 25 |
| | Lack of grease | | 54 | 54 |
| | Obstruction | | 54 | 54 |
| | Spring weakening | | 53 | 53 |
| | Improper pin position | | 50 | 50 |

The same algorithm used in Chapter 5 was used for the data of contactors A and C. One of the contactor's data were used for training and those of the other one were used for

validation. The results are shown in Figure 44 and Figure 45. In the case of MFCC + SVM, all data were classified as ‘improper pin position’ and as ‘lack of grease’ or ‘normal’ in the MFCC + KNN case. The reason for this result is that each contactor has its own unique features, and data from the same contactor can be classified without any problem as the model can capture its characteristics; however, when it comes to classifying a different contactor’s data, the model does not have the characteristics of the target, and is trained based on the characteristics of a different contactor, which may cause confusion and misclassifies data into different classes. The number of features used in this analysis is 3528, but the number of features that are important for classification may be limited.

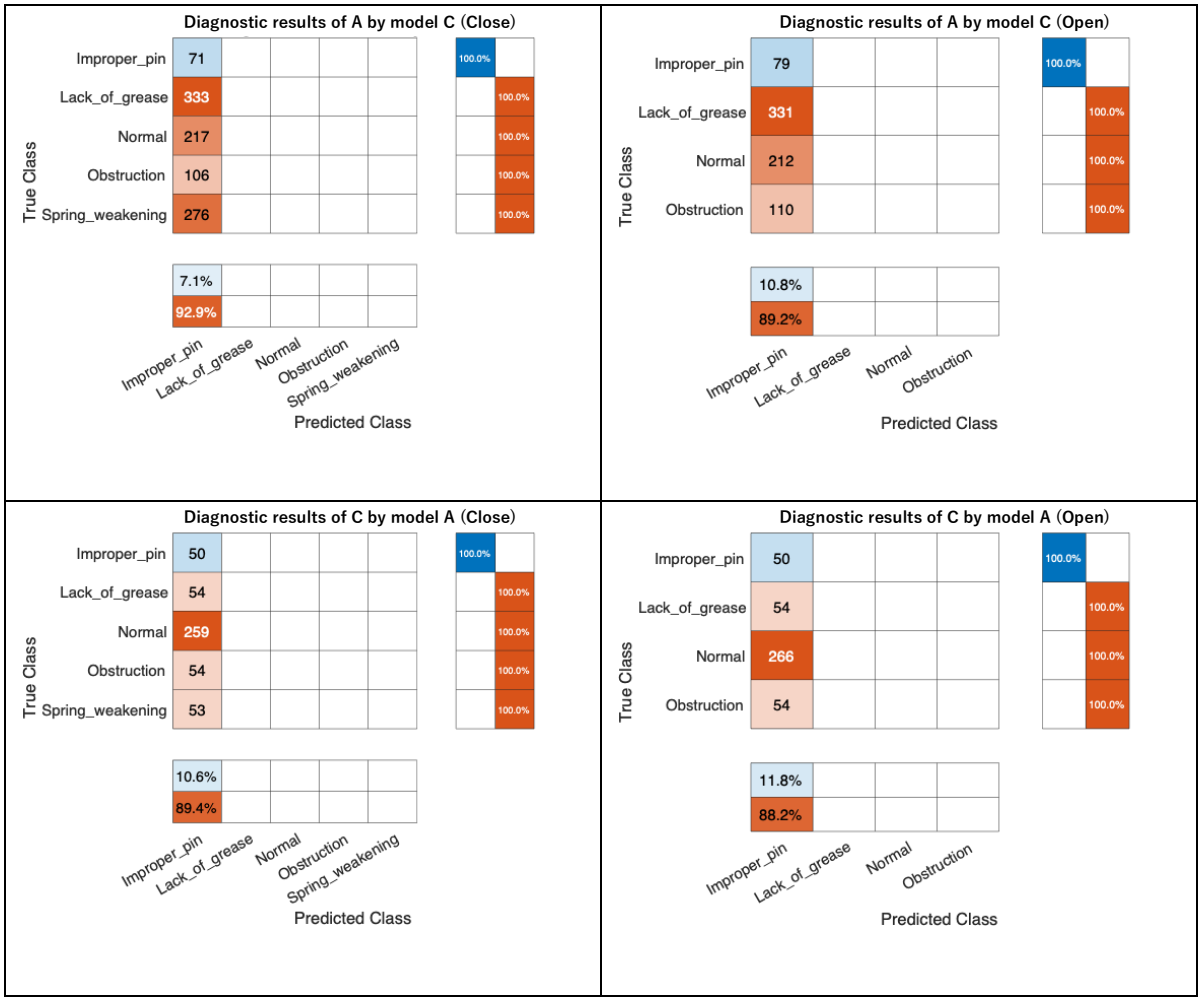


Figure 44. Transferability performance (MFCC + SVM)

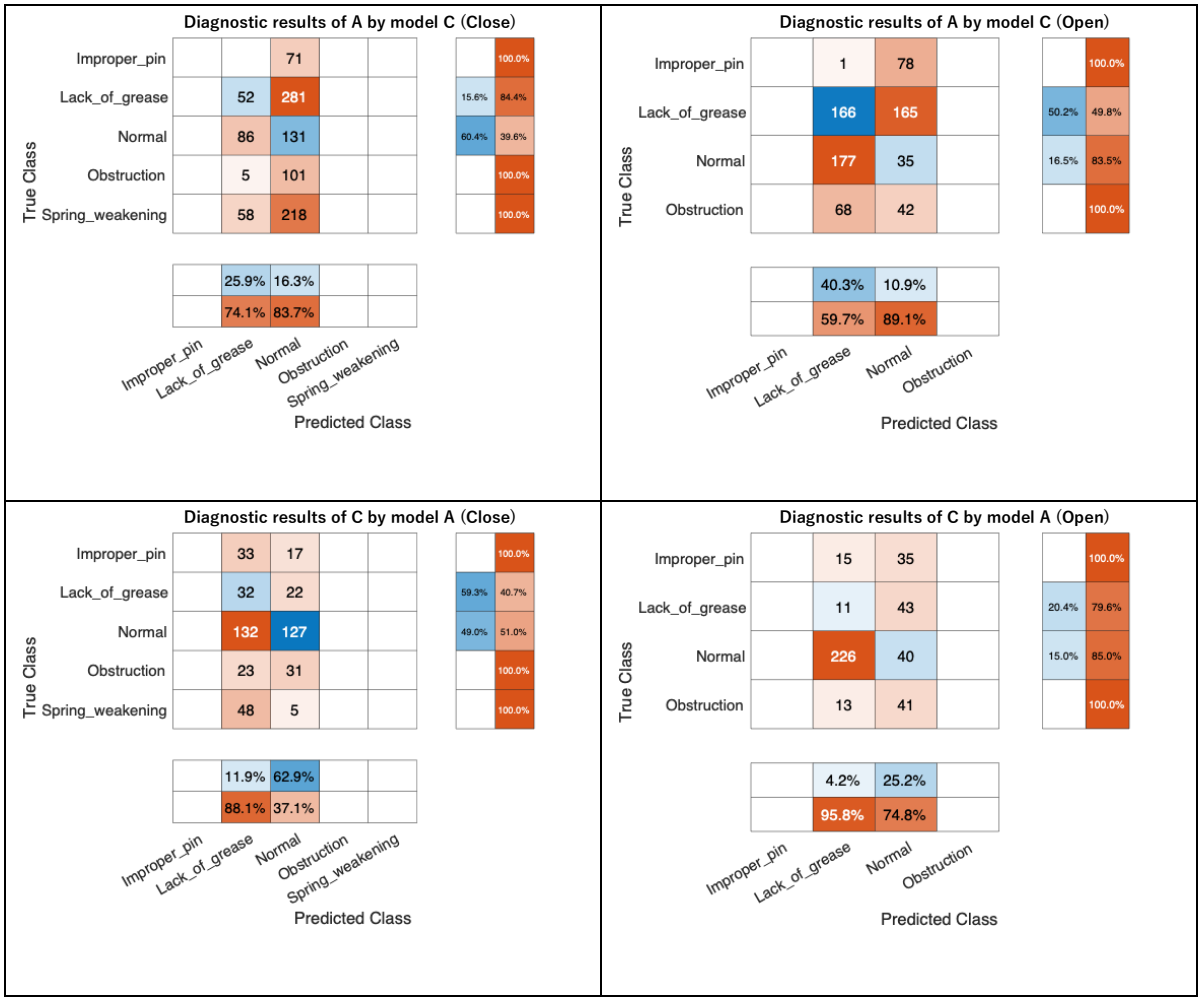


Figure 45. Transferability performance (MFCC + KNN)

## 6.3 Feature selection

To improve model transferability, it is necessary to remove the unique characteristics and find the common ones for each fault. To investigate which features are important in classifying each fault, the importance of each feature was investigated using techniques called Principal Component Analysis (PCA) and Minimum Redundancy Maximum Relevance (MRMR). PCA and MRMR are two commonly used techniques to reduce the dimensionality of data in the field of machine learning and data analysis [150, 151]. Investigation was done by using 'obstruction' closed data that were likely to have common characteristics in the data of both contactors. Randomly selected 50 normal and obstruction data were used for training,

regardless of the contactor, although there were more than 50 obstruction data in contactor C, because there were only about 50 obstruction data in contactor A.

### 6.3.1 Principal Component Analysis

PCA is a linear dimensionality reduction technique used to reduce the number of features in a dataset while retaining most of the important information. The main idea behind PCA is to project high-dimensionality data onto a lower-dimensionality subspace, where the data variance is maximised. The advantages of PCA include its ability to reduce the dimensionality of large datasets, identify underlying patterns in the data, and improve the computational efficiency of machine learning algorithms. However, PCA assumes that the data are linearly correlated, and it may not work well if the data have a non-linear structure. Therefore, an investigation was conducted to see how the transferability performance could be improved by using PCA. The Explained Variance Ratio (EVR) must be determined when using PCA. The EVR is a metric used in PCA to assess the amount of information captured by each principal component in a dataset. It measures the proportion of the total variance in the original data that is explained by each principal component and is typically expressed as a percentage. In the investigation, the MATLAB pca function was used for calculation of features, and EVR was varied from 80% to 95% in 5% increments. The accuracy was measured in each case. The results are shown in Table 20 and Table 21. The analysis result of the contactor A data for the model trained by contactor C data is described as ‘result of A by model C’. The results show that using PCA does not improve the transferability of the model for the data of either contactor. The PCA was expected to select important features for detecting ‘obstruction’ and improve transferability performance, but no improvement in performance was observed using either classifier. Since PCA is a dimensionality reduction technique and does not consider the

classification importance of the features, this may be the reason why PCA could not improve transferability performance.

Table 20. Transferability performance for obstruction (MFCC + PCA + SVM)

| EVR [%] | Result of A by model C | | Result of C by model A | |
|---|---|---|---|---|
| | Recall [%] | F1 score [%] | Recall [%] | F1 score [%] |
| 80 | 17.9 | 30.2 | 0.0 | 0.0 |
| 85 | 29.2 | 44.9 | 0.0 | 0.0 |
| 90 | 18.9 | 31.7 | 0.0 | 0.0 |
| 95 | 18.9 | 31.7 | 0.0 | 0.0 |

Table 21. Transferability performance for obstruction (MFCC + PCA + KNN)

| EVR [%] | Result of A by model C | | Result of C by model A | |
|---|---|---|---|---|
| | Recall [%] | F1 score [%] | Recall [%] | F1 score [%] |
| 80 | 100.0 | 29.4 | 95.3 | 55.2 |
| 85 | 100.0 | 29.4 | 89.6 | 50.5 |
| 90 | 100.0 | 29.4 | 100.0 | 50.8 |
| 95 | 100.0 | 29.4 | 90.6 | 49.5 |

### 6.3.2 Minimum Redundancy Maximum Relevance

MRMR is a feature selection technique used to select the most informative features from a dataset by maximising the relevance of the features to the target variable and minimising the redundancy between the selected features. The main advantage of MRMR is that it can identify the most important features in a dataset, which can improve the accuracy of machine learning models and reduce overfitting. However, MRMR can be computationally expensive and may not work well if the data have a high degree of correlation between the features [150]. Therefore, an investigation was conducted on how the transferability performance of each classifier could be improved by using MRMR. For feature calculation, the fscmrmr function was used. Table 22 and Table 23 show the classification accuracy when MRMR is used for each classifier. It was found that it is possible to improve the transferability by using only a small number of important features, both SVM and KNN can classify data with high accuracy, and better performance can be acquired with fewer features. Comparing the results for SVM and KNN, it appears that SVM performs better when using fewer features.

Table 22. Transferability performance for obstruction (MFCC + MRMR + SVM)

| Number of features used | Result of A by model C | | Result of C by model A | |
|---|---|---|---|---|
| | Recall [%] | F1 score [%] | Recall [%] | F1 score [%] |
| 30 | 74.1 | 44.0 | 98.1 | 74.1 |
| 10 | 83.3 | 61.2 | 100.0 | 97.3 |
| 5 | 100.0 | 71.1 | 100.0 | 94.7 |
| 2 | 100.0 | 77.1 | 100.0 | 100.0 |

Table 23. Transferability performance for obstruction (MFCC + MRMR + KNN)

| Number of features used | Result of A by model C | | Result of C by model A | |
|---|---|---|---|---|
| | Recall [%] | F1 score [%] | Recall [%] | F1 score [%] |
| 30 | 99.1 | 55.0 | 83.3 | 52.0 |
| 10 | 70.8 | 50.2 | 79.6 | 62.3 |
| 5 | 62.3 | 67.0 | 98.1 | 71.1 |
| 2 | 95.3 | 97.1 | 100.0 | 79.4 |

MRMR uses relative information to capture non-linear relationships between features, whereas PCA is a linear transformation technique that captures the maximum variance in the data. While PCA can reduce the dimensionality of the data, it may not always select the most informative features for prediction tasks. On the other hand, MRMR can select relevant features that are most informative for the task at hand, leading to improved accuracy. This is why MRMR can improve the transferability of the model. The distribution of features selected by MRMR is shown in Figure 46. It can be confirmed that normal and obstruction data of contactors A and C are clearly separated.

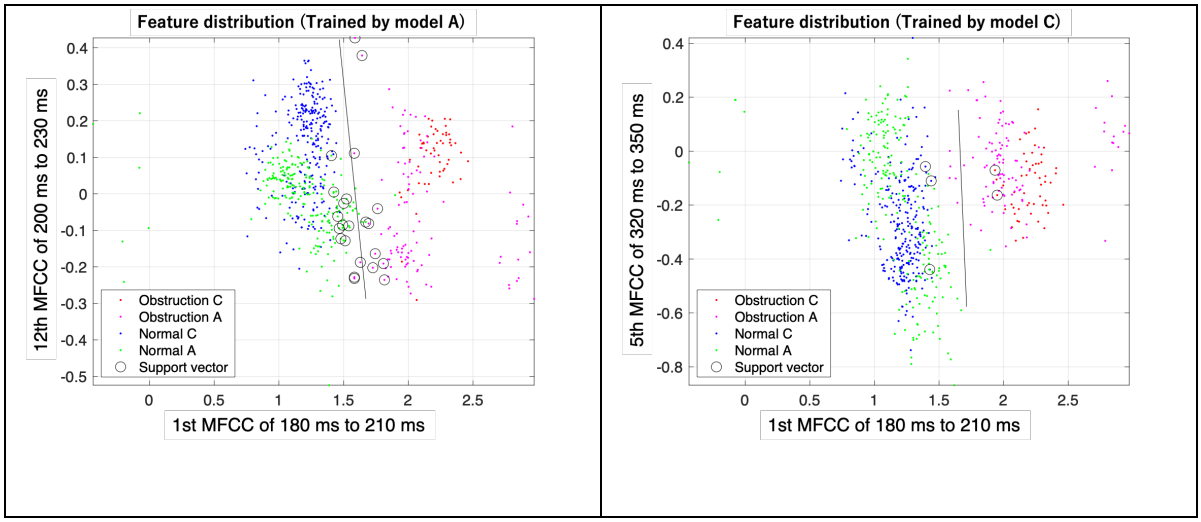


Figure 46. Distribution of selected features

Analysis of both contactors' data revealed that the most important feature was the MFCC, calculated from window frames in the 180 ms to 210 ms part of the analysis data. In the presence of obstruction, this MFCC was found to become large. Figure 47 shows the MFCC for normal and obstruction conditions. In both cases of contactors A and C, it can be seen that the value near the 19th position of the first MFCC becomes stronger. A larger first coefficient of MFCC indicates a smaller distribution of frequency components in this analysis window frame. For comparison, Figure 47 also shows a spectrogram of the data in this analysis window frame. It was confirmed that the frequency distribution range was smaller when there was an obstruction compared with the normal case. In this experiment, a piece of cloth was used for the obstruction, which seems to have absorbed the high-frequency sound generated by the impact of the blades and reduced the distribution of the frequency components, and this is expected to happen when dust accumulates on the blade. Furthermore, because changes occur in the MFCC of the analysis window frame including the moment when the obstruction collides with the blade, if the size of the obstruction is larger than in this case, it is expected that the value of the MFCC of the former analysis window frame will change. The spectrograms and MFCC for 1 mm and 5 mm obstructions are shown in Figure 48. In the case of a 5 mm

obstruction, the blade collides with the object faster, resulting in a collision sound before 200 ms. This increases the value of MFCC of the former time frame compared to the 1 mm case. From this verification, it was confirmed that any contactor with an obstruction causes a change in the MFCC when the blade collides with it. It was also clarified that the size of the obstruction can be diagnosed by the position of the changing MFCC.

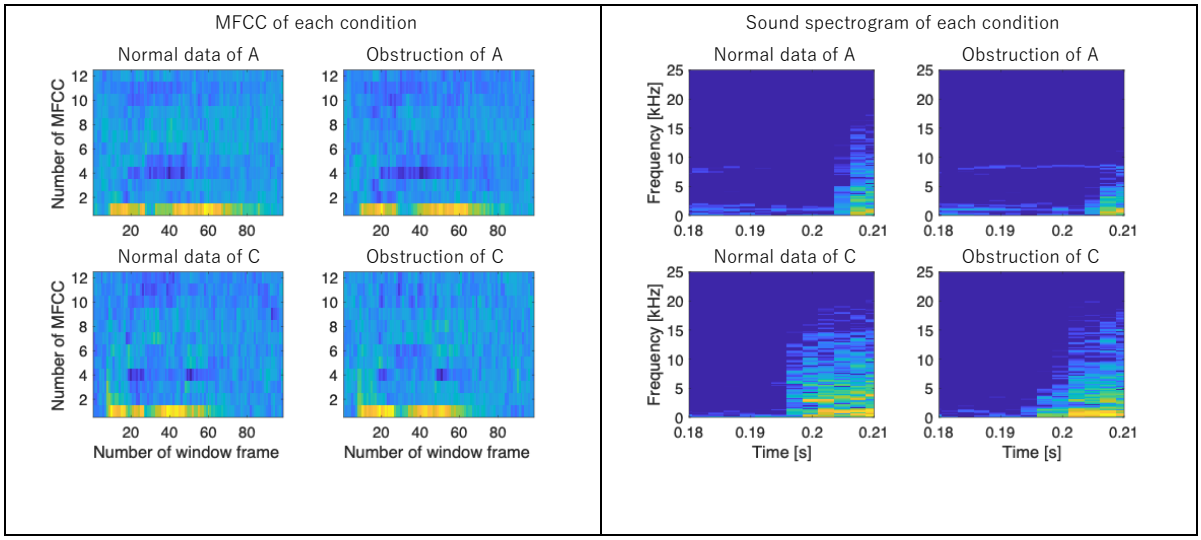


Figure 47. MFCC and sound spectrogram for each condition

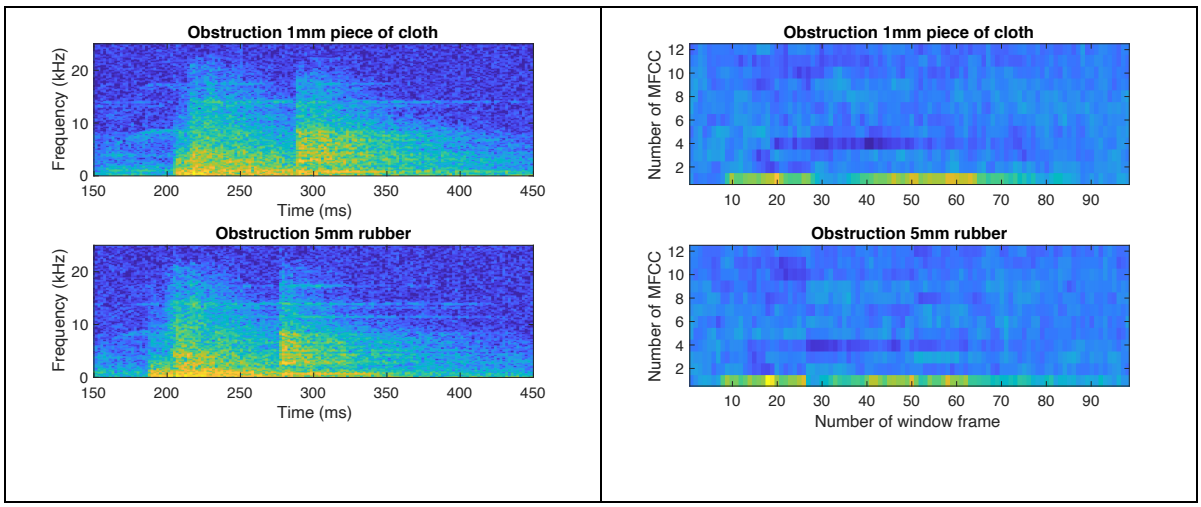


Figure 48. Sound spectrogram and MFCC for obstruction

## 6.4 Feature selection using MRMR

Since feature selection by MRMR was found to be effective for the detection of obstructions, the same technique was applied to other faults (lack of grease, spring weakening, and improper pin position) and those features were used for classification. The results are shown in Table 24, Table 25, Table 26, and Table 27. The tables are divided by the operating direction of the contactor and classifier. From the results, it was found that the model had high transferability with both SVM and KNN for closed data, even for spring weakening.

In the case of a lack of grease, data from contactor A (data A) could be detected with high accuracy, but data from contactor C (data C) could not. One possible reason is the level of grease removal. When data C were acquired, the experimental time was limited, and grease was removed in a short time. It is possible that a small amount of grease remained on the sliding surface of the moving parts, which is difficult to swipe in a short time. Even though the area to which grease was applied was cleaned up, the grease might not have been removed completely. On the other hand, when data A were acquired, there was enough time for the experiment, and the grease removal was carefully carried out. The grease was removed from the application area, the contactor was operated several times, and the grease was wiped off again. Removal of the grease adhering to the moving parts was also performed as much as possible. Therefore, the grease was almost completely removed in data A, while a small amount of grease possibly remained in data C, which may have made classification of data C difficult.

It also turned out that there is little transferability for improper pin position. In the case of this fault, there may be no significant change in the operation of the contactor, as the connecting pin was simply shifted from its original position and still connected the moving parts and plunger firmly with no wobbling. Because there were no significant differences,

common characteristics may not have emerged in both contactors. If the operation had been repeated more than a few hundred times with the pin out of proper position, it is expected that the condition would have further worsened or an unexpected force would be loaded, resulting in a difference in operation.

It was found that there is little transferability of models for open data. As for the lack of grease, it is conceivable that a larger difference occurs in the closed data in which parts move faster under the condition without grease. In the case of an obstruction, unlike for the closed data, in which the blade collides with an object at high speed, there was no significant difference in acoustic data as the blade simply moves away from the object. As closed data have the same trend, there is also little difference in open data between the normal and improper pin position data and it seems to be difficult to find the common features in both contactors. In the case of spring weakening, tape was used to simulate the fault. As a result, the open data for spring weakening behaved differently from the actual fault; therefore, spring weakening open data were not used in this study. More details can be found in Chapter 5.

Table 24. Transferability performance of closed data (MFCC + MRMR + SVM)

| Fault mode | Result of A by model C | | Result of C by model A | |
|---|---|---|---|---|
| | Recall [%] | F1 score [%] | Recall [%] | F1 score [%] |
| Lack of grease | 97.6 | 79.7 | 96.3 | 37.3 |
| Spring weakening | 92.8 | 88.7 | 100.0 | 78.5 |
| Improper pin position | 0.0 | 0.0 | 0.0 | 0.0 |
| Obstruction | 100.0 | 77.1 | 100.0 | 100.0 |

Table 25. Transferability performance of open data (MFCC + MRMR + SVM)

| Fault mode | Result of A by model C | | Result of C by model A | |
|---|---|---|---|---|
| | Recall [%] | F1 score [%] | Recall [%] | F1 score [%] |
| Lack of grease | 26.3 | 38.1 | 0.0 | 0.0 |
| Improper pin position | 53.2 | 42.6 | 0.0 | 0.0 |
| Obstruction | 13.6 | 16.1 | 100.0 | 28.9 |

Table 26. Transferability performance of closed data (MFCC + MRMR + KNN)

| Fault mode | Result of A by model C | | Result of C by model A | |
|---|---|---|---|---|
| | Recall [%] | F1 score [%] | Recall [%] | F1 score [%] |
| Lack of grease | 95.8 | 79.2 | 85.2 | 30.5 |
| Spring weakening | 87.3 | 86.8 | 84.9 | 73.8 |
| Improper pin position | 0.0 | 0.0 | 0.0 | 0.0 |
| Obstruction | 95.3 | 97.1 | 100.0 | 79.4 |

Table 27. Transferability performance of open data (MFCC + MRMR + KNN)

| Fault mode | Result of A by model C | | Result of C by model A | |
|---|---|---|---|---|
| | Recall [%] | F1 score [%] | Recall [%] | F1 score [%] |
| Lack of grease | 33.8 | 44.1 | 0.0 | 0.0 |
| Improper pin position | 58.4 | 42.9 | 0.0 | 0.0 |
| Obstruction | 20.0 | 23.3 | 100.0 | 28.9 |

## 6.5 Performance variation by fault level

Comparing the spring weakening results in Table 24 and Table 26, the data of contactor A have higher transfer performance. This might be because of a difference in the level of the fault, since data A contain fault data for 1 mm, 3 mm, and 5 mm but data C contain only 1 mm data. It is conceivable that higher-levels faults are more easily detected and common features are more prominent; therefore, differences in transferability performance by level were investigated. Data for contactor C were used for training and data of each level for contactor A were used for validation. The results are shown in Table 28. Transferability performance for spring weakening for each levelComparing the 1 mm, 3 mm, and 5 mm results, it was found that the expected high transferability performance of the high-severity faults was incorrect. The performance for 3 mm data was the highest, and the performance for 5 mm was lower than that of than others. This doesn't mean that 5 mm faults are difficult to detect, but that a model trained by only 1 mm, minor-level fault data, cannot detect 5 mm faults with high accuracy. It is

probable that the important features for detecting minor faults (1 mm and 3 mm) and those for severe fault (5 mm) are different and that is why the performance for 5 mm faults was degraded.

Table 28. Transferability performance for spring weakening for each level

(result of A by model C, closed data)

| Fault level | MFCC + MRMR + SVM | | MFCC + MRMR + KNN | |
|---|---|---|---|---|
| | Recall [%] | F1 score [%] | Recall [%] | F1 score [%] |
| 1 mm | 92.7 | 80.9 | 87.8 | 80.3 |
| 3 mm | 97.6 | 83.8 | 92.1 | 83.0 |
| 5 mm | 69.2 | 40.4 | 61.5 | 40.0 |

It was expected that if the features extracted from the minor faults were used for detection of severe faults, diagnostic performance could be higher compared to that for minor ones, as severe faults should have significant differences in features, but it was found that the distribution of selected features differed between minor and severe faults by investigation. When the features calculated from data C (1 mm) are selected by MRMR, the first delta delta MFCC in the data from 310 ms to 340 ms is the most important. Delta delta MFCCs are the second temporal derivatives of the MFCCs. They are used to capture the changes in the spectral features over time and provide additional information about the dynamic behaviour of the acoustic signal. In other words, there is a difference in the rate of change of the first MFCC when comparing normal and spring weakening data for contactor C. The distribution of this

feature of data A was also investigated for each fault level, and those features are shown in Figure 49. As the feature is selected from data C, the distribution of data C is clearly separated.

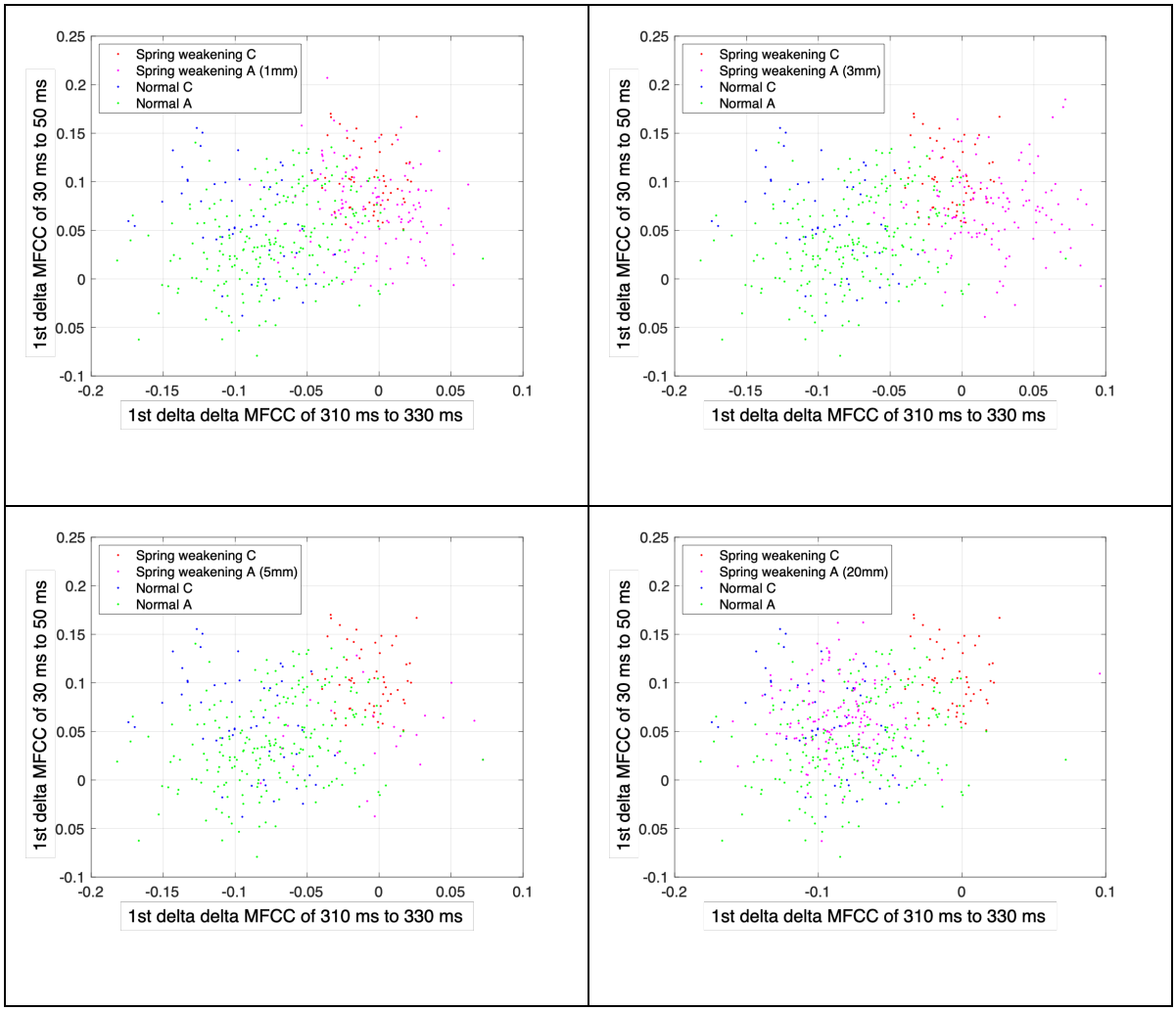


Figure 49. Distribution of features selected from data C

In the case of 1 mm and 3 mm (minor faults), the features of data A are also clearly separated as they are for data C. Therefore, model C was able to classify minor faults of data A with high accuracy. However, in the case of 5 mm, classification becomes difficult because the features are not separated, and the normal and fault features are mixed. For further investigation, the 20 mm fault level data were obtained from contactor A and the distribution of the features was investigated. The distribution is shown in Figure 49 as well. Normal and fault features were mixed as at the 5 mm level, and this is why the severe data cannot be classified with high

accuracy by model C. Important features of data A for 1 mm and 3 mm (minor faults) were also investigated by MRMR, and it was found that the first delta delta MFCC of 290 ms to 310 ms was the most important, and this is very close to the feature in the case of data C (first delta delta MFCC in the data from 310 ms to 340 ms). However, when it comes of the levels of 5 mm and 20 mm (severe faults), the second MFCC of 210 ms to 240 ms and the first MFCC of 390 ms to 420 ms were selected. From these results, it was found that the delta delta MFCC is important in the case of minor levels of spring weakening. Delta delta MFCCs are the second temporal derivatives of the MFCCs, usually used to capture the changes in the spectral features over time; it is conceivable that in the case of minor spring weakening, the initial position of the spring is slightly different, so that a subtle difference occurs when the blade accelerates, and it also makes differences in the delta delta MFCC. On the other hand, in the case of severe weakening (5 mm and 20 mm), the initial position is very different and the distance between the moving blade and the fixed blade is small. As a result, it is expected that the moving blades are not accelerated sufficiently and that makes a large difference in acoustic data. This analysis showed that the severity of the fault changes the optimal features for diagnosing the condition. The effective features for each level found in this study are listed in Table 29. As optimal features for each fault level are different, it is also expected that the progress of a fault can be followed by monitoring these features simultaneously. There is a change in delta delta MFCC at the beginning of the fault, and when the fault becomes serious, MFCC begins to change.

Table 29. Effective features for diagnosing each level of spring weakening fault

| Fault mode | Effective feature |
|---|---|
| Spring weakening (1 mm & 3 mm) | First delta delta MFCC of 290 ms to 340 ms |
| Spring weakening (5 mm) | Second MFCC of 210 ms to 240 ms |
| Spring weakening (20 mm) | First MFCC of 390 ms to 420 ms |

## 6.6 The effect of noise

Finally, an investigation was conducted on how resistant the transferability of the model is to noise. The closed data of contactors A and C were used for the investigation and white noise was added to the data to investigate how the accuracy varies with noise. The SPL of added noise were 55 dB, the same as those added in Chapter 5. The results are shown in Table 11 and the accuracy without noise (described in Table 24 and Table 26) is summarised again in Table 30 for comparison.

Table 30. Transferability of the fault diagnosis without noise

| Feature | Classifier | Fault | Result of A by model C | | Result of C by model A | |
|---|---|---|---|---|---|---|
| | | | Recall [%] | F1 score [%] | Recall [%] | F1 score [%] |
| MFCC | SVM | Lack of grease | 97.6 | 79.7 | 96.3 | 37.3 |
| | | Spring weakening | 92.8 | 88.7 | 100.0 | 78.5 |
| | | Obstruction | 100.0 | 77.1 | 100.0 | 100.0 |
| | KNN | Lack of grease | 95.8 | 79.2 | 85.2 | 30.5 |
| | | Spring weakening | 87.3 | 86.8 | 84.9 | 73.8 |
| | | Obstruction | 95.3 | 97.1 | 100.0 | 79.4 |

Table 31. Transferability of the fault diagnosis with 55 dB noise

| Feature | Classifier | Fault | Result of A by model C | | Result of C by model A | |
|---|---|---|---|---|---|---|
| | | | Recall [%] | F1 score [%] | Recall [%] | F1 score [%] |
| MFCC | SVM | Lack of grease | 93.4 | 73.4 | 1.9 | 0.9 |
| | | Spring weakening | 81.2 | 66.0 | 86.8 | 67.2 |
| | | Obstruction | 90.6 | 94.1 | 100.0 | 93.9 |
| | KNN | Lack of grease | 86.2 | 70.7 | 0.0 | 0.0 |
| | | Spring weakening | 78.6 | 66.9 | 69.8 | 43.5 |
| | | Obstruction | 87.7 | 88.2 | 100.0 | 76.1 |

In the case of a lack of grease, the result for data A is more accurate than that for data C, as is the case without noise shown in Table 30. In the absence of noise, some data were correctly classified in the case of the result for data C, but after the addition of noise most faults were misclassified as normal, and Recall became almost 0%. The reason for the decrease in the F1 score of the result of A is that the number of FPs (number of normal data misclassified as faults) increased. It is thought that the noise drowned out the difference between normal and fault data and caused the increase of FP. In the case of spring weakening, the trend of classification accuracy is similar to that in the case without noise. Accuracy is lowered by adding noise, and in the case of KNN, the number of misclassifications is large, making it difficult to apply it in practical use. As for obstruction, it was found that the fault can be detected with sufficient accuracy even when there is noise. Considering the analysis results of this

chapter, it seems that SVM shows better transferability performance when there is noise. When there is no noise, the transferability for some faults is lower than that for KNN; SVM is still accurate enough. In addition to this, as SVM has better accuracy in diagnosing faults as proven in Chapter 5, it is concluded that SVM provides the best performance for contactors.

In order to enhance the transferability of the fault detection model, it is important to narrow down the features of faults common to contactors. It was found that the transferability performance was different for each fault, and high performance was obtained even when there was noise. A lack of grease can be detected with high accuracy for the contactor A data. The reason why the contactor C data could not be detected is that the wiping off of grease from contactor C was insufficient and the difference between normal and fault data was slight. In this verification, it was found that even if a small amount of grease is left over from wiping, the contactor works properly. In order to improve the transferability of the model for lack of grease, it is necessary to obtain data with the grease completely wiped off and conduct a further investigation.

## 6.7 Summary and findings in this chapter

This chapter investigates the transferability of the fault detection model by using contactor data. Normal and simulated fault data were obtained from two contactors, and data from one contactor was used for training and those from the other used for validation. In the first verification, MFCC, used in Chapter 4 and found to be effective, was used, but the transferability could not be confirmed. This was thought to be because too many features which are not related to detecting the fault were used. Therefore, PCA and MRMR were used to narrow down the features to be used.

The results showed that high transferability performance can be obtained when MRMR is used for feature selection. It was also found that when MRMR is used, performance becomes better when the number of features is reduced. High performance can be obtained in the cases of obstruction and spring weakening; however, it could not be confirmed in the case of improper pin position. This is probably since even when the pin is about to come off, the operation of the contactor itself is not much different from the normal condition. It also could not be obtained for a lack of grease for contactor A data, as grease removal was not complete. It seems that clear differences compared to normal conditions are required to obtain transferability performance.

It was clarified that the important features for the detection of spring weakening differ depending on the fault level. By using this, not only the level of a fault but also monitoring of the progress of the fault can be expected.

Finally, the effect of noise on the transferability performance was investigated. When there is noise, the transferability performance can be confirmed for spring weakening and obstruction, although the performance is reduced. As for a lack of grease, the performance dropped significantly when the contactor C data were analysed. This might be caused by insufficient grease removal as described above, and no significant difference could be confirmed compared to the normal condition.

The investigation in this chapter revealed that choosing the number of features using MRMR results in high transferability performance. This performance was confirmed using both SVM and KNN classifiers. Since this performance does not degrade even when there is noise, it can be expected to be applicable for practical use.

The analysis in this chapter revealed the answers to the following research questions that could not be answered in Chapters 4 and 5 among those listed in Chapter 1.

- Can a fault detection model trained from one machine be transferable to other machines?

It was found that it is possible to obtain transferability by selecting features using MRMR. High performance can be obtained in the case of spring weakening and obstruction which cause a large difference from normal conditions. It is difficult to obtain transferability when there are no significant differences from the normal condition, such as in the initial state of a lack of grease, but it is expected to be detectable when a fault progresses, and the grease almost disappears. Considering the results of analysis in Chapter 5, the following conclusions can be drawn. If the simulated fault data can be obtained from the monitoring target, the model can detect even faults with little difference from normal conditions, such as a lack of grease and improper pin position, by training the model with all the MFCCs calculated from the obtained data. If it is not possible to obtain simulated fault data from the monitoring target, it is possible to detect the faults, such as obstruction and spring weakening, which differ significantly from normal conditions by selecting features by MRMR from data from the same type of machine. In addition to this, it was found that important features are different depending on the level of a fault, suggesting the possibility of monitoring the progression of faults.

# CHAPTER 7 CONCLUSIONS

## 7.1 Summary of the findings

In this study, the hypothesis was made that STME faults can be detected and diagnosed from acoustic data in the early stage, and to test this hypothesis, a literature search, experiments, and analysis were performed.

It was found from previous research that MFCC and WPDE as features and SVM and KNN as classifiers are expected to be useful for fault diagnosis of STME. A fault diagnosis algorithm was developed using these techniques and used to analyse the data obtained in the experiments to determine which combination had the highest accuracy.

Some STME uses different driving units even if the movement of the parts is similar, and there are differences in the speed and characteristics of the acoustic data. Because of this, STME is categorised into two types in this study. One is slow STME switching slowly, such as point machines and doors, and the other is fast STME switching at fast speed, such as contactors and circuit breakers. In the experiments, data were acquired from two types of STME to verify the proposed method is effective for general STME, by investigating the performance of the proposed method for two different types of STME. A point machine and contactors were used to acquire the data. The point machine and the contactor are both STME, and the movement of the machine itself is similar, but the operating sound is different. A point machine is a machine that operates over several seconds, and the operating sound has mainly low-frequency components, and a contactor works within a second and the operating sound extends to the high-frequency range.

Although some previous studies of condition monitoring using acoustic data did experiments with a single piece of STME, this study is novel in that data were obtained from multiple pieces of STME with significantly different operating characteristics. In addition to this, since most failures previously found to be detectable are serious ones that can be detected by means other than acoustic data, and most of them can be detected by the detection methods already installed in machines, this study targeted the early stage of faults that cannot be detected by conventional methods. A literature survey was conducted on the faults and frequency of occurrence in each type of STME, and it was decided to investigate contamination, dry slide chair, loose and over-tightened nuts, obstruction, and voltage drops in the point machine, and broken bolts, lack of grease, spring weakening, obstruction, and improper pin position in contactors.

To prove the hypothesis that these STME faults can be diagnosed from acoustic data in the early stage, this study provides answers to the following research questions:

- Which algorithm is most appropriate for fault diagnosis?

MFCC and WPDE were expected to be effective from previous research, so accuracy using these features was calculated and compared. It was found that using the MFCC as a feature is the more accurate for both the point machine and contactors. The combination of WPDE and classifiers was found to be able to diagnose point machine faults to some extent with accuracy for some types of faults, but many misdiagnoses occur. This is because the WPDE can capture significant acoustic changes, such as abnormal clutch sounds, caused by excessive tightening of nuts but cannot capture the difference of minute time-varying components caused when most minor faults happen. When WPDE was used for contactors, the accuracy did not decrease as much as when it was used for the point machine. This is because

contactors operate at high speed and the SPL of the operating sound is large, and there is a significant difference in the frequency domain when a fault occurs compared to the point machine.

As for classifiers, both SVM and KNN can diagnose faults with sufficiently high accuracy for both case studies, but the accuracy using KNN is slightly higher than that using SVM. The accuracy is almost the same when using KNN and SVM, but FN occur when using SVM. Although the number of FN that occur is small, FN mean missing faults, which is a problem directly linked to safety; therefore, it can be said KNN is the best classifier for fault diagnosis from the operating sound of STME.

- How accurate is the system and does that vary by fault?

In both case studies, all faults were found to be diagnosable with more than 95% accuracy using MFCC as the feature regardless of the classifier. In the case of the point machine, all faults could be diagnosed with more than 97% accuracy, and as most faults are diagnosed with nearly 100% accuracy, Recall is 99%. Although some misclassification of ‘loose nut’ and ‘obstruction’ occurs, it can be said that the diagnostic performance for all faults is sufficiently high. In the case of contactors, each fault can be diagnosed with an accuracy of more than 95%, and as most faults are diagnosed with nearly 100% accuracy, Recall is 99%. The diagnostic performance for all faults is high, but the accuracy for ‘lack of grease’ and ‘spring weakening’ is low compared with others, and there are some misdiagnoses with normal, suggesting that there is little difference between those faults and normal data. Although some misdiagnoses occur in some types of faults in both case studies, this system can diagnose all faults with over 95% accuracy.

- How tolerant is this proposed method to noise?

Since many machines are installed outdoors, noise with an SPL equivalent to light rain (37 dB) and heavy rain (55 dB) was added to the data to investigate its effect on classification accuracy. As a result, it was found that the proposed method is sufficiently tolerant to noise for both cases. Especially for contactors, the classification accuracy did not decrease much even when considerable noise equivalent to trains passing nearby (80 dB) was added. It is considered that the SPL of the operating sound of the contactor is larger than that of the point machine and the effect of noise is lower. In other words, the effect of noise can be reduced by increasing the SPL of the target operating sound as much as possible. It is desirable to install the microphone closer to the target or install a sound barrier between the target and the noise source, to increase the SPL.

- Which place is the most appropriate for the microphone to monitor the target?

Analysis of the two case studies revealed that placing the microphone close to the monitoring target's drive unit and increasing the SPL of the operating sound of the target machine are important to improve accuracy. It is desirable to place the microphone near the drive part where the motors and gears are installed, for equipment as large as a point machine. This is because even if something abnormal occurs near the rail, the abnormal force or vibration is transmitted to the driving part, or the related abnormality occurs to the driving parts. This is evidenced by the fact that the accuracy of the microphone near the point machine was higher than that of the microphone on the track in the case of 'obstruction' and 'dry slide chair' of the point machine. When an obstruction or dry slide chair occurs, the sound of the rail colliding with the obstruction or the sound of the rail being dragged will of course change, but the position of the parts and the force of the load also change due to the fault, and a larger abnormal sound

is generated in the locking mechanism, gears, clutch, and motor. Therefore, it is desirable to place the microphone near the driving unit.

It was also found that it is better to install the microphone inside the cabinet when the target machine is installed inside a cabinet. This is because noise mixed in such as operating sound from other machines can be reduced because of the cabinet, and the SPL of the operating sound of the target equipment can be raised. Previous studies using acoustic data have not examined the location of acoustic data acquisition. This study revealed that the accuracy can be improved regardless of the type of fault by placing the microphone near the driving unit. This finding will be useful for future research using acoustic data.

- Can a fault detection model trained from one machine be transferable to other machines?

It was proved that the fault detection model has transferability by selecting important features using MRMR. In the verification, normal and simulated fault data were acquired using two contactors. The model trained by data acquired from one machine could not diagnose faults of other machines by using all features. Overfitting seemed to occur for one machine because many features were used for training. In this study, a feature selection technique called MRMR was used to select the important features and it was proved that it is possible to improve the transferability of the model by narrowing down the features, in the case of ‘obstruction’ and ‘spring weakening’. This is because many of the features obtained from operating sound are not important and related to condition diagnosis, and it is considered that they behave as noise when diagnosing multiple machines. Therefore, it was possible to improve performance by selecting features that were important for classification, eliminating features that were not important, and using only those that were important for diagnosis. On the other hand, in the case of ‘improper pin position’ and ‘lack of grease’ when grease was not completely removed,

transferability could not be confirmed even when MRMR was used. This is probably since even when the pin is about to come off, the operation of the contactor itself is not much different from the normal condition. For 'lack of grease', it seems that clear differences could not be seen because the remaining grease smoothed the sliding surface of parts sufficiently so that there was no significant difference in operation compared to normal operation. MRMR makes it possible to select only important features common to all machines and remove other unrelated features in case there are significant differences between normal and abnormal conditions. This analysis revealed that to make the model transferable, it is necessary to select important features by MRMR. It was also found that when there are multiple levels of fault, such as spring weakening, important features differ by level, so when using the transferability of the model, it is necessary to select the optimal features using MRMR for each level of fault.

This analysis clarified that, in the case of using the transferability of the model, SVM is more accurate than KNN. Therefore, in this study, it is concluded that KNN is the best classifier for fault diagnosis using its target machine operating sound and SVM is the best for fault diagnosis using the transferability function.

Usually, after equipment is installed, its operation is checked. An operation check is also performed in the precise maintenance every few years. Some simulated fault data can be taken at this time, and using these data with KNN, it is possible to monitor the target equipment with high accuracy. If there is an operational risk in acquiring simulated fault data or when it takes time and effort to acquire simulated fault data from all facilities in the case of installing a large number of assets, those facilities can be monitored with high accuracy by acquiring simulated fault data from the same type of facility, selecting the calculated features with MRMR,

and diagnosing with SVM. For these reasons, it is concluded that the most appropriate classifier should be selected depending on the constraints of the target equipment.

The verification revealed the answers to each research question. It became clear from the first answer that the faults of both types of STME could be accurately diagnosed by using MFCC, KNN, and SVM. It is concluded that KNN and SVM are both adequate classifiers, but KNN is superior in that it has fewer FN. Since it is difficult to apply this method for practical use if there is a fault whose fault diagnosis accuracy is low, it was also investigated how much the accuracy changes with the fault. As a result, it was found that all faults could be diagnosed with high accuracy. In addition, since noise other than from the target machine might be mixed in in the real environment, noise was artificially added to examine its effect on the diagnostic accuracy. It was found that there was no significant effect on the diagnostic accuracy of this method even in the presence of environmental-level noise. Although it became clear that abnormalities could be diagnosed with high accuracy by sound, there was no knowledge of the best place to acquire data, so microphones were placed in several locations and the accuracy of each was compared. This revealed that the accuracy can be enhanced by placing the microphone near the machine's drive unit. Finally, it was verified whether there is transferability in the fault diagnosis model, because sometimes it is difficult to obtain simulated fault data from all machines. The results show that some models are transferable. When using training data acquired from one machine to monitor the same machine, it was proved that KNN is more accurate, but it was also revealed that SVM is more accurate when using the transferability of the model. Thus, it was concluded that high accuracy can be obtained by using KNN if simulated fault data can be acquired from the target, and using SVM if simulated fault data cannot be acquired, but can be acquired from the same type of STME.

The analysis in this study shows that the proposed method using MFCC and KNN can classify STME faults with high accuracy when simulated fault data can be obtained from the monitoring target. The results show that the accuracy does not change with the type of fault, and all faults can be classified with high accuracy. It was also found that the accuracy does not degrade when noise that could occur in a real environment where the target is really monitored, such as outdoors, is mixed in. It was also proved where to place the microphone for higher accuracy. In addition, even if the simulated fault data cannot be obtained from the target, it was found that some faults can be detected by obtaining simulated fault data from the same type of STME and selecting the features with MRMR and diagnosing them by SVM.

In summary, it can be said that the hypothesis that STME faults can be diagnosed using acoustic data is correct. In addition to this, the answers to the research questions were also uncovered, thus revealing useful facts to improve diagnostic accuracy. Investigation of the transferability of the model was also conducted and proved that faults can be detected even for machines without training fault data, by selecting features. This research is advanced in that it solved the problem of transferability, and field deployment would be anticipated to be successful.

## 7.2 Recommendation for future works

In this study, multiple experiments were conducted to obtain normal and simulated fault data, proving that these data can be classified with high accuracy. However, since the speed of sound varies with temperature and humidity, there is a possibility that the sound features will change with the seasons. The effect of seasonal variation should be investigated. It is desirable to install microphones on the target for a long period of time, take normal and simulated fault data of each season, and verify whether they can be classified with high accuracy.

Because it is difficult to obtain simulated fault data in all seasons, it is meaningful to investigate whether models trained on data acquired in one season can diagnose fault data in other seasons. If the data can be classified regardless of the season, there is a strong expectation that the method could be applied in the field in the rail industry.

Transferability of 'improper pin position' could not be confirmed in this study. This is thought to be because a large difference did not occur as the pin was only slightly out of position compared to normal, but if the contactor was repeatedly operated under this condition, a difference might occur at some point. The same thing might happen in the case of 'lack of grease'. When the transferability was investigated in this study, the fault detection accuracy of contactor C did not increase. It is thought that there was a little grease remaining and this was enough to lubricate the parts of the contactor. However, it is conceivable that if the contactor is operated repeatedly in this condition, a detectable difference may occur at some point. It is meaningful to examine at what point this abnormal condition can be detected when the contactor is repeatedly operated under this condition. Although the number of data used in this study is in the thousands, it is desirable to investigate the difference between the early and late stages of operation by acquiring and analysing more than tens of thousands of data over a long period of time with insufficient grease or misaligned pins. If this is clarified, the performance of transferability of 'improper pin position' and 'lack of grease' are expected to be improved. Analysis of data acquired over long period time also makes it possible to investigate transitions in the data, and the findings expected to be obtained by this will be valuable for research areas using sound.

The proposed method of this study made it possible to diagnose abnormalities by catching slight differences in the operation sound. However, it was not possible to analyse in

detail which part of the sound affects the fault diagnosis. Once this is known, more appropriate microphone locations, optimal sampling rate, frequency bands, and times to acquire will be revealed. These are important for practical application of this method. Data masking and using acoustic cameras are expected to address this problem. In this study, all of the acquired data were used for analysis, but it is possible to mask part of the data and examine which time data and frequency band data would reduce accuracy if masked. This would make it clear which time and which frequency bands of sound data are important for diagnosis. Once the time and frequency of sound that are important for condition diagnosis are known, it will be possible to detect where that sound is coming from by using an acoustic camera. An acoustic camera is a measuring instrument that combines a video camera with a microphone array using multiple microphones to identify the source of sound by the time difference between the sounds acquired by the individual microphones in the array. By analysing the frequency of the acquired sound, it is possible to visualise which frequency sound is generated from where. If the source of an important sound can be identified, placing the microphone close to the source can be expected to improve accuracy.

# LIST OF REFERENCES


[1] "Formal Inquiry: Derailment of train 1T60, 1245 hrs Kings Cross to Kings Lynn at Potters Bar on 10 May 2002," Rail Safety and Standards Board, 2005.

[2] H. P. B. I. Board, "Train derailment at potters bar 10 May 2002," Health & Safety Executive, 2003.

[3] "Rail Accident Report Derailment at Grayrigg 23 February 2007," Rail Accident Investigation Branch, 2011. [Online]. Available: https://assets.publishing.service.gov.uk/media/547c9037ed915d4c0d000199/R202008_081023_Grayrigg_v5.pdf

[4] "Tokaido Shinkansen temporarily stuck, signal trouble," ed: Nikkei Inc., 2018.

[5] Information on electrical equipment accidents [Online] Available: https://www.nite.go.jp/gcet/tso/shohopub/search

[6] "Root cause analysis for center substation 138 kV circuit breaker event on January 16, 2012," Indianapolis Power & Light Company, 2012. Accessed: 2022. [Online]. Available: https://www.in.gov/iurc/files/Center_Substation_Root_Cause_Analysis.pdf

[7] "Information on accidents and disasters." Kinki Branch of Chubu Kinki Industrial Safety and Inspection Department. https://www.safety-kinki.meti.go.jp/jikosaigai_jirei.html (accessed 2022).

[8] H. Umemoto, H. Nakao, H. Katsuya, F. Nakamura, and K. Mori, "Development of Railway Vehicle Passage Detection Sensor with Vibration Resistance " *Report of Nara Prefectural Institute of Industrial Development,* no. 39, pp. 15-19, 2013.

[9] "CSR Report 2015," East Japan Railway Company, 2016. [Online]. Available: https://www.jreast.co.jp/e/environment/pdf_2015/p18_21.pdf

https://www.jreast.co.jp/e/environment/2015.html

[10] "CSR Report 2017," East Japan Railway Company, 2018. [Online]. Available: https://www.jreast.co.jp/e/environment/pdf_2017/p051-053.pdf

https://www.jreast.co.jp/e/environment/2017.html

[11] G. Brambilla, P. Wilson, and D. Thompson, "Trackside Optical Fibre Acoustic Sensing (TOFAS)," ed: Engineering and Physical Sciences Research Council, 2016.

[12] "Network Rail using innovative fibre-optic technology to boost railway safety and performance." Network Rail. https://www.networkrailmediacentre.co.uk/news/network-rail-using-innovative-fibre-optic-technology-to-boost-railway-safety-and-performance (accessed 2022).

[13] N. Lehrasab and S. Fararooy, "Formal definition of single throw mechanical equipment for fault diagnosis," *Electronics Letters,* vol. 34, no. 23, pp. 2231-2232, 1998.

[14] "fault," Signalling and security apparatus for railways / Communication in transmission systems ed: International Electrotechnical Commission, 2017.

[15] "failure," Signalling and security apparatus for railways / Communication in transmission systems ed: International Electrotechnical Commission, 2017.

[16] "error," Dependability / Reliability related concepts: failures ed: International Electrotechnical Commission, 2015.
[17] J. Moubray, *Reliability-centered maintenance*, 2nd ed. Industrial Press Inc., 2001.
[18] J. Lee, H. Choi, D. Park, Y. Chung, H. Y. Kim, and S. Yoon, "Fault Detection and Diagnosis of Railway Point Machines by Sound Analysis," *Sensors (Basel),* vol. 16, no. 4, Apr 16 2016, doi: 10.3390/s16040549.
[19] Y. Cao, Y. Sun, G. Xie, and P. Li, "A Sound-Based Fault Diagnosis Method for Railway Point Machines Based on Two-Stage Feature Selection Strategy and Ensemble Classifier," *IEEE Transactions on Intelligent Transportation Systems,* pp. 1-10, 2021-01-01 2021, doi: 10.1109/tits.2021.3109632.
[20] *HW 1000/2000 Point Machine – Student Notes*, Issue 4 ed. Network Rail 2003.
[21] W. Lu, W. Jiang, H. Wu, and J. Hou, "A fault diagnosis scheme of rolling element bearing based on near-field acoustic holography and gray level co-occurrence matrix," *Journal of Sound and Vibration,* vol. 331, no. 15, pp. 3663-3674, 2012.
[22] S. K. Yadav, K. Tyagi, B. Shah, and P. K. Kalra, "Audio signature-based condition monitoring of internal combustion engine using FFT and correlation approach," *IEEE Transactions on instrumentation and measurement,* vol. 60, no. 4, pp. 1217-1226, 2010.
[23] N. Huang, L. Fang, G. Cai, D. Xu, H. Chen, and Y. Nie, "Mechanical fault diagnosis of high voltage circuit breakers with unknown fault type using hybrid classifier based on LMD and time segmentation energy entropy," *Entropy (Basel, Switzerland),* vol. 18, no. 9, pp. 322-322, 2016, doi: 10.3390/e18090322.
[24] S. Wan and L. Chen, "Fault diagnosis of high-voltage circuit breakers using mechanism action time and hybrid classifier," *IEEE Access,* vol. 7, pp. 85146-85157, 2019.
[25] R. Heng and M. J. M. Nor, "Statistical analysis of sound and vibration signals for monitoring rolling element bearing condition," *Applied Acoustics,* vol. 53, no. 1-3, pp. 211-226, 1998.
[26] N. Baydar and A. Ball, "A comparative study of acoustic and vibration signals in detection of gear failures using Wigner–Ville distribution," *Mechanical systems and signal processing,* vol. 15, no. 6, pp. 1091-1107, 2001.
[27] N. Baydar and A. Ball, "Detection of gear failures via vibration and acoustic signals using wavelet transform," *Mechanical Systems and Signal Processing,* vol. 17, no. 4, pp. 787-804, 2003.
[28] K. Shibata, A. Takahashi, and T. Shirai, "Fault diagnosis of rotating machinery through visualisation of sound signals," *Mechanical Systems and Signal Processing,* vol. 14, no. 2, pp. 229-241, 2000.
[29] U. Benko, J. Petrovčič, Đ. Juričić, J. Tavčar, and J. Rejec, "An approach to fault diagnosis of vacuum cleaner motors based on sound analysis," *Mechanical Systems and Signal Processing,* vol. 19, no. 2, pp. 427-445, 2005.
[30] H. Liu, L. Li, and J. Ma, "Rolling bearing fault diagnosis based on STFT-deep learning and sound signals," *Shock and Vibration,* vol. 2016, 2016.
[31] A. Glowacz, W. Glowacz, Z. Glowacz, and J. Kozik, "Early fault diagnosis of bearing and stator faults of the single-phase induction motor using acoustic signals," *Measurement,* vol. 113, pp. 1-9, 2018.
[32] RSSB, "Mapping current remote condition monitoring activities to the system reliability framework," 2009.

[33] "Development of novel S&C motion mechanisms:- Design concept report [TRL 3]," in "IN2RAIL, Innovative Intelligent Rail," Network Rail, 2018.

[34] S. J. Hassankiadeh, "Failure analysis of railway switches and crossings for the purpose of preventive maintenance," *Transport Science,* 2011.

[35] F. P. García Márquez, R. W. Lewis, A. M. Tobias, and C. Roberts, "Life cycle costs for railway condition monitoring," *Transportation research. Part E, Logistics and transportation review,* vol. 44, no. 6, pp. 1175-1187, 2008, doi: 10.1016/j.tre.2007.12.003.

[36] K. Izumi, Y. Hori, and T. Ukai, "Measures against machine failures," *Technical review, JR East,* vol. No.17, 2006. [Online]. Available: https://www.jreast.co.jp/development/tech/contents17.html.

[37] P. Weston, L. Saadé, and J. Y. Shih, "D2.1 S&C Failure Analysis Report " in "Project: 7117 AIR5," University of Birmingham, 2018.

[38] M. Hamadache, S. Dutta, O. Olaby, R. Ambur, E. Stewart, and R. Dixon, "On the Fault Detection and Diagnosis of Railway Switch and Crossing Systems: An Overview," *Applied Sciences,* vol. 9, no. 23, 2019, doi: 10.3390/app9235129.

[39] T. Asada, "Novel condition monitoring techniques applied to improve the dependability of railway point machines," University of Birmingham, 2013.

[40] F. P. G. Marquez, D. J. P. Tercero, and F. Schmid, "Unobserved component models applied to the assessment of wear in railway points: A case study," *European Journal of Operational Research,* vol. 176, no. 3, pp. 1703-1712, 2007.

[41] M. Hamadache, S. Dutta, R. Ambur, O. Olaby, E. Stewart, and R. Dixon, "Residual-based fault detection method: application to railway switch & crossing (S&C) system," in *2019 19th International Conference on Control, Automation and Systems (ICCAS)*, 2019: IEEE, pp. 1228-1233.

[42] Y. Cheng and H. Zhao, "Fault detection and diagnosis for railway switching points using fuzzy neural network," in *2015 IEEE 10th Conference on Industrial Electronics and Applications (ICIEA)*, 2015: IEEE, pp. 860-865.

[43] A. Guclu, H. Yılboga, O. F. Eker, F. Camci, and I. Jennions, "Prognostics with autoregressive moving average for railway turnouts," in *Annual Conference of the PHM Society*, 2010, vol. 2, no. 1.

[44] H. Adachi, M. Kikuchi, and Y. Watanabe, "Electric switch machine failure detection using data-mining technique," *Quarterly Report of RTRI,* vol. 47, no. 4, pp. 182-186, 2006.

[45] O. F. Eker, F. Camci, and U. Kumar, "Failure diagnostics on railway turnout systems using support vector machines," in *International Workshop and Congress on eMaintenance: 22/06/2010-24/06/2010*, 2010: Luleå tekniska universitet, pp. 248-251.

[46] Z. Wei, A. Núñez, Z. Li, and R. Dollevoet, "Evaluating degradation at railway crossings using axle box acceleration measurements," *Sensors,* vol. 17, no. 10, p. 2236, 2017.

[47] F. P. García, D. J. Pedregal, and C. Roberts, "Time series methods applied to failure prediction and detection," *Reliability Engineering & System Safety,* vol. 95, no. 6, pp. 698-703, 2010.

[48] N. Bolbolamiri, M. S. Sanai, and A. Mirabadi, "Time-domain stator current condition monitoring: Analyzing point failures detection by Kolmogorov-Smirnov (KS) test," *Int. J. Electr. Comput. Energ. Electron. Commun. Eng,* vol. 6, no. 6, pp. 587-592, 2012.

[49] M. Vileiniskis, R. Remenyte-Prescott, and D. Rama, "A fault detection method for railway point systems," *Proceedings of the Institution of Mechanical Engineers, Part F: Journal of Rail and Rapid Transit,* vol. 230, no. 3, pp. 852-865, 2015, doi: 10.1177/0954409714567487.

[50] N. Wright, R. Gan, and C. McVae, "Software and machine learning tools for monitoring railway track switch performance," 2016.

[51] J. A. Silmon and C. Roberts, "Improving railway switch system reliability with innovative condition monitoring algorithms," *Proceedings of the Institution of Mechanical Engineers, Part F: Journal of Rail and Rapid Transit,* vol. 224, no. 4, pp. 293-302, 2010, doi: 10.1243/09544097jrrt313.

[52] T. Asada and C. Roberts, "Improving the dependability of DC point machines with a novel condition monitoring system," *Proceedings of the Institution of Mechanical Engineers, Part F: Journal of Rail and Rapid Transit,* vol. 227, no. 4, pp. 322-332, 2013, doi: 10.1177/0954409713481748.

[53] F. Zhou *et al.*, "Remote condition monitoring and validation of railway points," *Computing & Control Engineering Journal,* vol. 13, no. 5, 2002.

[54] A. Guclu, H. Yilboga, O. F. Eker, and F. Camci, "Classification of uncertain data streams using modified k-nearest neighbor method: A case study on railway turnouts," in *Proceedings of the International Symposium on Innovations in Intelligent SysTems and Applications, Kayseri, Turkey*, 2010, pp. 21-24.

[55] T. Asada and C. Roberts, "Development of an effective condition monitoring system for AC point machines," in *5th IET Conference on Railway Condition Monitoring and Non-Destructive Testing (RCM 2011)*, 2011: IET, pp. 1-6.

[56] F. P. G. Márquez and J. M. C. Muñoz, "A pattern recognition and data analysis method for maintenance management," *International Journal of Systems Science,* vol. 43, no. 6, pp. 1014-1028, 2012.

[57] T. Böhm, "Accuracy improvement of condition diagnosis of railway switches via external data integration," *Structural health monitoring,* pp. 1550-1558, 2012.

[58] X. M. Mo, Y. Fang, and Y. G. Yang, "Method on the fault detection and diagnosis for the railway turnout based on the current curve of switch machine," in *Applied Mechanics and Materials*, 2013, vol. 427: Trans Tech Publ, pp. 1022-1027.

[59] K. Zhang, K. Du, and Y. Ju, "Algorithm of railway turnout fault detection based on PNN neural network," in *2014 seventh international symposium on computational intelligence and design*, 2014, vol. 1: IEEE, pp. 544-547.

[60] K. Zhang, "The railway turnout fault diagnosis algorithm based on BP neural network," in *2014 IEEE International Conference on Control Science and Systems Engineering*, 2014: IEEE, pp. 135-138.

[61] W. Jin *et al.*, "Development and evaluation of health monitoring techniques for railway point machines," in *2015 IEEE Conference on Prognostics and Health Management (PHM)*, 2015: IEEE, pp. 1-11.

[62] F. Zhou, L. Xia, W. Dong, X. Sun, X. Yan, and Q. Zhao, "Fault diagnosis of high-speed railway turnout based on support vector machine," in *2016 IEEE International Conference on Industrial Technology (ICIT)*, 2016: IEEE, pp. 1539-1544.

[63] H. Kim, J. Sa, Y. Chung, D. Park, and S. Yoon, "Fault diagnosis of railway point machines using dynamic time warping," *Electronics Letters,* vol. 52, no. 10, pp. 818-819, 2016.

[64] S. Huang, F. Zhang, R. Yu, W. Chen, F. Hu, and D. Dong, "Turnout fault diagnosis through dynamic time warping and signal normalization," *Journal of Advanced Transportation,* vol. 2017, 2017.

[65] D. Ou, M. TAng, R. Xue, and H. Yao, "Hybrid fault diagnosis of railway switches based on the segmentation of monitoring curves," *Eksploatacja i Niezawodność,* vol. 20, no. 4, 2018.

[66] S. Huang, X. Yang, L. Wang, W. Chen, F. Zhang, and D. Dong, "Two-stage turnout fault diagnosis based on similarity function and fuzzy c-means," *Advances in Mechanical Engineering,* vol. 10, no. 12, p. 1687814018811402, 2018.

[67] D. Ou, R. Xue, and K. Cui, "A data-driven fault diagnosis method for railway turnouts," *Transportation research record,* vol. 2673, no. 4, pp. 448-457, 2019.

[68] H. Yilboga, Ö. F. Eker, A. Güçlü, and F. Camci, "Failure prediction on railway turnouts using time delay neural networks," in *2010 IEEE International Conference on Computational Intelligence for Measurement Systems and Applications*, 2010: IEEE, pp. 134-137.

[69] O. F. Eker, F. Camci, A. Guclu, H. Yilboga, M. Sevkli, and S. Baskan, "A simple state-based prognostic model for railway turnout systems," *IEEE Transactions on Industrial Electronics,* vol. 58, no. 5, pp. 1718-1726, 2011.

[70] F. Camci, O. F. Eker, S. Başkan, and S. Konur, "Comparison of sensors and methodologies for effective prognostics on railway turnout systems," *Proceedings of the Institution of Mechanical Engineers, Part F: Journal of Rail and Rapid Transit,* vol. 230, no. 1, pp. 24-42, 2016.

[71] P. Mistry, P. Lane, and P. Allen, "Railway point-operating machine fault detection using unlabeled signaling sensor data," *Sensors,* vol. 20, no. 9, p. 2692, 2020.

[72] Z. Li, Z. Yin, T. Tang, and C. Gao, "Fault diagnosis of railway point machines using the locally connected autoencoder," *Applied Sciences,* vol. 9, no. 23, p. 5139, 2019.

[73] C. Bian, S. Yang, T. Huang, Q. Xu, J. Liu, and E. Zio, "Degradation state mining and identification for railway point machines," *Reliability Engineering & System Safety,* vol. 188, pp. 432-443, 2019, doi: 10.1016/j.ress.2019.03.044.

[74] D. Ou, Y. Ji, L. Zhang, and H. Liu, "An online classification method for fault diagnosis of railway turnouts," *Sensors,* vol. 20, no. 16, p. 4627, 2020.

[75] V. Atamuradov, K. Medjaher, F. Camci, P. Dersin, and N. Zerhouni, "Railway Point Machine Prognostics Based on Feature Fusion and Health State Assessment," *IEEE Transactions on Instrumentation and Measurement,* vol. 68, no. 8, pp. 2691-2704, 2019, doi: 10.1109/tim.2018.2869193.

[76] F. P. G. Márquez and D. J. Pedregal, "Applied RCM2 algorithms based on statistical methods," *International Journal of Automation and Computing,* vol. 4, no. 2, pp. 109-116, 2007.

[77] I. Matei, J. de Kleer, A. Feldman, M. Zhenirovskyy, and R. Rai, "Classification based diagnosis: Integrating partial knowledge of the physical system," in *2019 Annual Conference of the PHM Society. Scottsdale, USA: PHM Society. doi*, 2019, vol. 10.

[78] O. F. Eker and F. Camci, "State‐based prognostics with state duration information," *Quality and Reliability Engineering International,* vol. 29, no. 4, pp. 465-476, 2013.

[79] V. Atamuradov, K. Medjaher, F. Camci, P. Dersin, and N. Zerhouni, "Degradation-level assessment and online prognostics for sliding chair failure on point machines," *IFAC-PapersOnLine,* vol. 51, no. 24, pp. 208-213, 2018.

[80] O. Eker, F. Camci, and U. Kumar, "SVM based diagnostics on railway turnouts," *International Journal of Performability Engineering,* vol. 8, no. 3, p. 289, 2012.

[81] N. Obata, T. Ichikura, H. Narita, and H. Tanaka, "Development of an ES2-type point machine (monitoring of point machine)," *WIT Transactions on The Built Environment,* vol. 114, pp. 677-686, 2010.

[82] Z. Shi, Z. Liu, and J. Lee, "An auto-associative residual based approach for railway point system fault detection and diagnosis," *Measurement,* vol. 119, pp. 246-258, 2018, doi: 10.1016/j.measurement.2018.01.062.

[83] C. Letot *et al.*, "A data driven degradation-based model for the maintenance of turnouts: A case study," *IFAC-PapersOnLine,* vol. 48, no. 21, pp. 958-963, 2015.

[84] Z. Shi, "A Comparative Study of Performance Assessment and Fault Diagnosis Approaches for Reciprocating Electromechanical Mechanism," University of Cincinnati, 2016.

[85] T. Böhm, "Remaining useful life prediction for railway switch engines using classification techniques," *International Journal of Prognostics and Health Management,* vol. 8, 2017.

[86] G. Wang, T. Xu, T. Tang, T. Yuan, and H. Wang, "A Bayesian network model for prediction of weather-related failures in railway turnout systems," *Expert systems with applications,* vol. 69, pp. 247-256, 2017.

[87] N. IWASAWA, S. RYUO, K. KAWASAKI, and A. HADA, "Development of System for Supporting Lock Position Adjustment Work for Electric Point Machine," *Quarterly Report of RTRI,* vol. 56, no. 3, pp. 200-205, 2015.

[88] F. Wang, Z. Zhong, G. Wang, and T. Tang, "A penalized convolution model for oil leakage detection in electrohydraulic railway point systems," *IEEE Transactions on Instrumentation and Measurement,* vol. 70, pp. 1-9, 2020.

[89] Y. Sun, Y. Cao, G. Xie, and T. Wen, "Condition Monitoring for Railway Point Machines Based on Sound Analysis and Support Vector Machine," *Chinese Journal of Electronics,* vol. 29, no. 4, pp. 786-792, 2020, doi: 10.1049/cje.2020.06.007.

[90] Y. Sun, Y. Cao, G. Xie, and T. Wen, "Sound based fault diagnosis for RPMs based on multi-scale fractional permutation entropy and two-scale algorithm," *IEEE Transactions on Vehicular Technology,* vol. 70, no. 11, pp. 11184-11192, 2021.

[91] Y. Sun, Y. Cao, and P. Li, "Contactless Fault Diagnosis for Railway Point Machines based on Multi-Scale Fractional Wavelet Packet Energy Entropy and Synchronous Optimization Strategy," *IEEE Transactions on Vehicular Technology,* 2022.

[92] T. S. Shanthi and C. Lingam, "Review of feature extraction techniques in automatic speech recognition," *International Journal of Scientific Engineering and Technology,* vol. 2, no. 6, pp. 479-484, 2013.

[93] P. Shen, Z. Changjun, and X. Chen, "Automatic speech emotion recognition using support vector machine," in *Proceedings of 2011 international conference on electronic & mechanical engineering and information technology*, 2011, vol. 2: IEEE, pp. 621-625.

[94] K. C. Wang, "Time-frequency feature representation using multi-resolution texture analysis and acoustic activity detector for real-life speech emotion recognition," *Sensors (Basel),* vol. 15, no. 1, pp. 1458-78, Jan 14 2015, doi: 10.3390/s150101458.

[95] C. H. Chen, W. T. Huang, T. H. Tan, C. C. Chang, and Y. J. Chang, "Using K-Nearest Neighbor Classification to Diagnose Abnormal Lung Sounds," *Sensors (Basel),* vol. 15, no. 6, pp. 13132-58, Jun 4 2015, doi: 10.3390/s150613132.

[96] Y. Chung, S. Oh, J. Lee, D. Park, H. H. Chang, and S. Kim, "Automatic detection and recognition of pig wasting diseases using sound data in audio surveillance systems," *Sensors (Basel),* vol. 13, no. 10, pp. 12929-42, Sep 25 2013, doi: 10.3390/s131012929.

[97] V. Singh and N. Meena, "Engine fault diagnosis using DTW, MFCC and FFT," in *Proceedings of the First International Conference on Intelligent Human Computer Interaction*, 2009: Springer, pp. 83-94.

[98] F. V. Nelwamondo, T. Marwala, and U. Mahola, "Early classifications of bearing faults using hidden Markov models, Gaussian mixture models, mel-frequency cepstral coefficients and fractals," *International Journal of Innovative Computing, Information and Control,* vol. 2, no. 6, pp. 1281-1299, 2006.

[99] T. Maniak, C. Jayne, R. Iqbal, and F. Doctor, "Automated intelligent system for sound signalling device quality assurance," *Information Sciences,* vol. 294, pp. 600-611, 2015.

[100] V. N. Vapnik, "An overview of statistical learning theory," *IEEE transactions on neural networks,* vol. 10, no. 5, pp. 988-999, 1999.

[101] K. Venkata Rao and P. B. G. S. N. Murthy, "Modeling and optimization of tool vibration and surface roughness in boring of steel using RSM, ANN and SVM," *Journal of Intelligent Manufacturing,* vol. 29, no. 7, pp. 1533-1543, 2016, doi: 10.1007/s10845-016-1197-y.

[102] H. Qiu, J. Lee, J. Lin, and G. Yu, "Wavelet filter-based weak signature detection method and its application on rolling element bearing prognostics," *Journal of sound and vibration,* vol. 289, no. 4-5, pp. 1066-1090, 2006.

[103] J. Zarei and J. Poshtan, "Bearing fault detection using wavelet packet transform of induction motor stator current," *Tribology international,* vol. 40, no. 5, pp. 763-769, 2007.

[104] K. Heinrich and R. Kretzschmar, "Transrapid maglev system," 1989.

[105] M. Hashimoto, "Driving Control Characteristic Using the Inverter System at Yamanashi Maglev Test Line," in *The 15th International Conference on Magnetically Levitated Systems and Linear Drives*, 1998.

[106] T. Uzuka, "Faster than a speeding bullet: An overview of Japanese high-speed rail technology and electrification," *IEEE Electrification magazine,* vol. 1, no. 1, pp. 11-20, 2013.

[107] P. L. Fletcher and W. Degen, "A summary of the final results and conclusions of the second international enquiry on the reliability of high voltage circuit-breakers," ed. London: London: IEE, 1995, pp. 24-30.

[108] A. Carvalho *et al.*, "Final report of the 2004–2007 international enquiry on reliability of high voltage equipment," *Electra,* vol. 264, pp. 49-53, 2012.

[109] A. A. Razi-Kazemi, M. Vakilian, K. Niayesh, and M. Lehtonen, "Circuit-Breaker Automated Failure Tracking Based on Coil Current Signature," *IEEE Transactions on Power Delivery,* vol. 29, no. 1, pp. 283-290, 2014, doi: 10.1109/tpwrd.2013.2276630.

[110] A. A. Razi ‐ Kazemi, "Circuit breaker condition assessment through a fuzzy ‐ probabilistic analysis of actuating coil's current," *IET Generation, Transmission & Distribution (Wiley-Blackwell),* vol. 10, no. 1, pp. 48-57, 2016, doi: 10.1049/iet-gtd.2014.1236.

[111] J. Ni, C. Zhang, and S. X. Yang, "An Adaptive Approach Based on KPCA and SVM for Real-Time Fault Diagnosis of HVCBs," *IEEE Transactions on Power Delivery,* vol. 26, no. 3, pp. 1960-1971, 2011, doi: 10.1109/tpwrd.2011.2136441.

[112] M. Runde, G. Ottesen, B. Skyberg, and M. Ohlen, "Vibration analysis for diagnostic testing of circuit-breakers," *IEEE Transactions on Power Delivery,* vol. 11, no. 4, pp. 1816-1823, 1996.

[113] J. Huang, X. Hu, and F. Yang, "Support vector machine with genetic algorithm for machinery fault diagnosis of high voltage circuit breaker," *Measurement,* vol. 44, no. 6, pp. 1018-1027, 2011, doi: 10.1016/j.measurement.2011.02.017.

[114] B. Feizifar, "A Novel Arcing Power-Based Algorithm for Condition Monitoring of Electrical Wear of Circuit Breaker Contacts," *IEEE Transactions on Power Delivery,* vol. 34, no. 3, pp. 1060-1069, doi: 10.1109/TPWRD.2018.2882013.

[115] T. Ji, L. Yi, W. Tang, M. Shi, and Q. Wu, "Multi-mapping fault diagnosis of high voltage circuit breaker based on mathematical morphology and wavelet entropy," *CSEE Journal of Power and Energy Systems,* vol. 5, no. 1, pp. 130-138, 2019, doi: 10.17775/CSEEJPES.2017.01060.

[116] W. Gao, R.-J. Wai, S.-P. Qiao, and M.-F. Guo, "Mechanical Faults Diagnosis of High-Voltage Circuit Breaker via Hybrid Features and Integrated Extreme Learning Machine," *IEEE access,* vol. 7, pp. 60091-60103, 2019, doi: 10.1109/ACCESS.2019.2915252.

[117] C. Hou, Y. Li, Y. Cao, J. Li, and Y. Cao, "Analysis on vibration and acoustic joint mechanical fault diagnosis of high voltage vacuum circuit based on wavelet packet energy relative entropy," vol. 1, ed: IEEE, 2016, pp. 1-4.

[118] J. Huang, X. Hu, and X. Geng, "An intelligent fault diagnosis method of high voltage circuit breaker based on improved EMD energy entropy and multi-class support vector machine," *Electric Power Systems Research,* vol. 81, no. 2, pp. 400-407, 2011, doi: 10.1016/j.epsr.2010.10.029.

[119] N. Huang, H. Chen, G. Cai, L. Fang, and Y. Wang, "Mechanical Fault Diagnosis of High Voltage Circuit Breakers Based on Variational Mode Decomposition and Multi-Layer Classifier," *Sensors (Basel),* vol. 16, no. 11, Nov 10 2016, doi: 10.3390/s16111887.

[120] Q. Yang, J. Ruan, Z. Zhuang, and D. Huang, "Fault Identification for Circuit Breakers Based on Vibration Measurements," *IEEE transactions on instrumentation and measurement,* vol. 69, no. 7, pp. 4154-4164, 2020, doi: 10.1109/TIM.2019.2946470.

[121] C. Sánchez‐Giraldo, C. L. Bedoya, R. A. Morán‐Vásquez, C. V. Isaza, and J. M. Daza, "Ecoacoustics in the rain: understanding acoustic indices under the most common geophonic source in tropical rainforests," *Remote Sensing in Ecology and Conservation,* vol. 6, no. 3, pp. 248-261, 2020.

[122] C. Bedoya, C. Isaza, J. M. Daza, and J. D. López, "Automatic identification of rainfall in acoustic recordings," *Ecological Indicators,* vol. 75, pp. 95-100, 2017.

[123] M. F. M. Idris, M. M. Musa, and S. M. Ayob, "Noise Generated by Raindrop on Metal Deck Roof Profiles: It's Effect towards People Activities," *Procedia-Social and Behavioral Sciences,* vol. 36, pp. 485-492, 2012.

[124] L. Heinemann and H. Chi, "Technology benchmark of operating mechanisms for high voltage switchgear," *ABB AG, Mannheim, Germany,* 2011.

[125] H. A. Seki, T, "History of Switchgear," *The Nissin electric review,* vol. 62, 2017.

[126] M. Toyoda, "Technological transition of electric circuit breakers," *The Journal of The Institute of Electrical Engineers of Japan,* vol. 127, no. 9, pp. 607-610, 2007. [Online]. Available: https://www.jstage.jst.go.jp/article/ieejjournal/127/9/127_9_607/_pdf.

[127] M. S. Kosakada, T, "Trends in Maintenance and Renewal of Substation Facilities," *Toshiba review,* vol. 63, no. 12, pp. 2-6, 2008.

[128] M. Kendon, M. McCarthy, S. Jevrejeva, A. Matthews, T. Sparks, and J. Garforth, "State of the UK Climate 2020," *International Journal of Climatology,* vol. 41, pp. 1-76, 2021.

[129] J. M. Agency, "Average monthly rainfall in 2021 in Tokyo area." [Online]. Available: https://www.data.jma.go.jp/obd/stats/etrn/view/monthly_s1.php?prec_no=44&block_no=47662&year=2021&month=&day=&view=a1.

[130] P. Dubout, "The sound of rain on a steel roof," *Journal of sound and vibration,* vol. 10, no. 1, pp. 144-150, 1969, doi: 10.1016/0022-460X(69)90133-3.

[131] D. Griffin and K. Ballagh, "A Consolidated Theory for Predicting Rain Noise," *Building acoustics,* vol. 19, no. 4, pp. 221-248, 2012, doi: 10.1260/1351-010X.19.4.221.
[132] D. Griffin, "Accuracy of prediction methods for rain noise levels," 2016.
[133] S. S. Stevens, J. Volkmann, and E. B. Newman, "A scale for the measurement of the psychological magnitude pitch," *The journal of the acoustical society of america,* vol. 8, no. 3, pp. 185–190, 1937.
[134] Y. Shao and D. Wang, "Robust speaker recognition using binary time-frequency masks," in *2006 IEEE International Conference on Acoustics Speech and Signal Processing Proceedings*, 2006, vol. 1: IEEE, pp. I-I.
[135] J. Daniel and M. James H, *Speech and language processing: An introduction to natural language processing, computational linguistics, and speech recognition*. 2007.
[136] L. Rabiner and B.-H. Juang, *Fundamentals of speech recognition*. Prentice-Hall, Inc., 1993.
[137] H. Harvianto, L. Ashianti, J. Jupiter, and S. Junaedi, "Analysis and voice recognition In Indonesian language using MFCC and SVM method," *ComTech: Computer, Mathematics and Engineering Applications,* vol. 7, no. 2, pp. 131-139, 2016.
[138] T. Fukumori, M. Nakayama, T. Nishiura, and H. Nanjo, "Performance evaluation of noisy shouted speech detection based on acoustic model with rahmonic and mel-frequency cepstrum coefficients," *IEICE Technical Report; IEICE Tech. Rep.,* vol. 116, no. 477, pp. 283-286, 2017.
[139] F. Z. Chelali and A. Djeradi, "Text dependant speaker recognition using MFCC, LPC and DWT," *International Journal of Speech Technology,* vol. 20, no. 3, pp. 725-740, 2017, doi: 10.1007/s10772-017-9441-1.
[140] Y. Oishi, M. Goto, K. Ito, and K. Takeda, "Discrimination between Singing and Speaking Voices Using a Spectral Envelope and a Fundamental Frequency Derivative," *IPSJ Journal,* vol. 47, no. 6, pp. 1822-1830, 2006.
[141] D. S. S. Lee, B. J. Lithgow, and R. E. Morrison, "New fault diagnosis of circuit breakers," *IEEE Transactions on Power Delivery,* vol. 18, no. 2, pp. 454-459, 2003, doi: 10.1109/tpwrd.2003.809615.
[142] E. Alickovic, J. Kevric, and A. Subasi, "Performance evaluation of empirical mode decomposition, discrete wavelet transform, and wavelet packed decomposition for automated epileptic seizure detection and prediction," *Biomedical signal processing and control,* vol. 39, pp. 94-102, 2018.
[143] S. Badillo *et al.*, "An introduction to machine learning," *Clinical pharmacology & therapeutics,* vol. 107, no. 4, pp. 871-885, 2020.
[144] *Management of Wrong Side Failures*: British railways Signal & Telecommunications Engineering Department, 1989. [Online]. Available: https://www.rssb.co.uk/-/media/Project/RSSB/RssbWebsite/Documents/Registered/Standards/2020/09/16/10/39/GKEHH004-Iss-3.pdf.
[145] G. Britain and A. Hidden, *Investigation into the Clapham Junction railway accident*. HM Stationery Office, 1989.
[146] A. Sims, "Japanese rail workers build special tunnels to save turtles from train deaths," ed: The independent, 2015.
[147] B. Eccles, "The use of two nuts to prevent self loosening," *Fastener and Fixing magazine,* 2008. [Online]. Available: https://www.boltscience.com/pages/the-use-of-two-nuts-to-prevent-self-loosening.pdf.

[148] *Environmental Quality Standards for Shinkansen Superexpress Railway Noise*, M. o. t. E. G. o. Japan, 1993. [Online]. Available: https://www.env.go.jp/en/air/noise/railway.html

[149] P. H. Trombetta Zannin and F. Bunn, "Noise annoyance through railway traffic-a case study," *Journal of Environmental Health Science and Engineering,* vol. 12, pp. 1-12, 2014.

[150] H. Peng, F. Long, and C. Ding, "Feature selection based on mutual information criteria of max-dependency, max-relevance, and min-redundancy," *IEEE Transactions on pattern analysis and machine intelligence,* vol. 27, no. 8, pp. 1226-1238, 2005.

[151] H. Abdi and L. J. Williams, "Principal component analysis," *Wiley interdisciplinary reviews: computational statistics,* vol. 2, no. 4, pp. 433-459, 2010.